

学位論文

**Studies on seawater CO₂ chemistry in the tropical to
subtropical Pacific using *Porites* coral boron isotopes
for the last deglaciation and the industrial era**

(ハマサンゴホウ素同位体を用いた熱帯・亜熱帯太平洋における
産業革命以降・最終退氷期の海水炭酸系に関する研究)

平成 26 年 12 月 16 日 博士 (理学) 申請

東京大学大学院 理学系研究科

地球惑星科学専攻

窪田 薫

**Studies on seawater CO₂ chemistry in the tropical to
subtropical Pacific using *Porites* coral boron isotopes
for the last deglaciation and the industrial era**

Kaoru KUBOTA

Atmosphere and Ocean Research Institute &
Department of Earth and Planetary Science, The University of Tokyo

Submitted to the University of Tokyo
in partial fulfillment of the requirements for the Degree of Doctor of Philosophy

December 16, 2014

“Carbon is forever”

Mason Inman, *Nature Reports Climate Change* (2008)

Abstract

Boron isotope ratios ($\delta^{11}\text{B}$) of biogenic carbonates depend on seawater pH (pH_{SW}). To date, many stony corals have been reared in pH_{SW} -regulated aquariums, and $\delta^{11}\text{B}$ of skeletons that grew during the experiment have been measured. While the results clearly revealed pH_{SW} -dependency of $\delta^{11}\text{B}$ of coral skeletons, they revealed a large difference between measured $\delta^{11}\text{B}$ values and theoretically expected ones, too. In order to reconcile the difference, two approaches have been proposed. One approach regards $\delta^{11}\text{B}$ as a recorder of pH of calcification fluid (pH_{CF}), rather than pH_{SW} , because a line of evidence uncovers pH_{CF} is higher than pH_{SW} (biological pH up-regulation). The other approach presumes the difference as $\delta^{11}\text{B}$ offsets (empirical corrections). Whichever approaches are employed, however, culturing experiment-based $\delta^{11}\text{B}$ - pH_{SW} calibrations appear to reconstruct pH_{SW} that conflicts with the CO_2 chemistry observation. Therefore, another means to calibrate $\delta^{11}\text{B}$ - pH_{SW} is required. To meet the needs, massive *Porites* corals living in the natural environment have large potentials, because they are long-lived and have experienced anthropogenic pH_{SW} decreases since the Industrial Revolution (ocean acidification).

The research objectives of this thesis are (1) to obtain the field-based $\delta^{11}\text{B}$ - pH_{SW} calibrations and (2) to utilize them in paleoenvironmental studies. It is noteworthy that deep understandings of the $\delta^{11}\text{B}$ - pH_{SW} relationship will lead to not only a development of tools for carbon cycle studies but also understandings of the corals' response to ocean acidification. Firstly, the $\delta^{11}\text{B}$ - pH_{SW} calibrations using massive *Porites* corals collected from Chichijima (Ogasawara Islands, Japan) and Tahiti (Society Islands, French Polynesia) were shown (Chapter 2). Secondly, based on pH up-regulation mechanisms, effects of the ocean acidification for the last 100 years on the Chichijima coral calcification were discussed (Chapter 3). Thirdly, a paleoceanographic study using fossil *Porites* corals obtained from Tahiti under the program of Integrated Ocean Drilling Program (IODP) Expedition 310 was shown (Chapter 4). Lastly, the key findings of this thesis were discussed, and future avenues for this research were suggested (Chapter 5).

Boron isotopes - pH calibration using long-lived modern corals (Chapter 2): We measured a 100 year record of $\delta^{11}\text{B}$ of *Porites* coral obtained from Chichijima. Previously reported $\delta^{11}\text{B}$ values of Tahitian corals were also used after corrections of

different procedure-specific isotopic offsets. Comparing coral $\delta^{11}\text{B}$ records with pH_{SW} that was estimated from many CO_2 chemistry data and atmospheric CO_2 records, we established, for the first time, field-based calibrations for Chichijima and Tahiti. Using the established calibration, we reevaluated the previously reported pH_{SW} reconstructions from $\delta^{11}\text{B}$ of *Porites* corals obtained from Guam and Hainan islands. The results showed that empirically reconstructed pH_{SW} , as well as partial pressure of CO_2 in the seawater ($p\text{CO}_2_{\text{SW}}$), were more in line with CO_2 chemistry observations than those calculated using the culture-based calibration, and that the correction values were different depending on locations.

Effects of recent ocean acidification in the western North Pacific on Porites coral calcification (Chapter 3): To better understanding how organisms and ecosystems will adapt to or be damaged by ocean acidification, field observations are crucial. In this chapter, we showed clear evidence, based on $\delta^{11}\text{B}$ measurements, that ocean acidification is affecting the pH_{CF} in *Porites* coral collected at Chichijima. A rapid decline of $\delta^{11}\text{B}$ of coral skeleton since 1960 ($-0.17 \pm 0.07\text{‰}/\text{decade}$) was observed and was compared with pH_{SW} near the Ogasawara Islands over the 20th century. The results indicated that pH_{CF} has been changing sensitively to pH_{SW} and suggested that the calcification fluid of coral will become corrosive to aragonite in the future ($\text{pH}_{\text{CF}} = \text{ca. } 8.3$ when $\text{pH}_{\text{SW}} = \text{ca. } 8.0$ in 2050) at an earlier point than previously expected, despite the pH_{CF} up-regulation mechanism of coral.

Marine carbon cycle at the equatorial Pacific during the last deglaciation (Chapter 4): While biogeochemical and physical processes in the Southern Ocean are thought to be central to atmospheric CO_2 rise during the last deglaciation ($\sim 80 \mu\text{atm}$), the roles of the equatorial Pacific, where the largest CO_2 source exists at present, remains largely unconstrained. In this chapter we showed pH_{SW} and $p\text{CO}_2_{\text{SW}}$ variations during this period reconstructed from fossil *Porites* corals obtained at Tahiti based on empirical $\delta^{11}\text{B}$ - pH_{SW} calibration. The new data, together with recalibrated existing data, indicated that a significant $p\text{CO}_2_{\text{SW}}$ increase (pH_{SW} decrease), accompanied by anomalously large marine ^{14}C reservoir ages, occurred following not only the Younger Dryas, but also Heinrich Stadial 1. These findings indicated an expanded zone of equatorial upwelling and resultant CO_2 emission, which may be derived from higher subsurface DIC concentration.

Contents

Abstract	i
-----------------------	----------

Chapter 1

General Introduction	1
1-1. CO ₂ chemistry in seawater.....	2
1-2. Boron isotopes in seawater and carbonates.....	6
1-2-1. $\delta^{11}\text{B}$ -pH calibration (1): pH up-regulation.....	18
1-2-2. $\delta^{11}\text{B}$ -pH calibration (2): Empirical correction.....	18
1-3. Oceanography of the tropical to subtropical regions of Pacific Ocean.....	19
1-3-1. Temperature and salinity.....	19
1-3-2. Ocean current.....	22
1-3-3. Surface $p\text{CO}_2$ distribution and CO ₂ source versus sink.....	24
1-4. Carbon cycle since the last glacial period.....	25
1-4-1. The last deglaciation.....	29
1-4-2. After the Industrial Revolution.....	30
1-5. Research objectives and thesis structure.....	32

Chapter 2

Boron isotopes - pH calibration using long-lived modern corals	33
Chapter 2 Abstract	34
2-1. Introduction	35
2-2. Material and Methods	39
2-2-1. $\delta^{11}\text{B}$ measurements of Chichijima coral.....	39
2-2-2. $\delta^{11}\text{B}$ values of Tahiti and Marquesas corals.....	44
2-2-3. pH_{SW} estimation since 1970.....	44
2-2-4. pH_{SW} estimation since the Industrial Revolution.....	47
2-3. Results and Discussion	48
2-3-1. Comparison of $\delta^{11}\text{B}$ values measured in different methods.....	48
2-3-2. pH_{SW} estimation since 1970.....	50
2-3-3. pH_{SW} estimation since the Industrial Revolution.....	56
2-3-4. $\delta^{11}\text{B}$ - pH_{SW} calibration and errors.....	58

2-3-5. Location-specific difference of offset a	63
2-4. Conclusion	65

Chapter 3

Effects of recent ocean acidification in the western North Pacific on *Porites* coral calcification.....

Chapter 3 Abstract	68
3-1. Introduction	69
3-2. Material and Methods	72
3-2-1. $\delta^{11}\text{B}$ and $\delta^{13}\text{C}$ measurements of Chichijima coral	72
3-2-2. Seawater CO_2 chemistry	72
3-3. Results and Discussion	73
3-3-1. $\delta^{11}\text{B}$ variation	73
3-3-2. $\delta^{13}\text{C}$ variation	77
3-3-3. Relationships between $\delta^{11}\text{B}$ and $\delta^{13}\text{C}$	85
3-3-4. Sensitivity of pH_{CF} to pH_{SW} decrease	85
3-3-5. Environmental stressors for Chichijima corals and implications for future coral reefs	91
3-4. Conclusion	93

Chapter 4

Marine carbon cycle at the equatorial Pacific during the last deglaciation....

Chapter 4 Abstract	96
4-1. Introduction	97
4-2. Material and Methods	100
4-2-1. $\delta^{11}\text{B}$ - pH_{SW} calibration	100
4-2-2. $\delta^{11}\text{B}$ analysis of Tahitian fossil corals	100
4-2-3. Marine ^{14}C reservoir age compilation	103
4-3. Results and Discussion	104
4-3-1. pH_{SW} and pCO_2 SW reconstructions	104
4-3-2. Marine ^{14}C reservoir ages	106
4-3-3. SSS effects on TA and pCO_2 SW calculations	109
4-3-4. SST effects on pCO_2 SW reconstructions	111

4-3-5. Mechanisms to explain higher $\Delta p\text{CO}_2$ and R_{diff} during the last deglaciation	114
4-3-6. A similarity between R_{diff} and $p\text{CO}_2$ variability	115
4-3-7. Did the equatorial Pacific contribute to the deglacial CO_2 rise?	116
4-4. Conclusion	116
 Chapter 5	
General conclusion and future perspectives	119
5-1. General conclusion	120
5-2. Future perspectives	122
5-2-1. Perspectives on $\delta^{11}\text{B}$ -pH systematics	122
5-2-2. Direction of $\delta^{11}\text{B}$ -pH _{SW} calibration using long-lived calcifying organisms	125
5-2-3. Paleoclimatological perspectives	126
 Acknowledgements	129
References	131
Appendix	149

CHAPTER 1

General Introduction

As general introduction of this thesis, first of all, important parameters that control seawater CO₂ chemistry will be introduced. Secondly, boron isotope systematics in the seawater and the current knowledge of biological incorporations of boron isotopes into calcium carbonates that some marine organisms form will be explained. Thirdly, the oceanography of the tropical-subtropical region of the Pacific discussed in the thesis will be reviewed. Lastly, the carbon cycle since the last glacial period with several key paleoclimatological records will be summarized.

1-1. CO₂ chemistry in seawater

Surface seawater actively exchanges carbon dioxide (CO₂) with the overlying atmosphere (Fig. 1-1):



The air-sea exchanges of CO₂ are controlled by the partial pressure of CO₂ ($p\text{CO}_2$), gas transfer functions (function of temperature) and wind strength (e.g. [Takahashi et al., 2009](#)).

Dissolved CO₂ in seawater is dissociated into bicarbonate ion (HCO₃⁻):



and it is further dissociated into carbonate ion (CO₃²⁻):



As proton is emitted during the dissociation above, seawater CO₂ chemistry largely depends on pH (concentration of proton in logarithmic scale: $-\log_{10}[\text{H}^+]$) (Fig. 1-2). The saturation state of seawater with respect to aragonite (Ω_{arg}) is defined as:

$$\Omega_{\text{arg}} = \frac{[\text{Ca}^{2+}] * [\text{CO}_3^{2-}]}{K_{\text{sp}}} \quad (\text{Eq. 1-4})$$

where K_{SP} is a solubility product of aragonite that is a function of temperature, salinity and pressure.

Boron is also a major constituent of seawater CO_2 chemistry (Fig. 1-1), and it exists in two forms, boric acid ($B(OH)_3$) and borate ion ($B(OH)_4^-$), in seawater with pH of ~ 8 (Fig. 1-2). Boron concentration in seawater is a function of salinity (e.g., [Millero, 1979](#)):

$$B_T = [B(OH)_3] + [B(OH)_4^-] = 12.12 * \text{salinity} \quad (\text{Eq. 1-5})$$

Boric acid reacts with water, producing borate ion and proton:



Dissolved inorganic carbon (DIC) is defined as sum of carbon bearing ions:

$$DIC = [HCO_3^-] + [CO_3^{2-}] + [CO_2(aq)] \quad (\text{Eq. 1-7})$$

On the other hand, total alkalinity (TA), excess anions that keep charge balances of seawater, is defined as follows:

$$TA = [HCO_3^-] + 2[CO_3^{2-}] + [B(OH)_4^-] \quad (\text{Eq. 1-8})$$

As relative abundance of borate ion in TA is only a few percent (e.g., 3.8% when $DIC = 2,000 \mu\text{mol/kg}$, salinity = 35, and temperature = 25 °C), a contribution of borate ion to TA is neglected in general (and in this thesis, too). We can fully calculate CO_2 chemistry when pressure, temperature, salinity, and two of four parameters (DIC, TA, pH and pCO_2) are given (e.g. [Zeebe & Wolf-Gladrow, 2001](#)). It should be noted, unless otherwise stated, pH scale is the total hydrogen scale ([Gattuso & Hanson, 2011](#); [Riebesel et al., 2010](#); [Robbins et al., 2010](#); [Zeebe & Wolf-Gladrow, 2001](#)), and the dissociation constants are carbonic acid (CO_3^{2-} , HCO_3^-) derived from [Lueker et al. \(2000\)](#) and hydrogen sulfate (HSO_4^-) derived from [Dickson \(1990\)](#) in this thesis.

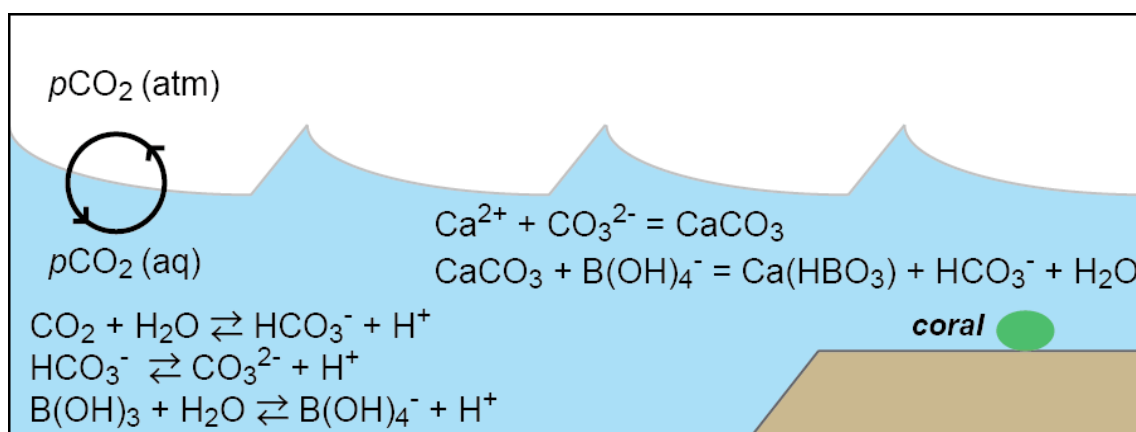


Fig. 1-1. A schematic diagram of seawater CO_2 chemistry in the surface ocean.

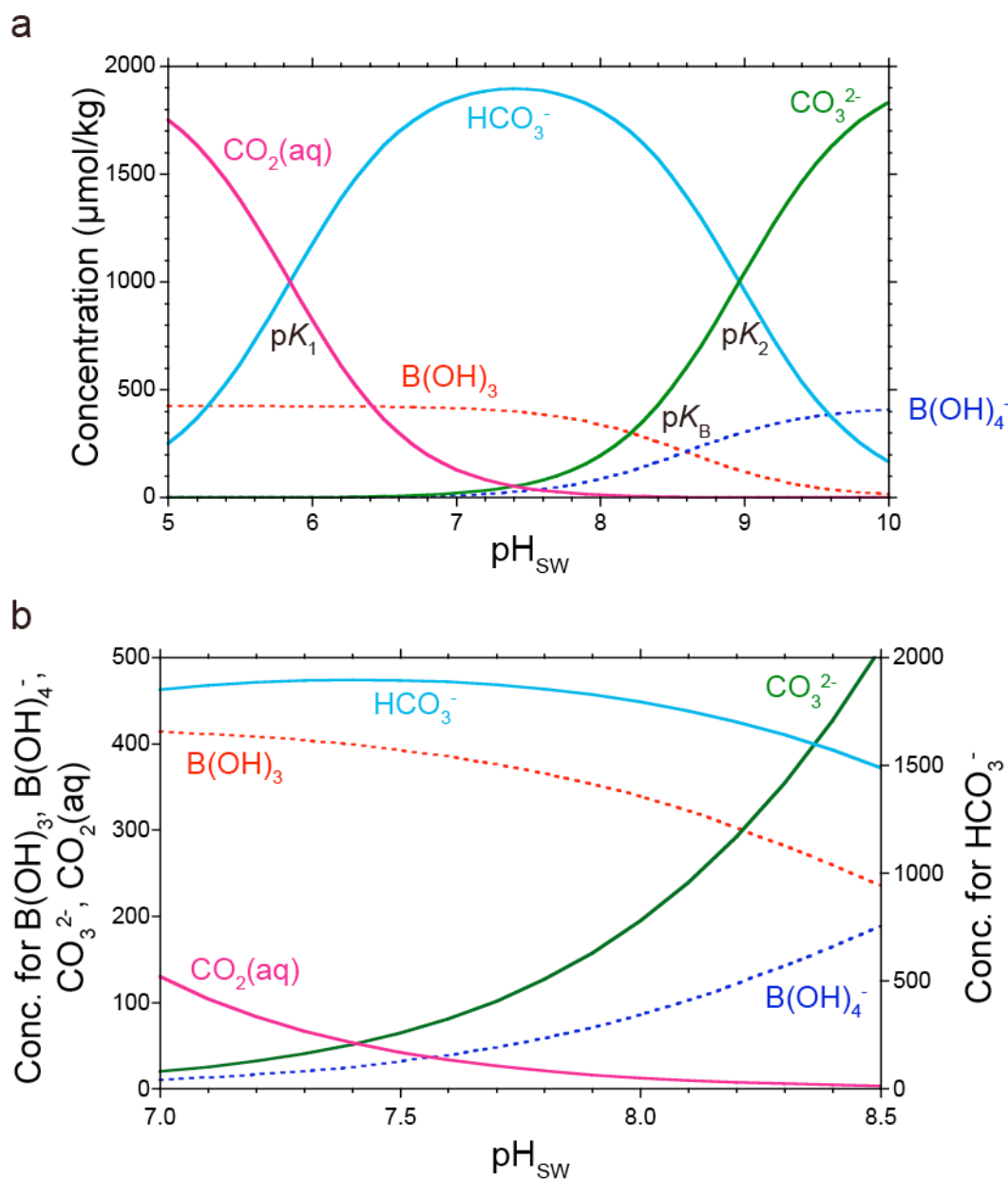
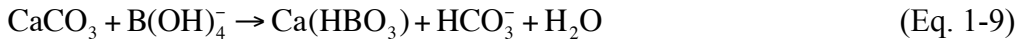


Fig. 1-2. (a) Concentration of each ion that constitutes CO_2 chemistry. The calculation was made using DIC of 2,000 $\mu\text{mol/kg}$, salinity of 35, and temperature of 25 °C. (b) Enlarged view of a. Note that concentration of bicarbonate ion is shown in right axis.

1-2. Boron isotopes in seawater and carbonates

Not only relative abundances of boric acid and borate ion, but also $\delta^{11}\text{B}$ of each species are pH-dependent (Fig. 1-3). The following equation is proposed to describe incorporations of boron into biogenic carbonates (Hemming & Hanson, 1992):



As seen in the equation, if borate ion B(OH)_4^- is incorporated into biogenic carbonates preferentially, $\delta^{11}\text{B}$ of carbonates ($\delta^{11}\text{B}_{\text{carbonate}}$) acts as a pH-meter following the equation:

$$\text{pH} = \text{p}K_{\text{B}} - \log \left(\frac{\delta^{11}\text{B}_{\text{SW}} - \delta^{11}\text{B}_{\text{carbonate}}}{\alpha_{3.4} * \delta^{11}\text{B}_{\text{carbonate}} - \delta^{11}\text{B}_{\text{SW}} + 10^3 * (\alpha_{3.4} - 1)} \right) \quad (\text{Eq. 1-10})$$

$\text{p}K_{\text{B}}$ is the dissociation constant of boric acid (Dickson, 1990). $\delta^{11}\text{B}_{\text{SW}}$ is the global average $\delta^{11}\text{B}$ of seawater (a recently compiled value is 39.61‰, Foster et al., 2010) and can be regarded as a constant throughout the Quaternary because a residence time of boron in the seawater is long enough (at least ~20 Ma, Spivack & Edmond, 1987). $\alpha_{3.4}$ is the fractionation factor between trigonal boric acid B(OH)_3 and tetrahedral borate ion B(OH)_4^- determined empirically through spectrometric pH measurements of borate buffer solutions containing only ^{11}B or ^{10}B (1.0272, Klochko et al., 2006).

As pioneering works, Vengosh *et al.* (1991) and Hemming & Hanson (1992) demonstrated that $\delta^{11}\text{B}$ values of modern marine carbonates, both aragonite and calcite, are roughly in line with the theoretically expected values (Table 1-1). Nowadays, boron isotopes of carbonate materials are measured by mainly two methodologies: thermal ionization mass spectrometry (TIMS) and multi-collector inductively coupled plasma mass spectrometry (MC-ICPMS) (Table 1-2). Although $\delta^{11}\text{B}$ measurements of biogenic carbonates using secondary ionization mass spectrometry (SIMS, e.g., Allison et al., 2014; Kasemann et al., 2009), high-resolution ICPMS (HR-ICPMS, e.g., Mirsa et al., 2014), and laser ablation ICPMS (LA-ICPMS, e.g., Kaczmarek et al., 2015) has also developed recently, they are omitted here. The TIMS method is further divided into two

ways depending on which ion is used in mass spectrometry, positive (P-TIMS) or negative (N-TIMS). McMullen *et al.* (1961) developed the P-TIMS method utilizing Na_2BO_2^+ ions (mass of 89 and 88). However, the precision of this methodology was worse than 2–3‰ at that time. After a while Spivack & Edmond (1987) improved the P-TIMS method introducing Cs_2BO_2^+ ion (mass of 309 and 308). Up until now, Ishikawa & Nagaishi (2011)'s P-TIMS method using Cs_2BO_2^+ ion reports the highest precision (0.08‰, 2σ) for $\delta^{11}\text{B}$ measurements of biogenic carbonates, which requires 50–100 ngB for the analysis (equivalent to 2–3 mg of coral aragonite). The N-TIMS method using BO_2^- ion (mass of 43 and 42), developed by Heumann (1982), is characterized by a high sensitivity, namely it requires a little sample amount (< 1 ngB). Although the precision of the N-TIMS method is relatively worse than P-TIMS method ($\sim 0.50\%$, 2σ), it is suitable for $\delta^{11}\text{B}$ measurements of small samples (e.g., foraminifers). Currently, the MC-ICPMS method is the most widely used for $\delta^{11}\text{B}$ measurements of biogenic carbonates because of a moderately high precision ($\sim 0.25\%$, 2σ), a swiftness of sample preparation, and availability of an autosampler (Table 1-2, and references therein). Foster (2008) developed the MC-ICPMS method using a sample-standard bracketing routine, and paved the way to measure $\delta^{11}\text{B}$ of 1–3 mg of foraminiferal calcite.

However, there are large gaps between the measured $\delta^{11}\text{B}$ of scleractinian corals cultured in pH-regulated aquariums and the theoretical curve of $\delta^{11}\text{B}$ of borate ion (Fig. 1-4, Table 1-3) (Holcomb *et al.*, 2014; Trotter *et al.*, 2011; Krief *et al.*, 2010; Raynaud *et al.*, 2004; Hönisch *et al.*, 2004). In order to draw Figs. 1-4 and 1-5, we firstly corrected the analytical procedure-specific isotopic offsets (Kubota *et al.*, 2014, modified after Zeebe & Wolf-Gladrow, 2001):

$$\delta^{11}\text{B}_{\text{carbonate-corrected}} = \delta^{11}\text{B}_{\text{SW-stacked}} + \frac{\delta^{11}\text{B}_{\text{SW-stacked}} + 10^3}{\delta^{11}\text{B}_{\text{SW-measured}} + 10^3} * (\delta^{11}\text{B}_{\text{carbonate-measured}} - \delta^{11}\text{B}_{\text{SW-measured}})$$

(Eq. 1-11)

The differences between $\delta^{11}\text{B}$ of biogenic carbonates and theoretically expected ones are ubiquitously seen in scleractinian and deep-sea corals, foraminifers, brachiopods, ostracods, pteropods, gastropods, mollusks, echinoderms, and calcareous algae (e.g.,

Table 1-1 and references therein). The only exception is benthic foraminifers (*Cibicidoides* spp.); their $\delta^{11}\text{B}$ values coincide with the theory (Rae et al., 2011). Trotter et al. (2011) explained the cause of the difference seen in scleractinian corals as biological modulation of carbonate chemistry in calcification fluid from which the skeleton is produced. McCulloch et al. (2012a, b) extended their idea to deep-sea corals. They regarded $\delta^{11}\text{B}$ of both scleractinian and deep-sea corals as a recorder of calcification fluid pH, not seawater pH (Table 1-3). More simply, on the other hand, Hönisch et al. (2007) regarded the difference as a "vital effect" and corrected it empirically. This approach is reasonable because what we need in paleoceanography is an empirical proxy.

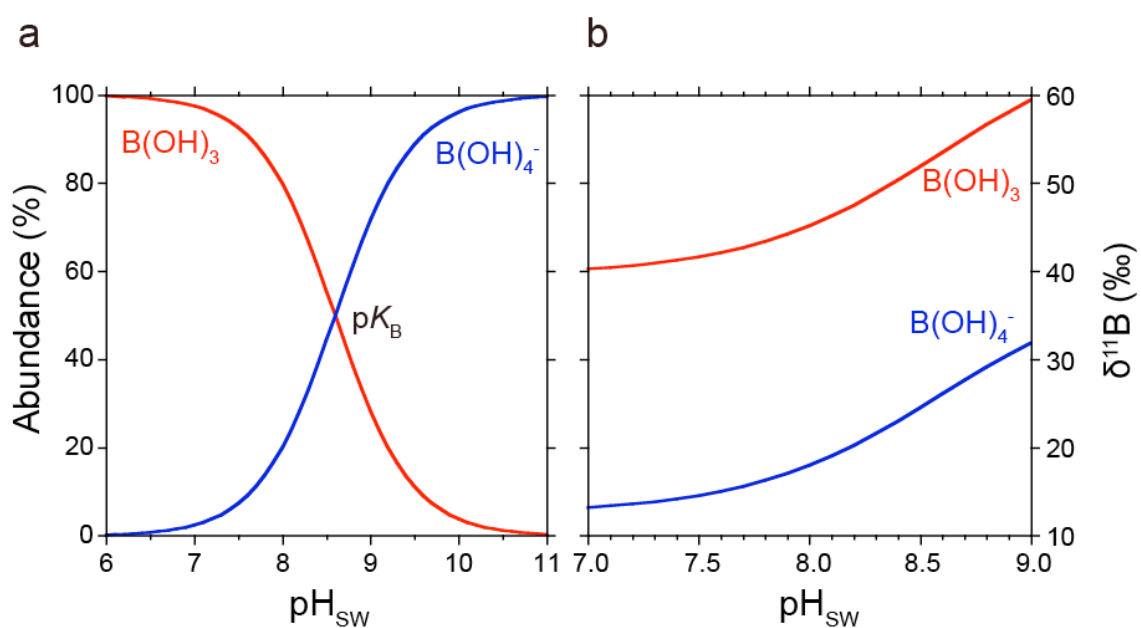


Fig. 1-3. (a) Relative abundance and (b) $\delta^{11}B$ of boric acid (red) and borate ion (blue). The calculation was made using the fractionation factor of Klochko *et al.* (2006), dissociation constants (pK_B) of boric acid of Dickson (1990) with salinity of 35 and temperature of 25 °C.

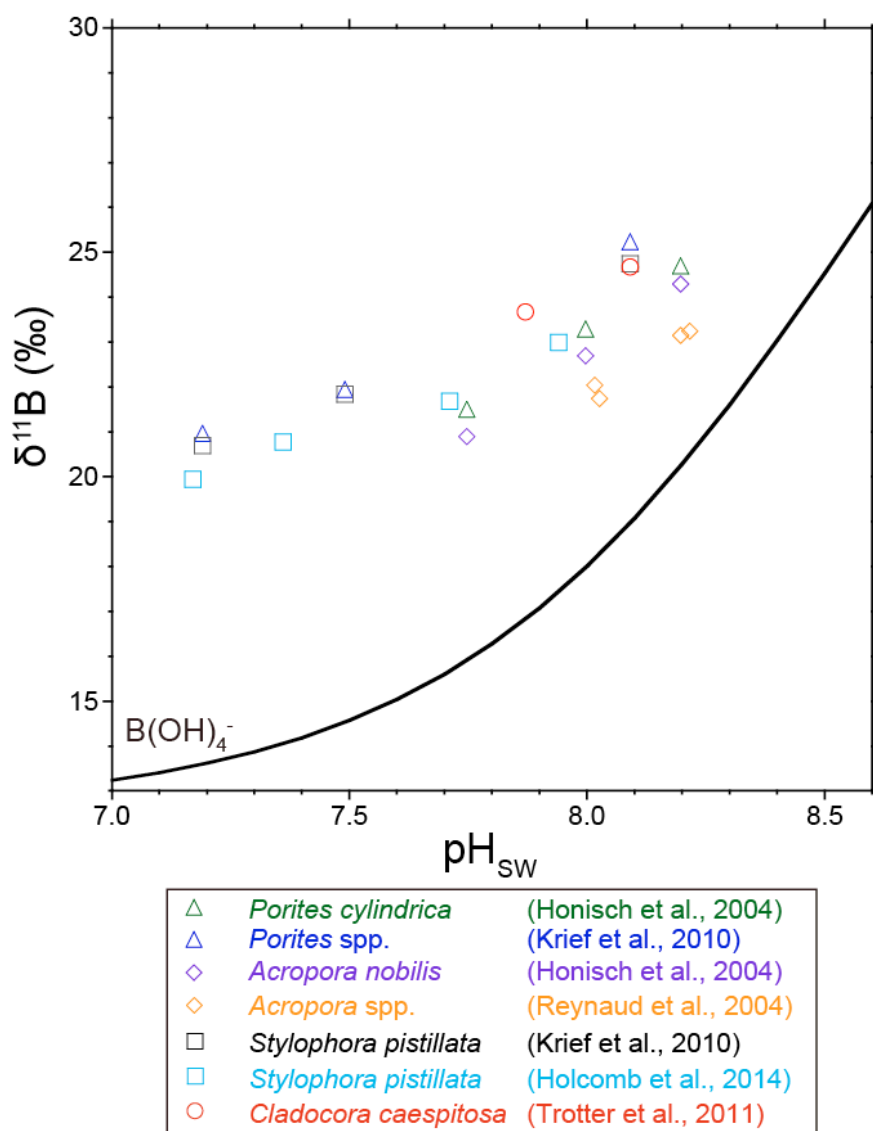


Fig. 1-4. Previously reported $\delta^{11}\text{B}$ values of cultured scleractinian corals (Table 1-3). Analytical procedure-specific isotopic offsets were corrected using Equation (1-11). The theoretical curve of $\delta^{11}\text{B}$ of borate ion is also plotted.

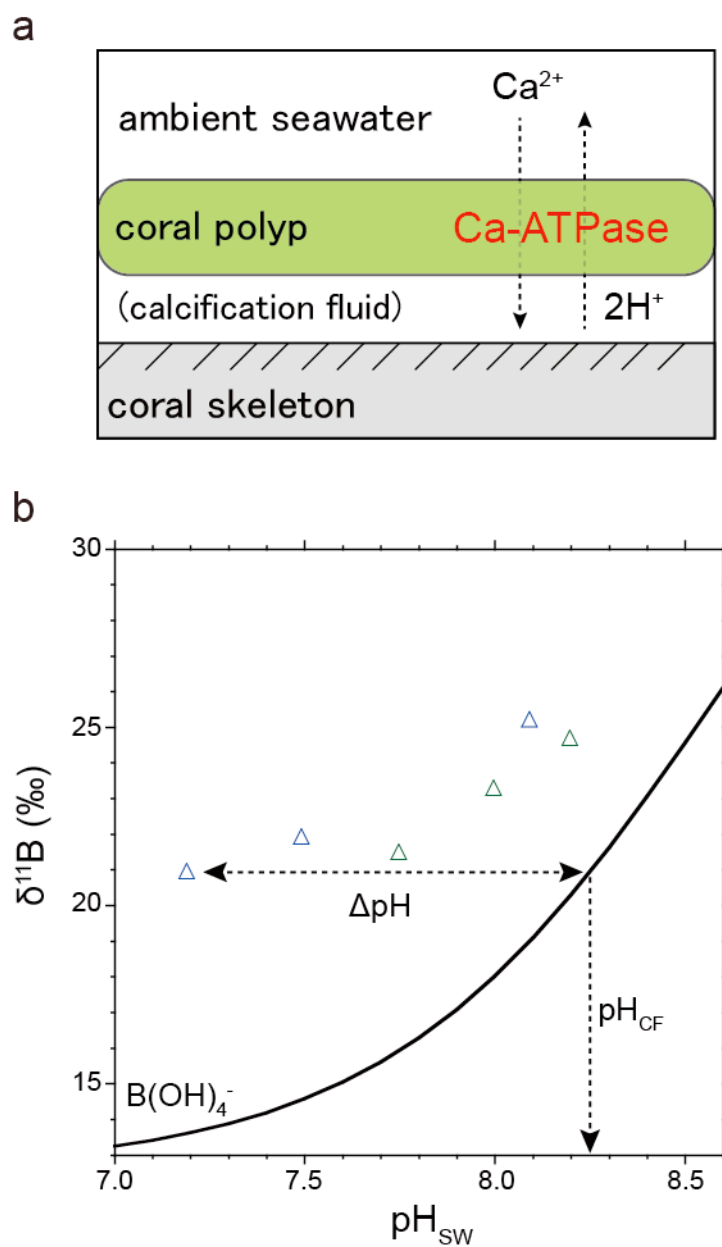


Fig. 1-5. (a) An illustration of calcification model proposed by Al-Horani *et al.* (2003). (b) Same as Fig. 1-4, but only Poritidae corals are shown. Arrows indicate pH_{CF} and ΔpH .

Table. 1-1. A summary of corals of which $\delta^{11}\text{B}$ values have documented in literatures.

Genus	Location	References
Scleractinian corals		
<i>Porites</i> (culture)		
massive <i>Porites</i> spp.	Eilat (Israel)	Krief et al., 2010
<i>Porites cylindrica</i>	Okinawa (Japan)	Hönisch et al., 2004
<i>Porites</i> (field, modern)		
massive <i>Porites</i> spp.	Chichijima (Japan)	This study
massive <i>Porites</i> spp.	Moorea (French Polynesia)	Douville et al., 2010 ; Gaillardet & Allegre, 1995
massive <i>Porites</i> spp.	Hainan (China)	Liu et al., 2014
massive <i>Porites</i> spp.	Guam (USA)	Shinjo et al., 2013
massive <i>Porites</i> spp.	GBR (Australia)	Wei et al., 2009 ; Pelejero et al., 2005
massive <i>Porites</i> spp.	Ishigaki (Japan)	This study (not shown) ; Kubota et al., 2014 ; McCulloch et al., 2014 ; Ishikawa & Nagaishi, 2011 ; Douville et al., 2010
massive <i>Porites</i> spp.	New Caledonia	Douville et al., 2010
massive <i>Porites</i> spp.	Luson (Philippines)	This study (not shown)
massive <i>Porites</i> spp.	Red sea	Gaillardet & Allegre, 1995
massive <i>Porites</i> spp.	Hawaii (USA)	Allison et al., 2014
massive <i>Porites</i> spp.	Jarvis (USA)	Allison et al., 2014
massive <i>Porites</i> spp.	GBR (Australia)	Vengosh et al., 1991
<i>Porites lutea</i>	New Caledonia	Rollion-Bard et al., 2003
<i>Porites lobata</i>	Hawaii (USA)	Allison et al., 2010
<i>Porites lobata</i>	Fanning (Kiribati)	Hemming et al., 1998
<i>Porites porites</i>	Florida (USA)	Hemming & Hanson, 1992

Continued

<i>Porites</i> (field, fossil)		
–	Tahiti (French Polynesia)	Kubota et al., 2014; Douville et al., 2010
–	Marquesas	Douville et al., 2010
–	Papua New Guinea	Kasemann et al., 2009
–	SCS (China)	Liu et al., 2014, 2009
<i>Acropora</i> (culture)		
<i>Acropora nobilis</i>	Okinawa (Japan)	Hönisch et al., 2004
<i>Acropora</i> spp.	New Caledonia	Raynaud et al., 2004
<i>Acropora</i> spp.	New Caledonia	Dissald et al., 2012
<i>Acropora</i> (field, modern)		
<i>Acropora cervicornis</i>	Jamaica	Hemming & Hanson, 1992
<i>Acropora</i> (field, fossil)		
–	Tahiti (French Polynesia)	Gaillardet & Allegre, 1995
–	Red Sea	Gaillardet & Allegre, 1995
–	La Reunion	Gaillardet & Allegre, 1995
–	Mauritius	Gaillardet & Allegre, 1995
–	Saint Thomas (USA)	Gaillardet & Allegre, 1995
<i>Cladocora</i> (culture)		
<i>Cladocora caespitosa</i>	Villefranche (France)	Trotter et al., 2011
<i>Cladocora caespitosa</i>	Villefranche (France)	Rollion-Bard et al., 2011
<i>Cladocora</i> (field, modern)		
<i>Cladocora caespitosa</i>	Levanto (Italy)	Trotter et al., 2011
<i>Cladocora caespitosa</i>	Ischia (Italy)	Trotter et al., 2011
<i>Pocilopora</i> (culture)		
<i>Pocillopora damicornis</i>	Eilat (Israel)	Allison et al., 2014

Continued

<i>Stylophora</i> (culture)		
<i>Stylophora pistilata</i>	Aqaba (Jordan)	Holcomb et al., 2014
<i>Stylophora pistilata</i>	Eilat (Israel)	Krief et al., 2010
<i>Stylophora</i> (field, modern)		
<i>Stylophora pistilata</i>	Eilat (Israel)	Vengosh et al., 1991
<i>Siderastrea</i> (field, modern)		
<i>Siderastrea siderea</i>	Jamaica	Hemming & Hanson, 1992
<i>Montastrea</i> (field, modern)		
<i>Montastrea</i> spp.	Jamaica	Hemming & Hanson, 1992
<i>Agaricia</i> (field, modern)		
<i>Agaricia agaricites</i>	Jamaica	Hemming & Hanson, 1992
<i>Pratygira</i> (field, modern)		
<i>Pratygira</i> spp.	Eilat (Israel)	Vengosh et al., 1991
<i>Fungia</i> (field, modern)		
<i>Fungia</i> spp.	Eilat (Israel)	Vengosh et al., 1991
<i>Goniastrea</i> (field, modern)		
<i>Agaricia agaricites</i>	Sumba (Indonesia)	Gaillardet & Allegre, 1995
Deep-sea corals		
<i>Caryophyllia smithii</i>		McCulloch et al., 2012b
<i>Desmophyllum dianthus</i>		McCulloch et al., 2012b ; Anagnostou et al., 2012
<i>Desmophyllum</i> spp.		Kasemann et al., 2009
<i>Enallopsammia rostrata</i>		McCulloch et al., 2012b
<i>Lophelia pertusa</i>		McCulloch et al., 2012b ; Rollion-Bard et al., 2011
<i>Madrepora oculata</i>		McCulloch et al., 2012b
<i>Keratoisis</i> spp.		Farmer et al., in press
<i>Corallium</i> spp.		McCulloch et al., 2012b

Table 1-2. A summary of methodologies to measure $\delta^{11}\text{B}$ of carbonate materials.

References		
Method	Corals (aragonite)	Foraminifers (calcite)
P-TIMS	This study; Kubota et al., 2014; Holcomb et al., 2014; McCulloch et al., 2012a, b; Trotter et al., 2011; Ishikawa & Nagaishi, 2011; Wei et al., 2009; Pelejero et al., 2005; Gaillardet & Allegre, 1995	
N-TIMS	Farmer et al., in press; Kasemann et al., 2009; Hönisch et al., 2004; Raynaud et al., 2004; Hemming et al., 1998; Hemming & Hanson, 1992; Vengosh et al., 1991	Hönisch et al., 2009; Hönisch & Hemming, 2005; Palmer & Pearson, 2003
MC-ICPMS	This study; Shinjo et al., 2013; Dissard et al., 2012; Anagnostou et al., 2012; Douville et al., 2010; Krief et al., 2010; Kasemann et al., 2009	This study; McCulloch et al., 2014; Liu et al., 2014; Henehan et al., 2013; Foster & Sexton, 2014; Seki et al., 2009; Yu et al., 2013; Foster, 2008

Table 1-3. Previously reported $\delta^{11}\text{B}$ values of scleractinian corals reared in aquariums with lowered pH_{sw} .

$^{(1)}\text{pH}_{\text{sw}} \pm$	$\text{p}K_{\text{B}}(\text{T}, \text{S})$	Coral genera	$\delta^{11}\text{B}_{\text{coral}}$ values (‰)		error (%, 2 σ)	pH_{CF}	ΔpH	Method	$\delta^{11}\text{B}_{\text{sw}}$ (‰)	Reference
			measured	corrected						
8.22	0.05	<i>Acropora</i>	24.0	23.4	0.50	8.42	0.21	N-TIMS	40.3	Reynaud et al., 2004
8.20	8.58 (25.3, 38.0)	spp.	23.9	23.3		8.38	0.19			
8.03	8.55 (28.2, 38.0)		22.5	21.9		8.32	0.30			
8.02	8.58 (25.1, 38.0)		22.8	22.2		8.31	0.29			
7.75	8.54 (28.3, 38.0)									
7.75	0.05	<i>Acropora</i>	21.1	21.0	0.31	8.25	0.50	N-TIMS	39.7	Hönisch et al., 2004
8.00	(27.0, 36.4)	<i>nobilis</i>	22.9	22.8		8.37	0.38			
8.20			24.5	24.4		8.48	0.28			
7.75	0.05	<i>Porites</i>	21.7	21.6	0.31	8.29	0.55	N-TIMS	39.7	Hönisch et al., 2004
8.00	(27.0, 36.4)	<i>cylindrica</i>	23.5	23.4		8.41	0.42			
8.20			24.9	24.8		8.50	0.31			
8.09	0.05	<i>Porites</i>	25.2	25.3	0.25	8.54	0.45	MC-ICPMS	39.5	Krief et al., 2010
7.49	(25.0, 40.7)	spp.	22.0	22.1		8.33	0.84			
7.19			21.0	21.1		8.26	1.07			
8.09	0.05	<i>Stylophora</i>	24.8	24.9	0.25	8.51	0.42	MC-ICPMS	39.5	Krief et al., 2010
7.49	(25.0, 40.7)	<i>pistillata</i>	21.8	21.9		8.32	0.83			
7.19			20.7	20.8		8.24	1.05			
8.09	0.02	<i>Cladocora</i>	25.3	24.8	0.27	8.61	0.52	P-TIMS	40.1	Trotter et al., 2011
7.87	(17.6, 38.1)	<i>caespitosa</i>	24.3	23.8		8.51	0.64			
	8.64 (20.5, 38.1)									

<i>Continued</i>											
7.17	0.07	8.58	<i>Stylophora</i>	20.4	19.9	0.25	8.18	1.01	P-TIMS	40.1	Holcomb et al., 2014
7.36	0.08	(25.0, 38.0)	<i>pistillata</i>	21.2	20.8		8.25	0.89			
7.71	0.08			22.2	21.7		8.31	0.60			
7.94	0.04			23.5	23.0		8.40	0.46			

(1) pH scales were integrated into the total hydrogen scale.

(2) Analytical procedure-specific isotopic offsets were corrected using Equation (1-11)

1-2-1. $\delta^{11}\text{B}$ -pH calibration (1): pH up-regulation

Corals up-regulate pH of calcification fluid (pH_{CF}) in order to realize more suitable conditions for calcification (Allison et al., 2014; Holcomb et al., 2014; Hendriks et al., 2015; Venn et al., 2013, 2011; McCulloch et al., 2012a,b; Trotter et al., 2011; Cohen & Holcomb, 2009; Al-Horani et al., 2003). For instance, pH_{CF} is ~ 1.1 (under the light) and 0.2–0.5 higher than seawater pH (pH_{SW}) for *Galaxea fascicularis* and *Stylophora pistillata*, respectively (Venn et al., 2013, 2011; Al-Horani et al., 2003). Recently Allison et al. (2014) showed that pH_{CF} of *Stylophora pistillata* directly measured using pH sensitive dye is in an excellent agreement with that estimated from $\delta^{11}\text{B}_{\text{coral}}$. The enzyme Ca^{2+} -ATPase likely plays a key role in this pH up-regulation because it has a function of pumping Ca^{2+} into the calcification fluid and removing two H^+ , which elevates pH_{CF} and $[\text{CO}_3^{2-}]$ (Figs. 1-2 and 1-5). Then increases of $[\text{Ca}^{2+}]$ and $[\text{CO}_3^{2-}]$ will lead to more saturated $\Omega_{\text{arg CF}}$, thus facilitating calcification. In the pH up-regulation, $\delta^{11}\text{B}_{\text{coral}}$ represents pH_{CF} , not pH_{SW} , and a deviation between them is defined as ΔpH (Trotter et al., 2011) (Fig. 1-5):

$$\text{pH}_{\text{CF}} = \text{p}K_{\text{B}} - \log\left(\frac{\delta^{11}\text{B}_{\text{SW}} - \delta^{11}\text{B}_{\text{coral}}}{\alpha_{3.4} * \delta^{11}\text{B}_{\text{coral}} - \delta^{11}\text{B}_{\text{SW}} + 10^3 * (\alpha_{3.4} - 1)}\right) \quad (\text{Eq. 1-12})$$

$$\Delta\text{pH} = \text{pH}_{\text{CF}} - \text{pH}_{\text{SW}} \quad (\text{Eq. 1-13})$$

ΔpH is always positive, namely $\delta^{11}\text{B}_{\text{coral}}$ locates in the left side of the theoretical curve in $\delta^{11}\text{B}$ -pH cross plot (lessor pH) (Figs. 1-4 and 1-5).

1-2-2. $\delta^{11}\text{B}$ -pH calibration (2): Empirical correction

On the other hand, Hönisch et al. (2007) proposed a more simplified equation by introducing "offset a (unit is ‰)" in the $\delta^{11}\text{B}$ - pH_{SW} calibration equation:

$$\text{pH}_{\text{SW}} = \text{p}K_{\text{B}} - \log\left(\frac{\delta^{11}\text{B}_{\text{SW}} - (\delta^{11}\text{B}_{\text{coral}} + a)}{\alpha_{3.4} * (\delta^{11}\text{B}_{\text{coral}} + a) - \delta^{11}\text{B}_{\text{SW}} + 10^3 * (\alpha_{3.4} - 1)}\right) \quad (\text{Eq. 1-14})$$

The offset a has a negative value, namely $\delta^{11}\text{B}_{\text{coral}}$ is plotted above the theoretical curve

(heavier $\delta^{11}\text{B}$) (Fig. 1-4).

1-3. Oceanography of the tropical and subtropical Pacific

Study regions discussed in this thesis is the tropical-subtropical Pacific. Modern and fossil corals obtained from Chichijima (Ogasawara Islands, 27°06'N 142°12'E) in the western North Pacific and Tahiti (Society Islands, 17°39'S 149°30'W) in the South Pacific are used. In the following sections, the sea surface temperature (SST) and salinity (SSS) regimes, the ocean current, and then the carbon cycle in the surface ocean of the tropical-subtropical Pacific will be summarized.

1-3-1. Temperature and salinity

In the western equatorial Pacific, the broad warm water mass called the Western Pacific Warm Pool (WPWP) exists (Fig. 1-6). On the other hand, in the eastern equatorial Pacific, there exists the outcrop of cold subsurface water due to inclined thermocline toward the west, called the cold tongue. Cold tongue is formed as a result of the equatorial upwelling and the advection of upwelled subsurface water at the coast off Peru (coastal upwelling) (Talley et al., 2011). Due to the heat transport by Kuroshio Current, the south coast of Japan is kept relatively warm regardless of its latitude. The annual mean temperature of Chichijima is 24.2 °C with the minimum temperature of 20.0 °C in winter (Fig. 1-6). On the other hand, as Tahiti locates in the southern rim of the WPWP, the temperature stays high through the year: the annual mean temperature is 27.4 °C and the seasonal variation is only 2.4 °C (Fig. 1-6). These islands lie in water whose temperature is over 18 °C, that is the distribution limit of *Porites* coral (Fallon et al., 1999). As a result, a cessation of *Porites* coral growth in the coldest season has never been documented (e.g., Chichijima, Felis et al., 2009; Tahiti, Cahyarini et al., 2009).

The Intertropical Convergence Zone (ITCZ) lying several degrees north of the equator brings heavy rain in the regions (Schneider et al., 2014). As a result, the lowest surface salinity in the tropical-subtropical Pacific is observed right bellow the ITCZ (Fig. 1-6) (Talley et al., 2011). Although the amplitude of the meridional ITCZ migration over the equatorial Pacific is small compared to the one over continents, it

migrates towards the warmer hemisphere seasonally: The ITCZ migrates northward ($\sim 9^\circ\text{N}$) in the boreal summer and southward ($\sim 2^\circ\text{N}$) in the austral summer (Schneider et al., 2014). The ITCZ drives the Hadley circulation in the troposphere, and its descending flow of dry air causes the aridification around subtropical regions. It yields positive evaporation-precipitation balances, and thus salinity increases in the subtropical surface water. This is why there exists the salinity maximum near the centers of the subtropical gyre in the North and South Pacific (Fig. 1-6). Another southward branch of rain band stretching towards Tahiti is called the South Pacific Convergence Zone (SPCZ, Fig. 1-6). Although it is the largest rain band in the southern hemisphere (Vincent, 1994), it has a slight influence on salinity variations in Tahiti. In Tahiti, SST is under influences from the WPWP, but salinity is neither affected by the ITCZ nor the SPCZ. The ITCZ also has a strong influence on Southeast Asian monsoon. In summer when the ITCZ migrates northward along the east coast of Eurasian Continent, it brings a heavy rain to the eastern Asia including the southern Japan. Dilution of surface seawater caused by freshwater influx from the surrounding continents is probably a reason why the north subtropical gyre shows the lower salinity than the south subtropical gyre (Fig. 1-6).

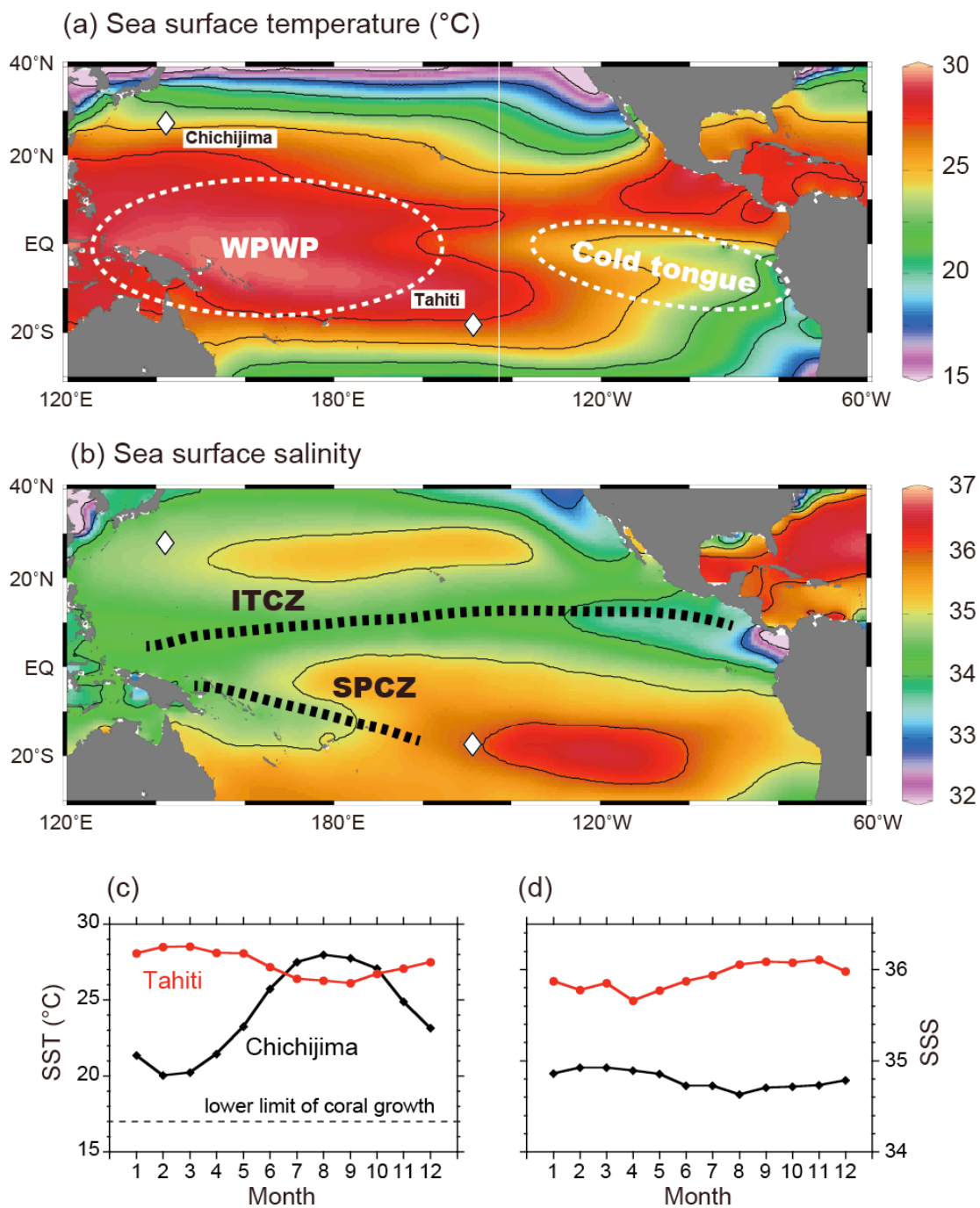


Fig. 1-6. (a,b) Climatological mean sea surface temperature and salinity. Data is from World Ocean Atlas 2009 downloaded via <http://odv.awi.de/en/data/> and plotted using Ocean Data View software version 4.6.2 (Schlitzer, 2014). WPWP, Western Pacific Warm Pool; ITCZ, Intertropical Convergence Zone; SPCZ, South Pacific Convergence Zone. (c,d) Monthly mean sea surface temperature and salinity at Chichijima and Tahiti.

1-3-2. Ocean current

The two islands locate within the subtropical gyre in both hemispheres. The North Equatorial Current (NEC) brings warm, nutrient-poor tropical water to the western Pacific. At $\sim 15^{\circ}\text{N}$, NEC splits into the western boundary current, the Kuroshio Current (Fig. 1-7). Kuroshio flows northward along the continental shelf of East Eurasia Continent, and turns its direction eastward at $\sim 30^{\circ}\text{N}$ to flow along the south coast of Japan. On the other hand, the South Equatorial Current (SEC) constitutes a northern rim of the subtropical gyre in the South Pacific. Because the SEC extends across the equator, the South Pacific subtropical gyre is more directly connected to the equator than the northern counterparts (Fig. 1-7) (Talley et al., 2011). Between the NEC and the SEC, there exists the Equatorial Counter Current (ECC) that flows eastward. Right below the equator, there exists one of the strongest oceanic current in the world, the Equatorial Undercurrent (EUC) that flows eastward along the thermocline (Talley et al., 2011).

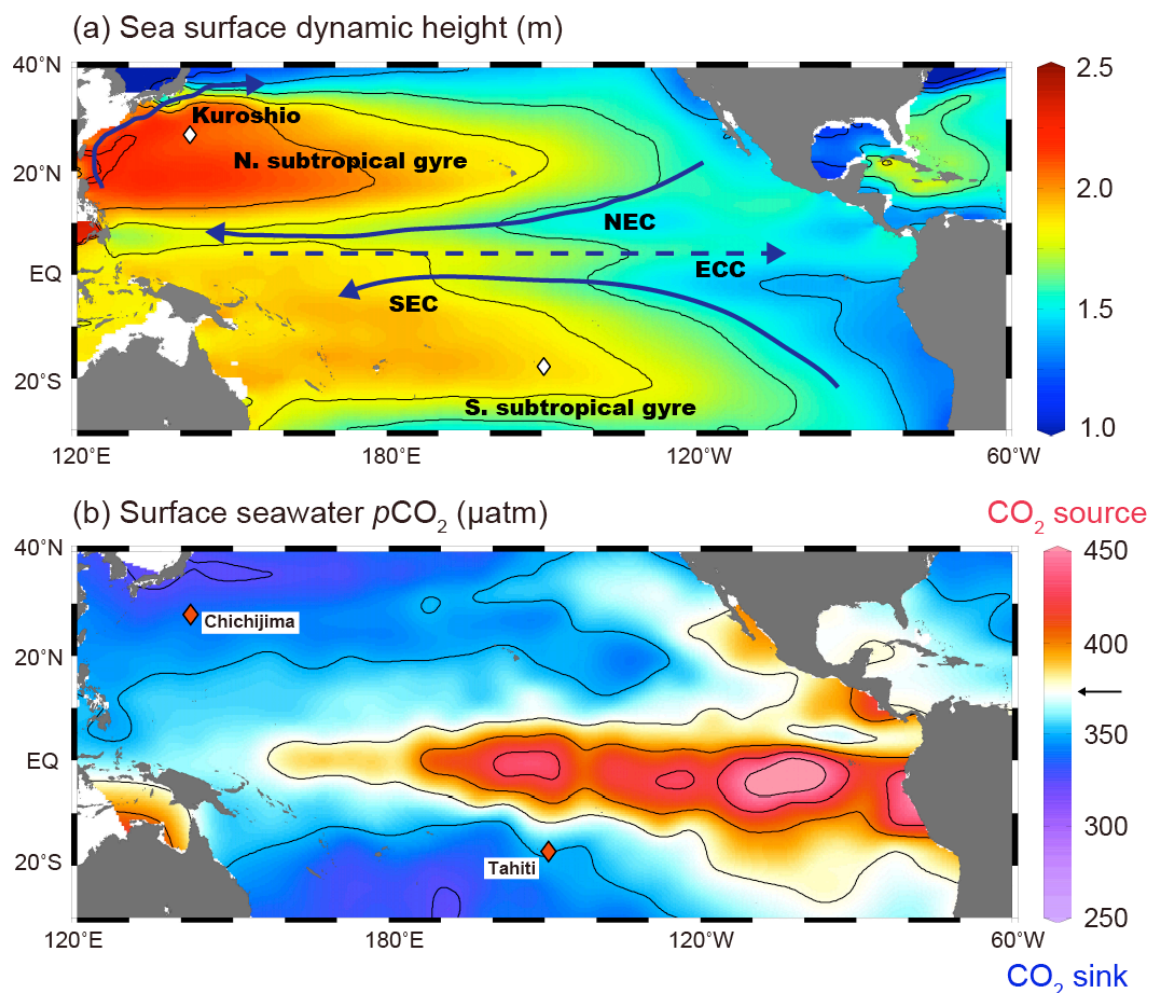


Fig. 1-7. (a) Climatological mean sea surface dynamic height (in units of m relative to the 1,000 m level) with arrows showing major surface ocean currents. Data source is “World Ocean Atlas 2009 > annual”. NEC, North Equatorial Current; ECC, Equatorial Counter Current; SEC, South Equatorial Current. (b) Distribution of surface seawater $p\text{CO}_2$ in the tropical-subtropical Pacific for the reference year AD 2000 (Takahashi et al., 2009). Arrow indicates atmospheric $p\text{CO}_2$ in 2000 (369.5 μatm). Red and blue colors represent CO_2 sources and sinks, respectively. Data source is “LDEO_Database_V2010 > Gridded_sumflax_2006c”. Both data were downloaded via <http://odv.awi.de/en/data/> and plotted using Ocean Data View software version 4.6.2 (Schlitzer, 2014).

1-3-3. Surface $p\text{CO}_2$ distribution and CO_2 source versus sink

The equatorial Pacific is currently the largest CO_2 “source” in the world as indicated by higher $p\text{CO}_2$ values than the atmospheric $p\text{CO}_2$ (Fig. 1-7) (Takahashi et al., 2009; Gruber et al., 2009; Sarmiento & Gruber, 2006). The direction and magnitude of CO_2 flux is mainly controlled by $p\text{CO}_2$ difference in the air-sea interface (e.g., Takahashi et al., 2009). The equatorial upwelling brings the nutrient- and DIC- rich cold subsurface water to the surface, which results in enhanced biological productivities. CO_2 outgassing from the sea to the air occurs, because biological carbon drawdown in the surface is insufficient due to a shortage of micronutrients such as iron (c.f., high-nutrient low-chlorophyll region; Sarmiento & Gruber, 2006). Seawater CO_2 chemistry in the equatorial upwelling region shows stochastic variabilities in seasonal to decadal timescales (e.g., Sutton et al., 2014; Feely et al., 2006, 2002).

On the contrary, the surface seawater in the subtropical gyre in both hemispheres are the modest CO_2 “sink” as characterized by the lower $p\text{CO}_2$ than the atmospheric $p\text{CO}_2$ (Fig. 1-7) (Ishii et al., 2011, 2001; Dore et al., 2009; Takahashi et al., 2009; Gruber et al., 2009; Sabine et al., 2004). In boreal summer, the surface water in the western North Pacific (Chichijima) becomes a weak source of CO_2 (Ishii et al., 2001; 2011), but this is not the case for that surrounds Tahiti in austral summer, namely Tahiti is a CO_2 sink throughout the year (Kubota et al., 2014). As a deep thermocline inhibits incorporations of subsurface nutrient, the surface seawater surrounding these islands is oligotrophic and can hardly sustain active biological productivities (e.g., Kubota et al., 2014; Ishii et al., 2011, 2001; Midorikawa et al., 2012, 2010). Therefore, the dominant driver of pH_{SW} and $p\text{CO}_{2\text{SW}}$ variability is the seasonal SST around the area (Kubota et al., 2014; Ishii et al., 2011; 2001).

1-4. Carbon cycle since the last glacial period

Although the direct atmospheric observation of atmospheric CO₂ only became possible after AD 1958 (Tans & Keeling, 2014), Antarctic ice and firn cores have recorded atmospheric $p\text{CO}_2$ ($p\text{CO}_{2\text{ atm}}$) fluctuations in the past (Fig. 1-8) (Marcott et al., 2014; Rubino et al., 2013; Lourantou et al., 2010; Lüthi et al., 2008). EPICA Dome C ice core has offered the longest $p\text{CO}_{2\text{ atm}}$ records over the last 800 thousand years before AD 1950 (ka BP) (Lüthi et al., 2008). In the eastern equatorial Atlantic, the $\delta^{11}\text{B}$ of the fossil planktonic foraminifer in the marine sediment core showed that surface seawater pH and $p\text{CO}_2$ (pH_{SW} and $p\text{CO}_{2\text{ SW}}$) fluctuations synchronized with $p\text{CO}_{2\text{ atm}}$ over the last 800 ka BP (Hönisch et al., 2009; Hönisch & Hemming, 2005). The $\delta^{11}\text{B}$ measurements of planktonic foraminifer further extended their records back to 2.1 million years ago (Ma), and they showed that $p\text{CO}_{2\text{ atm}}$ periodically fluctuated between 180 and 300 μatm coinciding with global ice sheet retreats and advances (Hönisch et al., 2009). Given that excellent correspondences between the peaks of $p\text{CO}_{2\text{ atm}}$ and ice-sheet volume, it is reasonable to think that the relationship has continued over the entire Quaternary (since 2.81 Ma). Therefore, the current $p\text{CO}_{2\text{ atm}}$ level ($\sim 400\ \mu\text{atm}$) is not only much higher than that of the late Holocene ($\sim 280\ \mu\text{atm}$) but also that of the Quaternary (Fig. 1-8), and may be so over the last 25 Ma (Beerling & Royer, 2011). Furthermore, the rate of modern $p\text{CO}_{2\text{ atm}}$ increase is unprecedentedly higher than that from other periods over the Cenozoic (65 Ma).

To study the carbon cycle for the last ~ 50 ka (constrained by half-life of radiocarbon and detection limit of the measurement), radiocarbon can be used as a tracer that travels from the stratosphere to the deepsea sediments. In the modern ocean, the oldest seawater, age of $\sim 2,000$ years, exists in the deep Pacific Ocean while the average of global surface seawater is ~ 400 years. Another important tracer studying carbon cycle is stable carbon isotope ($\delta^{13}\text{C}$). In general, $\delta^{13}\text{C}$ of DIC ($\delta^{13}\text{C}_{\text{DIC}}$) of the deep seawater has lighter value than that of the surface seawater because sinking particles that are remineralized in the deep sea have lighter $\delta^{13}\text{C}$, too (Sarmiento & Gruber, 2006). The sinking particles (marine snow) originate from phytoplanktons living in the surface layer of the ocean. As phytoplanktons selectively incorporate lighter carbon isotope into their bodies, the biological pump transports more ^{12}C than ^{13}C to the deep sea. Therefore the deep seawater that is isolated from the atmosphere for a long time tends to

be older and have lighter $\delta^{13}\text{C}_{\text{DIC}}$. As a result, modern Pacific deep water has older ages and has lighter $\delta^{13}\text{C}_{\text{DIC}}$ than those of the Atlantic deep water, as the former and the latter is respectively an exit and an entrance of the global conveyor belt of the seawater (Schmittner et al., 2013; Sarmiento & Gruber, 2006; Broecker & Peng, 1992).

In the following section we will introduce carbon cycles from two recent periods during the Quaternary, "the last deglaciation" and "after the Industrial Revolution", when the earth experienced the rapid increases of $p\text{CO}_2_{\text{atm}}$ through natural and human activities. These two $p\text{CO}_2_{\text{atm}}$ increases occurred in totally different mechanisms (Fig. 1-9). During the last deglaciation, $p\text{CO}_2_{\text{atm}}$ increased as a result of redistribution of carbon among major reservoirs (e.g., deep seawater, terrestrial biomass, and the atmosphere). As $p\text{CO}_2_{\text{atm}}$ increased from 180 to 280 μatm during the last deglaciation, $p\text{CO}_2$ and DIC of the surface layer of the ocean increased, too (Figs. 1-8 & 1-9). TA was probably higher (by $\sim 80 \mu\text{mol/kg}$) during the LGM because the salinity was $\sim 1.2 \text{ g/kg}$ higher as a result of increased freshwater storage on land (e.g., Adkins et al., 2002). Since the Industrial Revolution, on the other hand, anthropogenic CO_2 has entered into the surface layer of the ocean from the atmosphere, causing DIC increases. The time scale of the CO_2 addition is so fast that the ocean has not reached to the steady state. It is noteworthy that TA remains unchanged since the Industrial Revolution because CO_2 invasion against the ocean does not influence TA (e.g., Zeebe & Wolf-Gradlow, 2001) (Fig. 1-9).

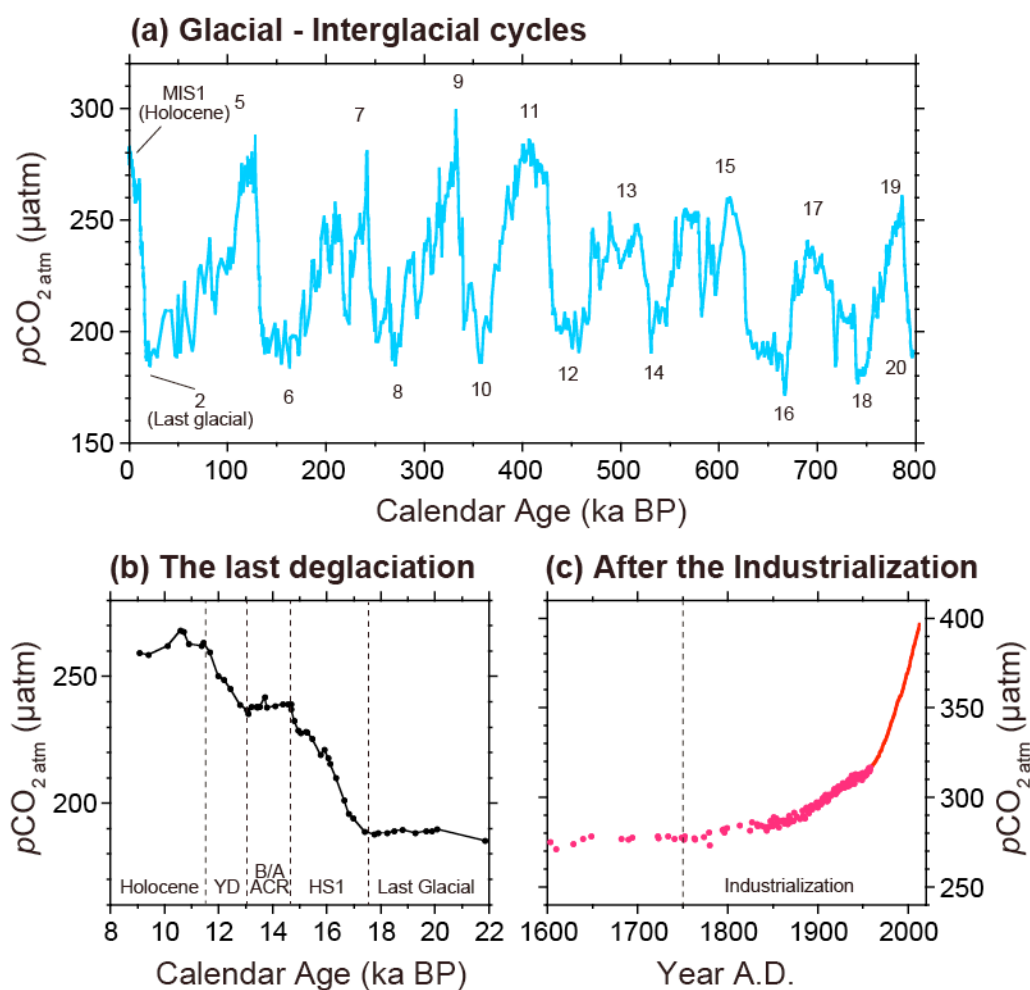


Fig. 1-8. Variations of $p\text{CO}_{2\text{ atm}}$ in three different time-windows. **(a)** $p\text{CO}_{2\text{ atm}}$ records of Antarctic ice core (Lüthi et al., 2008). $p\text{CO}_{2\text{ atm}}$ varied cyclically: $\sim 280\ \mu\text{atm}$ during interglacial and $\sim 180\ \mu\text{atm}$ during glacial periods. Marine Isotope Stages (MIS) are given in Arabic numerals. **(b)** As **a**, but higher resolution records during the last deglaciation (Lourantou et al., 2010). $p\text{CO}_{2\text{ atm}}$ increased by $\sim 50\ \mu\text{atm}$ during HS1 and $\sim 30\ \mu\text{atm}$ during the YD. HS1, Heinrich Stadial 1; B/A, Bolling/Allerod; ACR, Antarctic Cold Reversal; YD, Younger Dryas. **(c)** $p\text{CO}_{2\text{ atm}}$ during 1959–2013 are measured at the Mauna Loa Observatory in Hawaii (red) (Tans & Keeling, 2014) and those prior to 1959 are reconstructed records from Antarctic ice core (magenta) (Rubino et al., 2013). After the Industrial Revolution $p\text{CO}_{2\text{ atm}}$ increased by $120\ \mu\text{atm}$ and reached to $400\ \mu\text{atm}$ nowadays.

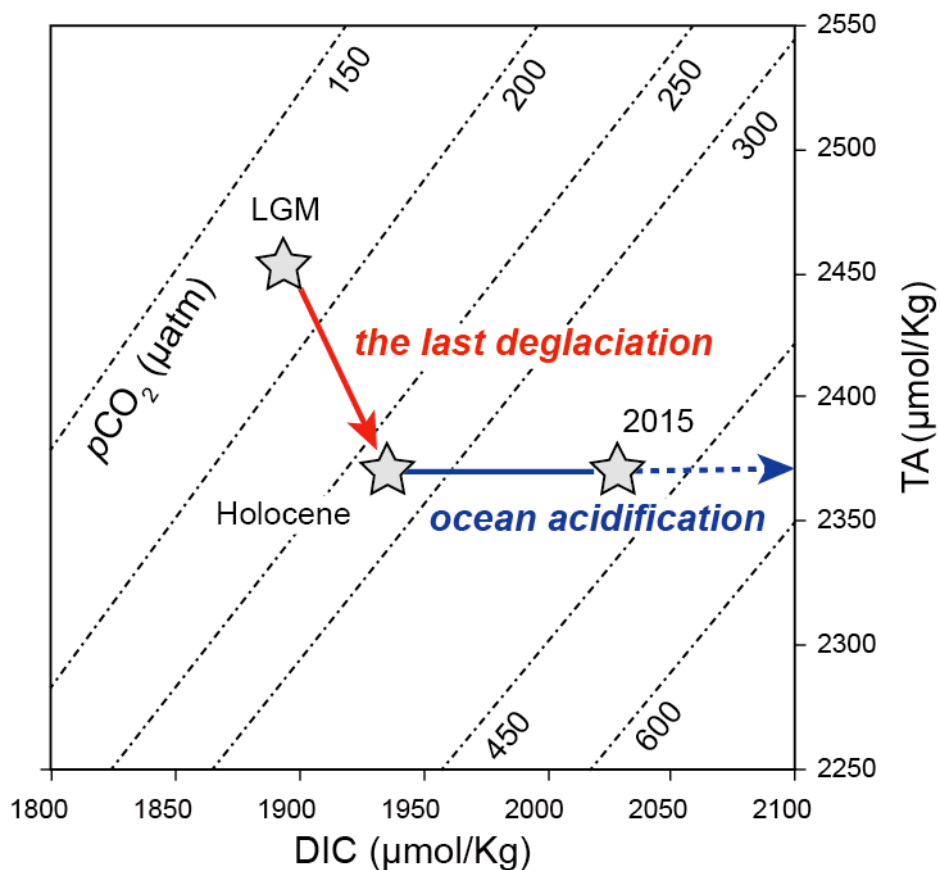


Fig. 1-9. A DIC-TA plot of the surface seawater that is well ventilated with the overlying atmosphere. The calculation was made using salinity and temperature of 35.9 and 27.1 °C (climatological values of Tahiti). TA is 2360 $\mu\text{mol/kg}$ at present and was by ~ 80 $\mu\text{mol/kg}$ higher during the LGM. The LGM DIC was calculated from $p\text{CO}_2$ $_{\text{sw}}$ of 180 μatm and the LGM TA. Since the Industrial Revolution, the anthropogenic CO_2 addition have caused DIC increases while keeping TA constant (ocean acidification).

1-4-1. The last deglaciation

Physical and biogeochemical dynamics in the Southern Ocean surrounding Antarctica has proposed to play a central role to control glacial - interglacial $p\text{CO}_2_{\text{atm}}$ fluctuations, because carbon reservoirs in the ocean is ~60 times as large as that of the atmosphere (e.g., [Martínez-García et al., 2014](#); [Schmitt et al., 2012](#); [Sigman et al., 2010](#), [Sarmiento & Gruber, 2006](#)). The hypothetical carbon stored in the glacial ocean is called "glacial abyssal carbon reservoir". In fact, the existence of extremely aged (depleted in ^{14}C) seawater has been reported through analyzing fossil benthic foraminifer and deepsea corals' skeletons in the last glacial Southern Ocean ([Burke & Robinson, 2012](#); [Rose et al., 2010](#); [Skinner et al., 2015, 2009](#)).

During the last deglaciation, climatic shifts from the last glacial to the present interglacial, $p\text{CO}_2_{\text{atm}}$ increased by ~50 μatm during Heinrich Stadial 1 (HS1, 17.5–14.6 ka BP), followed by additional ~30 μatm during the Younger Dryas (YD, 12.9–11.5 ka BP) (Fig. 1-8). During HS1 and the YD, both $\delta^{13}\text{C}$ of atmospheric CO_2 ($\delta^{13}\text{C}_{\text{atm}}$) and decay-corrected radiocarbon concentration of atmospheric CO_2 ($\Delta^{14}\text{C}_{\text{atm}}$) decreased. This supports the hypothesis that the stored carbon in the glacial ocean returned to the atmosphere during these periods (e.g., [Schmitt et al., 2012](#); [Skinner et al., 2010](#); [Marchitto et al., 2007](#); [Spero & Lea, 2002](#)). Similarities seen between Antarctic air temperatures and $p\text{CO}_2_{\text{atm}}$ strongly suggest the Southern Ocean was the most important place to control glacial - interglacial carbon cycles. To date, different mechanisms have been proposed to explain lower $p\text{CO}_2_{\text{atm}}$ during the last glacial and rapid increases in $p\text{CO}_2_{\text{atm}}$ during glacial terminations. They are included oceanography-dominant mechanisms such as oceanic and atmospheric circulations (e.g., [Kwon et al., 2012](#); [Skinner et al., 2010](#); [Anderson et al., 2009](#); [Toggweiler et al., 2006](#)), Antarctic sea ice and brine rejection feedback (e.g., [Bouttes et al., 2011, 2010](#)), biology-dominant mechanisms such as iron fertilization ([Martínez-García et al., 2014](#); [Ziegler et al., 2013](#)) and silica leakage (e.g., [Matsumoto et al., 2002](#); [Brzezinski et al., 2002](#)), and combination of them (e.g., [Sigman et al., 2010](#); [Kohfeld et al., 2005](#); [Archer et al., 2000](#); [Sigman & Boyle, 2000](#)). However, the clear explanation of $p\text{CO}_2_{\text{atm}}$ variability has been controversial (e.g., [Matsumoto & Yokoyama, 2013](#); [Thomas et al., 2009](#)).

1-4-2. After the Industrial Revolution

Since the beginning of the industrial era (AD 1750), the ocean has absorbed about one quarter of emitted CO₂ as a result of human activities; such as fossil fuel burning, land use changes, and cement production (Ciais et al., 2013; Francey et al., 2013; Le Quéré et al., 2009; Sabine et al., 2005; Key et al., 2004). The extra DIC addition has disturbed the seawater CO₂ chemistry by lowering pH_{SW} and CO₃²⁻ concentrations (Fig. 1-9). This is the phenomenon so-called "ocean acidification" (OA). In the present surface layer of the ocean, pH_{SW} is 8.1 on average, which is a weak alkaline. Thus, OA means that ocean becomes more acidic, not acid liquid (pH < 7). pH_{SW} has decreased by ~0.1 after the Industrial Revolution as most surface seawater is a CO₂ sink (Doney et al., 2014; Gattuso & Hansson, 2011; Feely et al., 2009; Tans et al., 2009; Sabine et al., 2005; Key et al., 2004). This is especially evident that in the North Atlantic Ocean and the Southern Ocean, where deep and intermediate water formations and vigorous biological primary production occur, absorbed CO₂ is efficiently transported into the subsurface (Sallée et al., 2012; Ito et al., 2010; Gruber et al., 2009; Sabine et al., 2004). A large fraction of absorbed CO₂ currently distributes in the interior of the South Pacific Ocean due to its large surface area for air-sea CO₂ exchange and production of Subantarctic Mode Water (SAMW) and Antarctic Intermediate Water (AAIW) that subduct along the pycnocline south of 30 °S (Sallée et al., 2012; Iudicone et al., 2011; Ito et al., 2010). Depending on the future course of CO₂ emission, pH_{SW} is anticipated to further decrease about 0.3-0.4 by the end of this century (Doney et al., 2014; Feely et al., 2009; Tans et al., 2009; Orr et al., 2005; Caldeira & Wickett, 2003).

Numerous culturing experiments conducted in aquariums with lowered pH_{SW} have suggested that many calcifying organisms such as corals, foraminifers and mollusks are generally vulnerable to OA (Hoegh-Guldberg et al., 2011; Pandolfi et al., 2011; Doney et al., 2009; Kleypas & Yates, 2009; Fabry et al., 2008; Gattuso & Hansson, 2008; Orr et al., 2005). This phenomenon is supported by field observations at naturally acidified sites by volcanic CO₂ seeps such as Milne Bay (Papua New Guinea), Iwotorishima (Japan), and Ischia (Italy) that acidified seawater eliminates calcifying organisms and leads to proliferation of non-calcifying organisms such as softcoral and macroalgae (e.g., Inoue et al., 2013; Fabricius et al., 2011; Hall-Spencer et al., 2008).

Due to isotopic dilution by ¹²C-enriched CO₂ emitted from fossil fuel burning and

deforestation, $\delta^{13}\text{C}_{\text{atm}}$ is decreasing since the Industrial Revolution with an observed acceleration after 1960 (Rubino et al., 2013; Francey et al., 1999). In the same reason outlined in the previous section, burning of fossil fuel and terrestrial biomass will produce lighter $\delta^{13}\text{C}_{\text{atm}}$ as they are ^{12}C -rich. The phenomenon is called " ^{13}C Suess effect" named after its discoverers (Revelle & Suess, 1957). $\delta^{13}\text{C}_{\text{DIC}}$ of surface layers of the oceans is also decreasing (Schmittner et al., 2013; Keeling et al., 2004; Quay & Stutsman, 2003; Quay et al., 2003, 1992; Gruber et al., 1999). As calcifying organisms that live in the surface layer of the oceans utilize oceanic carbon to secrete their CaCO_3 skeleton, it is also decreasing at a similar rate with $\delta^{13}\text{C}_{\text{atm}}$ depending on regional efficiency of CO_2 ventilation (Dassié et al., 2013; Swart et al., 2010; Nozaki et al., 1978).

Fossil fuel-derived carbon is depleted in ^{14}C ("dead" carbon) because millions of years have passed since petroleum and coal was produced. In addition to $\delta^{13}\text{C}_{\text{atm}}$, ^{14}C in atmospheric CO_2 , ^{14}C in DIC, and ^{14}C in living organisms are decreasing faster than the decay rate since the beginning of the industrial era (Druffel, 2002; Nozaki et al., 1978). This phenomenon is called " ^{14}C Suess effect" distinguishing it from the ^{13}C Suess effect (Nozaki et al., 1978). After the 1960s, the ^{14}C Suess effect has been overwhelmed by anthropogenic ^{14}C pollution caused by nuclear tests (bomb ^{14}C) (Grottoli & Eakin, 2007; Druffel, 2002; Nozaki et al., 1978).

1-5. Research objectives and thesis structure

The boron isotopes ($\delta^{11}\text{B}$) are the most promising proxy to estimate atmospheric $p\text{CO}_2$ prior to 800 ka BP and to understand dynamic CO_2 chemistry, for example, in the coastal and upwelling regions (e.g., Kubota et al., 2014; Foster et al., 2014; Douville et al., 2010; Palmer & Pearson, 2003). However, there are no $\delta^{11}\text{B}$ - pH_{SW} calibrations using long-lived corals collected in the natural environment. The needs to establish a field-based calibration equation is that culturing-based calibrations can hardly reconstruct reasonable pH_{SW} that is in line with observations of seawater CO_2 chemistry (discussed in detail in Chapter 2). There are many regions where we can estimate pH_{SW} time-series through simple calculations of CO_2 chemistry with aid of previous efforts to reconstruct atmospheric CO_2 level and to estimate anthropogenic CO_2 absorption by the ocean. In such regions past $\delta^{11}\text{B}$ variations of long-lived corals should be calibrated with already-known pH_{SW} rather than be used to reconstruct pH_{SW} .

The primary objective of this thesis is to obtain a field-based $\delta^{11}\text{B}$ - pH_{SW} calibration. Firstly a methodology to obtain an empirical $\delta^{11}\text{B}$ - pH_{SW} equation for massive *Porites* corals collected at Chichijima and Tahiti will be introduced (Chapter 2). pH_{SW} variations since the Industrial Revolution are estimated from atmospheric $p\text{CO}_2$ records, because air-sea $p\text{CO}_2$ differences ($\Delta p\text{CO}_2$) has been kept constant around these islands. Secondly, changes of pH_{CF} of Chichijima coral (estimated from $\delta^{11}\text{B}$ based on the pH up-regulation) will be discussed, highlighting effects of OA on calcification in particular (Chapter 3). Thirdly, the empirical $\delta^{11}\text{B}$ - pH_{SW} calibration for Tahiti obtained in Chapter 2 will be applied to $\delta^{11}\text{B}$ of fossil *Porites* corals in order to reconstruct pH_{SW} and $p\text{CO}_2_{\text{SW}}$ during the last deglaciation (Chapter 4). Lastly, the key findings of this thesis will be summarized, and future avenues for this research will be suggested (Chapter 5).

CHAPTER 2

Boron isotopes - pH calibration using long-lived modern corals

Chapter 2 Abstract

Boron isotopes ($\delta^{11}\text{B}$) of marine biogenic carbonates can reconstruct pH_{SW} , $p\text{CO}_2_{\text{SW}}$, and potentially atmospheric CO_2 concentration in the geological past. To date, $\delta^{11}\text{B}$ - pH_{SW} calibration has been proposed through culturing experiments of calcifying organisms under artificially acidified seawater. However, as for scleractinian corals, reconstructed pH_{SW} using the culture-based calibration do not agree well with seawater CO_2 chemistry observations. Thus, another approach is needed to establish a more reliable calibration. To attain the purpose, we measured a 100 year record of $\delta^{11}\text{B}$ of *Porites* coral obtained from Chichijima, Ogasawara Archipelago, Japan. Previously reported $\delta^{11}\text{B}$ values of Tahitian corals were also used after corrections of different procedure-specific isotopic offsets. We compared coral $\delta^{11}\text{B}$ records with pH_{SW} variation that was estimated from many CO_2 chemistry data and atmospheric CO_2 records, and established, for the first time, field-based calibrations for Chichijima and Tahiti. Using the established calibration, we reevaluated the previously reported two examples of pH_{SW} reconstructions from $\delta^{11}\text{B}$ of *Porites* corals obtained from Guam and Hainan islands. The results showed that empirically reconstructed pH_{SW} as well as $p\text{CO}_2_{\text{SW}}$ were more in line with CO_2 chemistry observations than those calculated using the culture-based calibration, and that the correction values were different depending on locations.

2-1. Introduction

There are two motivations to develop past seawater CO₂ chemistry proxy. Firstly, to constrain atmospheric pCO₂ and climate sensitivity of the earth during warmer periods in the past (e.g., Pliocene epoch and Paleocene-Eocene Thermal Maximum) is one of the most important research subjects in paleoclimatology, because these periods are regarded as past-analogs of increasing atmospheric CO₂ level and subsequent global warming (Beerling & Royer, 2011; Seki et al., 2009). Secondly, it is urgently required to understand natural variability of CO₂ chemistry of biogeochemically, ecologically, and economically important regions; such as, equatorial upwelling, eastern boundary current - upwelling system, coral reefs, and estuaries (Hendriks et al., 2015; Kubota et al., 2014; Gruber et al., 2012), and their future responses, vulnerabilities, and resilience to environmental pollution of CO₂ (e.g., ocean acidification).

To date, a lot of studies have reared various genera of corals under artificially acidified seawater and measured $\delta^{11}\text{B}$ of coral skeletons to understand $\delta^{11}\text{B}$ -pH_{SW} systematics (Holcomb et al., 2014; Dissard et al., 2012; Trotter et al., 2011; Krief et al., 2010; Raynaud et al., 2004; Hönisch et al., 2004) (Fig. 1-4, Table 1-3). However, it does not appear that the culture-based $\delta^{11}\text{B}$ -pH_{SW} (and pCO_{2 SW}) calibration for *Porites* corals can reconstruct reasonable pH_{SW} and pCO_{2 SW} during the last millennia (Kubota et al., 2014; Liu et al., 2014; Shinjo et al., 2013). For instance, Liu et al. (2014) calculated surface pH_{SW} from $\delta^{11}\text{B}$ of *Porites* spp. that was collected at Hainan Island (18.2°N, 109.5°E, Fig. 2-2) using a reported pH_{SW}-pH_{CF} relationship for cultured *Porites* coral (Trotter et al., 2011), but the reconstructed pH_{SW} decrease after the Industrial Revolution to the present was as much as 0.3, which is far different from the accepted value of ~0.1 (Doney et al., 2014; Gattuso & Hansson, 2011; Feely et al., 2009; Tans et al., 2009; Sabine et al., 2005; Key et al., 2004). Their reconstruction also indicated that pCO_{2 SW} in 2000 was 270 μatm when the calculation was made using TA of 2220.4 $\mu\text{mol/kg}$, SST of 26.9 °C, and SSS of 33.8, but it is unacceptably lower than the reported pCO₂ value of 360 μatm in the same year at the Southeast Asian Time-series Study (SEATS; 18°N, 116°E, Fig. 2-2) (Tseng et al., 2007). Similarly, Shinjo et al. (2013) reconstructed pH_{SW} at Guam (13.45°N, 144.76°E, Fig. 2-2) from $\delta^{11}\text{B}$ of *Porites* spp. using the same pH_{SW}-pH_{CF} relationship, but not only pH_{SW} values but also its decreasing trend, do not agree with pH_{SW} observation at the Station ALOHA

in Hawaii (Fig. 2-2) (Dore et al., 2009), although these islands are equally located inside of the north subtropical gyre and in weak CO₂ sink region (Fig. 2-1 & 2-2).

Therefore, we have to reconcile the discrepancy in order to use the $\delta^{11}\text{B-pH}_{\text{SW-pCO}_2}$ calibration in ecological and environmental studies. To establish the calibration, we employed massive *Porites* corals from Chichijima and Tahiti that live in the surface ocean with well-equilibrated atmospheric CO₂ (Fig. 2-1). Massive *Porites* corals, often used in paleoceanography, are characterized for its longevity, which means that they preserve, century-long geochemical records in their skeletons. Thus, in order to calibrate $\delta^{11}\text{B-pH}_{\text{SW}}$, we measured a 100 year record of $\delta^{11}\text{B}$ of long-lived *Porites* coral that was obtained at Chichijima and compared it with independently estimated pH_{SW} variations. In this strategy, the precision of $\delta^{11}\text{B}$ measurements are essential, because surface pH_{SW} decreases due to the anthropogenic DIC addition since the Industrial Revolution is ‘only’ ~0.1 (it is translated into ~1.0‰ in $\delta^{11}\text{B}$). As for Tahiti, as we could not obtain modern coral samples, we utilized previously published $\delta^{11}\text{B}$ values of *Porites* corals for the calibration (Douville et al., 2010; Gaillardet & Allegre, 1995).

To summarize, the purpose of this chapter is to establish the empirical $\delta^{11}\text{B-pH}_{\text{SW}}$ calibrations in order to use them in paleoclimatology and paleoceanography. In the calibration, we used a modern long-lived coral collected at Chichijima, two modern corals collected at Moorea (the west of Tahiti), and one fossil coral obtained at Marquesas (dated to 1750 AD) (Fig. 2-1). The difference of $\delta^{11}\text{B}$ values from the theoretically expected values, that is the offset a in Equation (1-14), are determined in Chichijima and Tahiti regions.

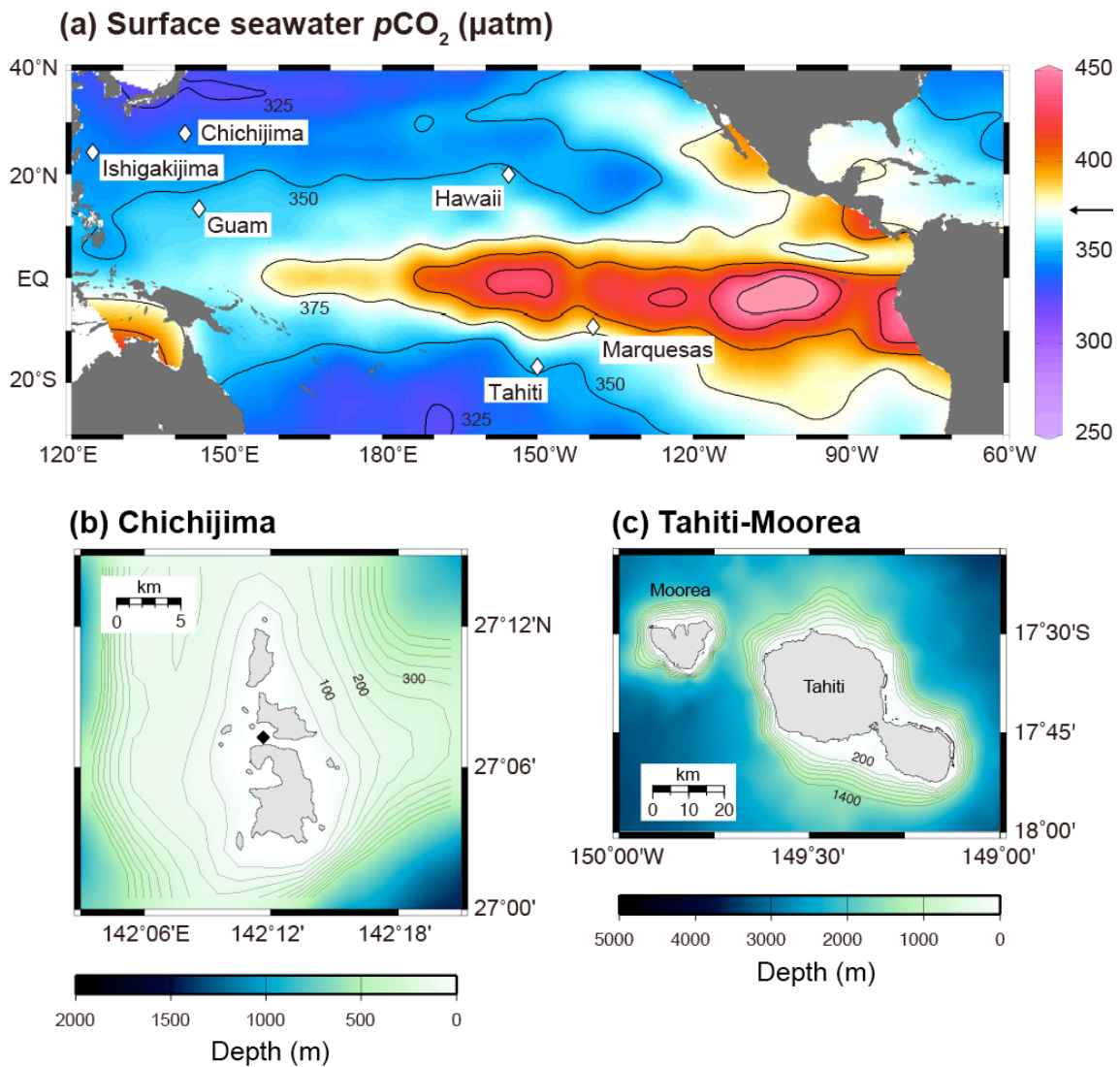


Fig. 2-1. (a) Same as **Fig. 1-7b**, but islands mentioned in this chapter are indicated in diamonds. (b,c) A bathymetric map around Chichijima and Tahiti. The modern coral of Chichijima was collected at locations well flushed with open ocean seawater (black diamond).

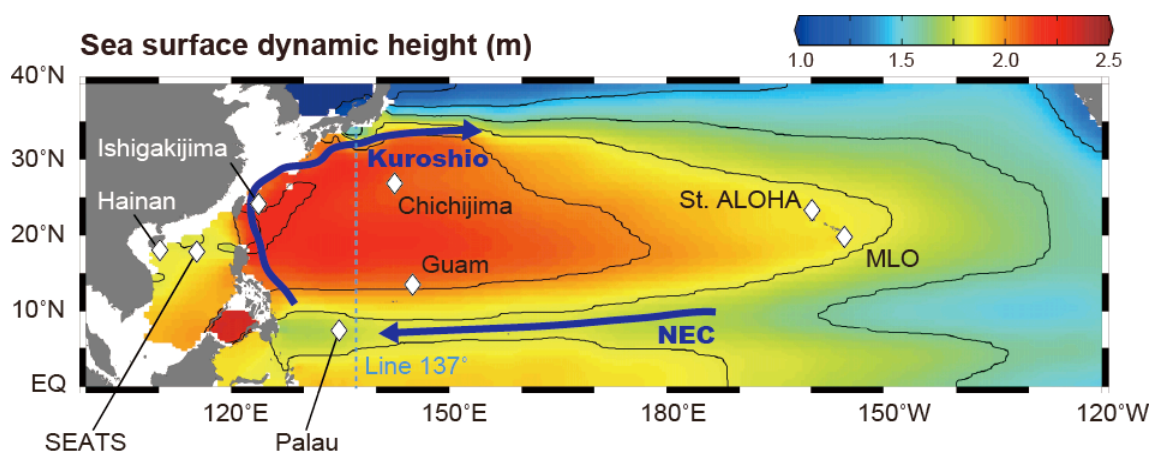


Fig. 2-2. Climatological mean sea surface dynamic height in the western North Pacific region (in units of m relative to the 1,000 m level). Blue arrows represent Kuroshio and the NEC.

2-2. Material & Methods

2-2-1. $\delta^{11}\text{B}$ measurements of Chichijima coral

A *Porites* spp. that lived in 5.6 m deep water was cored in 2002. A sampling location is not a closed environment (e.g., reef flat), but was an opened environment that receives good circulation of open ocean seawater (Fig. 2-1). This justifies the comparison of coral $\delta^{11}\text{B}$ variations with open ocean pH_{SW} . After sonification under distilled water, coral skeleton was drilled along the major growth direction and just 1-year resolution sub-samples, from 1873–2002 (one summer to the next summer) were obtained. We discarded the sub-samples from the top 4 years due to geochemical alterations (Felis et al., 2009). We also discarded those prior to 1910 because a previous study reports large climatic regime shift from 1905–1910 (Felis et al., 2009). To prepare 3-year resolution subsamples for $\delta^{11}\text{B}$ measurements (typically 3–6 mg of carbonate), we mixed the same amount of annual sample. $\delta^{11}\text{B}$ were measured using two methodologies: P-TIMS and MC-ICPMS. Ishikawa and Nagaishi (2011) reports the methodology using the P-TIMS and Tanimizu *et al.* (in prep.) reports that using the MC-ICPMS (Fig. 2-3).

For the P-TIMS method, after removing organic matter using a 30% H_2O_2 for ~12 hours, boron were purified by cation and anion exchange using AG 50W X12 and 1-X4 resin (Bio-Rad, USA). Then, cesium and mannitol were added to produce and stabilize cesium-borate complex. The solution was dried in a 60 °C oven for 12 hours. The obtained material was dissolved in distilled water and 309/308 isotopic ratio were measured using Thermo Finnigan TRITON at Kochi Institute for Core Sample Research. All reported $\delta^{11}\text{B}$ values are the average of replicate analyses (2–4 times, Table 2-1). Repeated analysis of the JCp-1 (Okai et al., 2004), homogenized powder of *Porites* coral skeleton collected at Ishigakijima (Fig. 2-1 & 2-2), yielded $24.28 \pm 0.14\text{‰}$ (2σ , $n = 14$) where boron isotopic ratios of coral samples were expressed as per mil deviations from the values of standard (NIST SRM 951):

$$\delta^{11}\text{B} = \left[\frac{(^{11/10}\text{B})_{\text{sample}}}{(^{11/10}\text{B})_{\text{std}}} - 1 \right] * 10^3$$

$$= \left[\frac{(^{309/308}\text{CS}_2\text{BO}_2)_{\text{sample}} - 0.00079}{(^{309/308}\text{CS}_2\text{BO}_2)_{\text{std}} - 0.00079} - 1 \right] * 10^3$$
(Eq. 2-1)

We used $\pm 0.14\%$ as the analytical uncertainty of $\delta^{11}\text{B}$ measurements of Chichijima coral.

For the MC-ICPMS method, the wet chemistry was the same as the P-TIMS method until the ion exchange. After the ion exchange, lithium-spike instead of caesium was added in order for the drift correction during measurements. $\delta^{11}\text{B}$ values were measured using a sample-standard bracketing routine on Thermo Finnigan NEPTUNE at Kochi Institute for Core Sample Research without replicate analysis. We used the recommended value of $\pm 0.25\%$ as the analytical uncertainty of $\delta^{11}\text{B}$ (Tanimizu et al., in prep.).

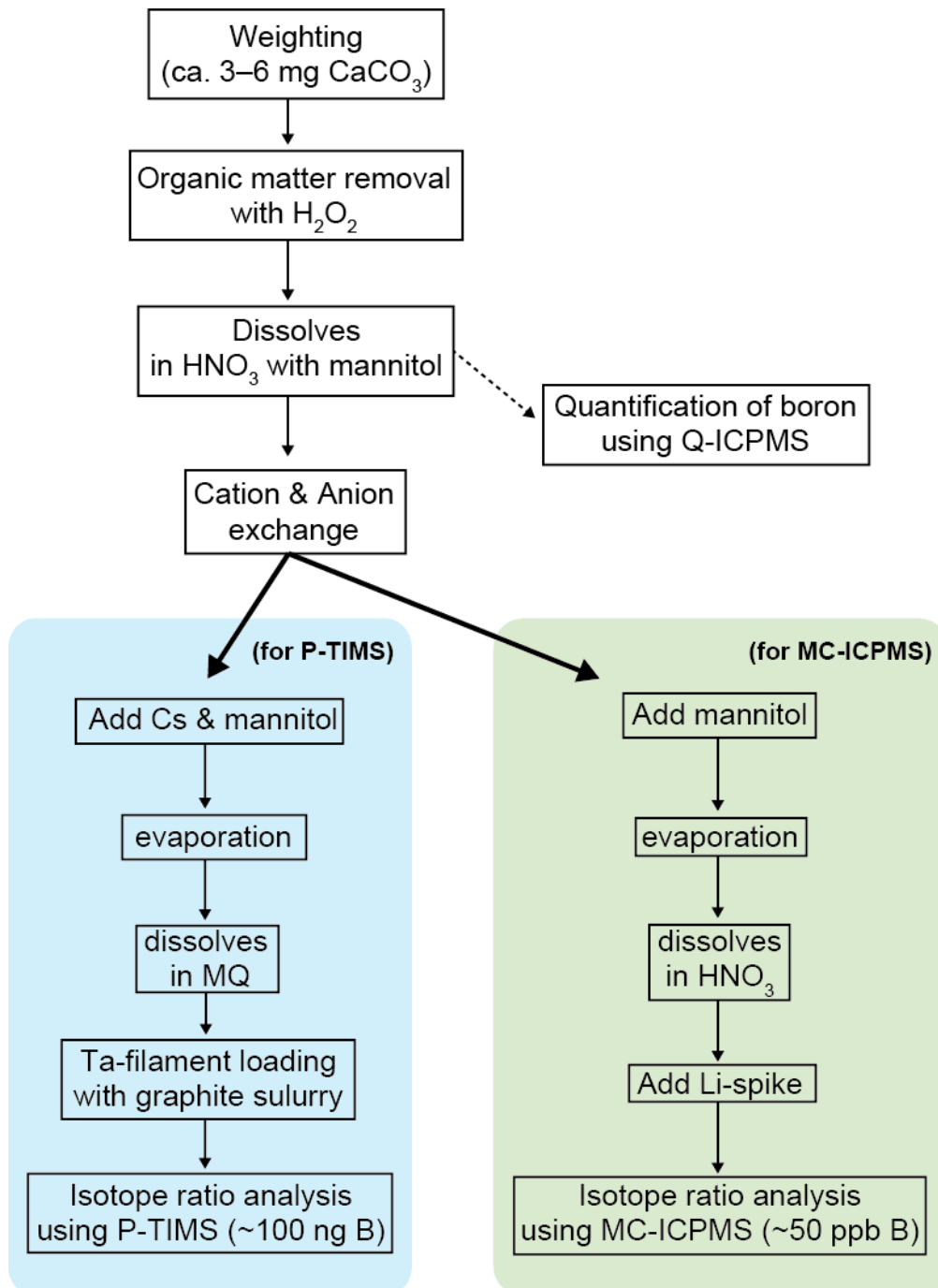


Fig. 2-3. Schematic procedures of boron isotope analyses of coral samples.

Table 2-1. Measured $\delta^{11}\text{B}$ values for Chichijima coral.

Sample name	$\delta^{11}\text{B}$ values		pH _{sw}	
	P-TIMS	MC-ICPMS		
	mean			
OGA02_3Y_1997	23.92	23.84	23.65	8.12
	23.95			
	23.71			
	23.77			
OGA02_3Y_1992	23.88	23.84	23.77	8.12
	23.81			
	23.79			
	23.87			
OGA02_3Y_1987	24.11	24.22	24.39	8.14
	24.26			
	24.30			
OGA02_3Y_1982	23.77	23.89	24.08	8.15
	23.97			
	23.92			
OGA02_3Y_1977	24.24	24.17	23.61	8.14
	24.11			
OGA02_3Y_1972	24.75	24.71	24.99	8.14
	24.69			
	24.70			
OGA02_3Y_1966	24.19	24.16	24.28	8.16
	24.13			
OGA02_3Y_1960	24.48	24.43	24.47	8.16
	24.44			
	24.37			
OGA02_3Y_1954	24.59	24.56	24.57	8.15
	24.54			
OGA02_3Y_1948	24.24	24.28	24.48	8.16
	24.31			

Continued

OGA02_3Y_1942	24.29	24.28	24.75	8.17
	24.26			
OGA02_3Y_1935	24.39	24.38	24.40	8.17
	24.38			
OGA02_3Y_1928	24.86	24.76	25.02	8.18
	24.72			
	24.71			
OGA02_3Y_1921	24.13	24.06	23.87	8.18
	24.03			
	24.01			
OGA02_3Y_1914	24.26	24.41	24.33	8.18
	24.53			
	24.43			

2-2-2. $\delta^{11}\text{B}$ values of Tahiti and Marquesas corals

In the $\delta^{11}\text{B}$ - pH_{SW} calibration We also used previously reported $\delta^{11}\text{B}$ values of corals that were obtained from Moorea, the west of Tahiti, and Marquesas (Fig. 2-1) (Douville et al., 2010; Gaillardet & Allegre, 1995). As these values are determined by different analytical procedures, firstly we corrected the analytical procedure-specific isotopic offset (Foster et al., 2010) using Equation (1-11). We used the recommended value of 39.61‰ for $\delta^{11}\text{B}_{\text{SW-stacked}}$ (Foster et al., 2010).

2-2-3. pH_{SW} estimation since 1970

Long-term pH_{SW} monitoring sites do not exist in the tropical-subtropical Pacific, except for the Station ALOHA (Dore et al., 2009) and the repeat hydrographic line at 137°E by Japanese Meteorological Agency (JMA) (e.g., Midorikawa et al., 2012, 2010; Ishii et al., 2011, 2001). Thus we estimated pH_{SW} variations from sporadic seawater CO_2 chemistry data that have been measured in the open ocean through research cruises. There are many international programs that measured various CO_2 chemistry parameters (i.e., DIC, TA, pH, $p\text{CO}_2$, and $f\text{CO}_2$), and the combined data to understand horizontal and vertical distributions, temporal variation, and amount of anthropogenic CO_2 incorporation by the ocean (e.g., WOCE, World Ocean Circulation Experiment; JGOFS; Joint Global Ocean Flux Study; GEOSECS, Geochemical Ocean Sections program; CLIVAR, Climate Variability and Predictability Project). In such efforts, the data compilation by Surface Ocean Carbon Atlas (SOCAT) has large and quality-controlled data sets of $f\text{CO}_2$ measurements in the open ocean surface layer. This data set is suitable for the purpose of this thesis because *Porites* corals live in the surface ocean in order to obtain sunlight for photosynthesis. Hence, in this thesis, we used SOCAT $f\text{CO}_2$ data (version 2, Bakker et al., 2014) to estimate pH_{SW} variation at Chichijima, Hawaii, Tahiti, and Marquesas. We extracted the data using 1.0° latitude by 5.0° longitude grids centered on Chichijima and Hawaii. As for Tahiti and Marquesas, we enlarged the grids (5° latitude by 10° longitude) to extract the data, because $f\text{CO}_2$ data is less abundant in the South Pacific and the equatorial Pacific than in the North Pacific. In the calculation, we used ancillary *in situ* data of SST and SSS to each $f\text{CO}_2$ data-point. For grid points where SSS data was not available, we imported

climatological salinity values from the World Ocean Atlas 2005. We estimated TA from TA-SSS relationships from Midorikawa *et al.* (2010) for Chichijima and Kutchinke *et al.* (2014) for Hawaii, Tahiti, and Marquesas, respectively:

$$TA = nTA * SSS / 35 = 2295 * SSS / 35 \quad (\text{Eq. 2-2, Midorikawa et al., 2010})$$

$$TA = 2300 + 66.3 * (SSS - 35) \quad (\text{Eq. 2-3, Kuchinke et al., 2014})$$

Midorikawa *et al.* (2010)'s relationship is based on continuous TA and SSS measurements by JMA at the 137°E line and Kuchinke *et al.* (2014)'s one is based on the compilation of discrete TA and SSS data by GLODAP and CLIVAR. We calculated DIC from fCO_2 and assuming TA using CO2Calc software (version 1.0, Robins *et al.*, 2010). Then we normalized DIC at a salinity of 35 (nDIC), and fitted it to an empirical function of the timing of measurement (year), SST, and SSS by multi-parameter regression (See Ishii *et al.* (2011) for detail):

$$\begin{aligned} nDIC &= DIC * 35 / SSS \\ &= f(yr, SST, SSS) \\ &= C_0 + C_1 * yr + C_2 * temp + C_3 * temp^2 + C_4 * temp^3 + C_5 * sal + \varepsilon \end{aligned} \quad (\text{Eq. 2-4})$$

Here $yr = \text{year} - 1994$, $temp = SST - T_{ave}$, and $sal = SSS - S_{ave}$. Average temperature (T_{ave}) and salinity (S_{ave}) was separately specified for Chichijima, Hawaii, Tahiti, and Marquesas (Table 2-2). The terms $C_0 \sim C_5$ are coefficients of multiple regressions, and ε represents the residual of the fitting (Table 2-2). The polynomial of $temp$ in the equation exhibits strong correlation with nDIC and SST (Ishii *et al.*, 2011).

Table 2-2. Parameters of multi-regression analysis.

Parameter	Location			
	Chichijima	Hawaii	Tahiti	Marquesas
C_0	1958.7	1965.9	1934.3	1961.7
C_1	1.15	1.22	0.76	1.07
C_2	-2.22	-3.49	-4.9	-17.5
C_3	0.30	0.76	0.53	-1.44
C_4	-0.05	-0.56	0.26	-2.32
C_5	-12.0	-13.5	1.51	-52.5
T_{ave} ($^{\circ}C$)	24.7	25.0	27.4	27.9
S	34.5	35.0	35.9	35.6
RMSE	6.7	5.8	5.5	7.4
R^2	0.74	0.58	0.54	0.84
N	1034	11205	1440	4314

2-2-4. pH_{SW} estimation since the Industrial Revolution

High-precision seawater CO₂ chemistry measurements are limited to the past 40 years, and Equation (2-4) can overestimate preindustrial pH_{SW} (e.g., preindustrial pH_{SW} at Tahiti is equivalent to ~8.45, [Kubota et al., 2014](#)) because of an assumption that nDIC increased linearly with time. Thus we extended pH_{SW} estimation prior to the Industrial Revolution using atmospheric *p*CO₂ records from a continuous observation at the Mauna Loa Observatory (MLO) and air trapped in the Antarctic ice sheet ([Tans & Keeling, 2014](#); [Rubino et al., 2013](#)). We used the method modified from Tans (2009), which uses an empirical pH_{SW} estimation equation based on atmospheric *p*CO₂, taking into account the reaction of borate with anthropogenic CO₂:

$$\text{pH}_{\text{SW}} = \text{pH}_{\text{pre-industrial}} - b * \log\left(\frac{p\text{CO}_{2\text{atm}}}{280}\right) \quad (\text{Eq. 2-5})$$

2-3. Results & Discussion

2-3-1. Comparison of $\delta^{11}\text{B}$ values measured in different methods

Firstly, we compared $\delta^{11}\text{B}$ variation measured by two methodologies: P-TIMS and MC-ICPMS (Fig. 2-4). Both records showed relatively steady values until 1966, and then decreased. It is consistent with the prediction that ocean acidification accelerated after 1960 reflecting atmospheric CO_2 level (Rubino et al., 2013; Francey et al., 1999; Etheridge et al., 1996). A cross-plot reveals that the relationship is not necessarily one to one (Fig. 2-4). Tanimizu *et al.* (in prep) points out that $\delta^{11}\text{B}$ value measured by the MC-ICPMS is systematically, $\sim 0.1\text{‰}$ higher than that measured by the P-TIMS. It is consistent with the fact that measured $\delta^{11}\text{B}$ values of JCp-1 in this thesis was 24.36‰ (2σ , $n = 4$), 0.08‰ higher than that measured by the P-TIMS ($24.28 \pm 0.14\text{‰}$, 2σ , $n = 14$). However, after correcting the offsets, a slight discrepancy between them still remains (Fig. 2-4). There is a possibility that discrepancy may be related to (1) heterogeneity of prepared subsample and (2) isotopic fractionation during the P-TIMS measurements due to isobaric ions interference derived from organic matter in the coral skeleton (Wu et al., 2012; Ishikawa & Nagaishi, 2011), or a combination of the two. To identify the reason for this discrepancy is an important future research theme, but it is beyond the scope of this thesis. In addition, $\delta^{11}\text{B}$ variation measured by the MC-ICPMS has larger amplitude than that measured by the P-TIMS. As we did not replicate $\delta^{11}\text{B}$ measurements and precision of the MC-ICPMS method is at present worse than the P-TIMS method, we will discuss the P-TIMS data only in the following sections and Chapter 3. $\delta^{11}\text{B}$ variation measured by the P-TIMS showed no statistically significant trend from 1907 to 1960, but showed statistically significant decreasing trend after 1960 ($-0.17 \pm 0.07\text{‰/decade}$, $p = 0.05$). It is consistent with the acceleration of ocean acidification after 1960.

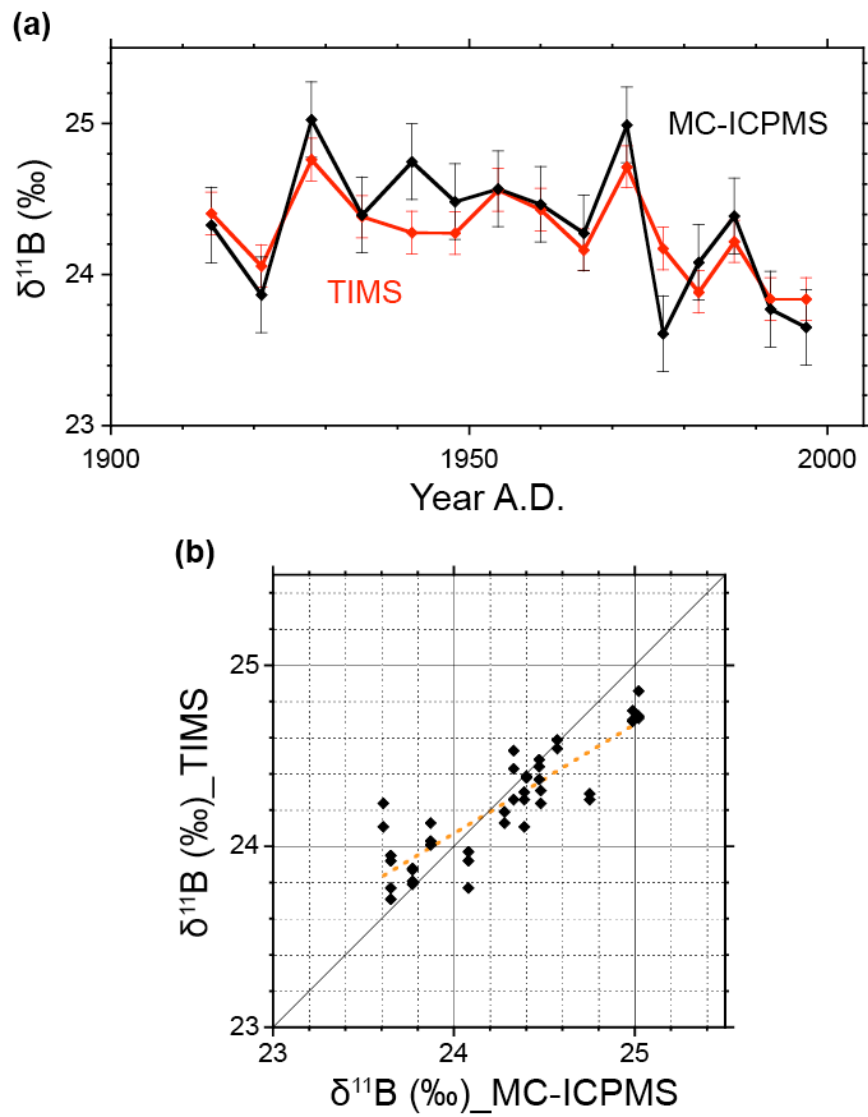


Fig. 2-4. Comparison of $\delta^{11}\text{B}$ values of Chichijima coral measured in P-TIMS and MC-ICPMS methods. (a) Variation since 1914. (b) P-TIMS versus MC-ICPMS. Linear regression line ($r = 0.87$, $p < 0.01$, $n = 41$) and one-to-one line are indicated in yellow and black.

2-3-2. pH_{SW} estimation since 1970

We obtained an empirical regression equation for Chichijima ($R^2 = 0.74$, $n = 1,034$), Hawaii ($R^2 = 0.58$, $n = 11,205$), Tahiti ($R^2 = 0.54$, $n = 1,440$), and Marquesas ($R^2 = 0.84$, $n = 4,314$) using the parameters summarized in Table 2-2. Root mean squares of ε were 6.7, 5.8, 5.5, and 7.4 $\mu\text{mol/kg}$, respectively. We used SST and SSS from the Simple Ocean Data Assimilation (SODA version 2.1.6, [Carton & Giese, 2008](#)) to estimate monthly values of nDIC for the years 1970–2008, and calculated pH_{SW} and $p\text{CO}_2\text{ SW}$ from DIC and assuming TA using CO2Calc (Fig. 2-5). Results show that around the studied islands, pH_{SW} is decreasing and $p\text{CO}_2\text{ SW}$ is increasing at a consistent rate with atmospheric $p\text{CO}_2$ since 1970 (Fig. 2-5). Reflecting SST seasonality, cyclic variation is seen in pH_{SW} and $p\text{CO}_2\text{ SW}$ variation of Chichijima, Hawaii, and Tahiti ([Kubota et al., 2014](#); [Ishii et al., 2011, 2002](#); [Dore et al., 2009](#)). Large pH_{SW} and $p\text{CO}_2\text{ SW}$ seasonality in Chichijima is due to large SST seasonality. On the other hand, Marquesas records show complex variation, reflecting stochastic nature of oceanography in the equatorial Pacific ([Sutton et al., 2014](#); [Feely et al., 2002](#)).

In order to evaluate the validity of the empirical regression equation, we compared pH_{SW} and $p\text{CO}_2\text{ SW}$ time series for Chichijima area with more continuous and abundant measurements at the Line 137°E (Masao Ishii, personal communications). JMA has measured seawater CO₂ chemistry repeatedly along this line since 1981. This different data set has two types: one is discrete monthly data for 26.5–27.5°N, 125–145°E (see [Midorikawa et al. \(2012\)](#) for detail), and the other is a time series data set for 27°N, 137°E grid point for the years 1993–2010 (Fig. 2-6). We observed only a slight difference in summer between my estimation and the discrete records by JMA (Fig. 2-6). This slight difference is also seen between discrete records and time series data by JMA. A weak biological productivity in summer is a probable cause, because this effect is not reflected in the multiparameter regressions (Masao Ishii, personal communications). Though the time series for 27°N, 137°E grid point (about 500 km west of Chichijima) was estimated using different methodologies from my estimation, these data are in excellent agreement (Fig. 2-6). For instance, it extracts CO₂ chemistry data from different areas; it sets different regression parameters; and it uses different SST and SSS data sets (that is, monthly 1° × 1° resolution records from the multivariate ocean variational estimation system (MOVE-G, [Usui et al., 2006](#))). This supports the validity

of pH_{SW} and $p\text{CO}_2_{\text{SW}}$ estimation in this thesis, and suggests that the time series from the Ogasawara area may represent the wide range of the western North Pacific.

Using CO_2 chemistry data around Hawaii, we further assessed the reliability of pH_{SW} and $p\text{CO}_2_{\text{SW}}$ estimation in this thesis, because there exists continuous pH_{SW} observation since 1988 (i.e., HOT, <http://hahana.soest.hawaii.edu/hot/>). It is important to note that SOCAT v2 data around Hawaii is especially abundant during 2005 and 2009, which enables the comparison in detail. The estimated pH_{SW} time series captures its seasonality quite well (Fig. 2-7). We observed a small underestimation of seasonality in estimated time series compared with pH_{SW} measurements at the Station ALOHA since 1988 (one is directly measured, and the other is calculated from DIC and TA; Dore et al., 2009) (Fig. 2-7). A part of underestimation may be due to biological productivity, as similar to Chichijima. It should be noted that the small discrepancy in pH_{SW} seasonality has a negligible effect on annual mean pH_{SW} .

In order to estimate pH_{SW} and $p\text{CO}_2_{\text{SW}}$ differences between Tahiti and Marquesas, we made calculations removing the second term in Equation (2-4). Through this treatment, long-term pH_{SW} decreases and $p\text{CO}_2$ increases are detrended. Since Marquesas is located closer to the equatorial upwelling zone than Tahiti, pH_{SW} ($p\text{CO}_2_{\text{SW}}$) is lower (higher) by 0.04 (43.9 μatm) (Fig. 2-8). All calculations considered this offset through this thesis.

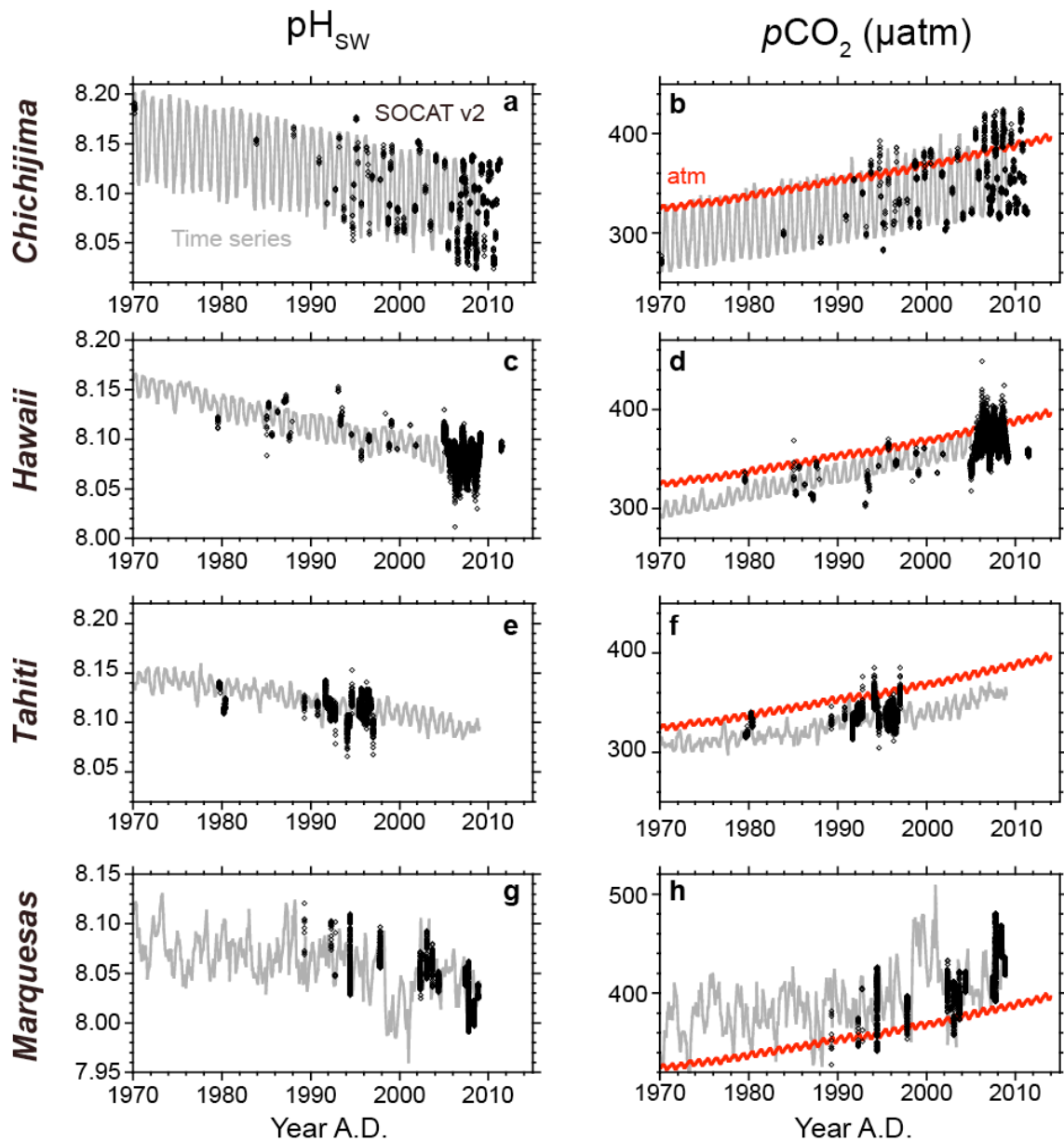


Fig. 2-5. pH_{sw} and pCO_2 variation during 1980–2015 in the vicinity of (a,b) Chichijima, (c,d) Hawaii, (e,f) Tahiti, and (g,h) Marquesas. Calculations were made using SOCATv2 $f\text{CO}_2$ datasets (black diamonds) (Bakker et al., 2014) and time-series were estimated by multi-regression analysis (gray lines) (Ishii et al., 2011). Atmospheric pCO_2 measured in the MLO is also plotted (red lines) (Tans & Keeling, 2014).

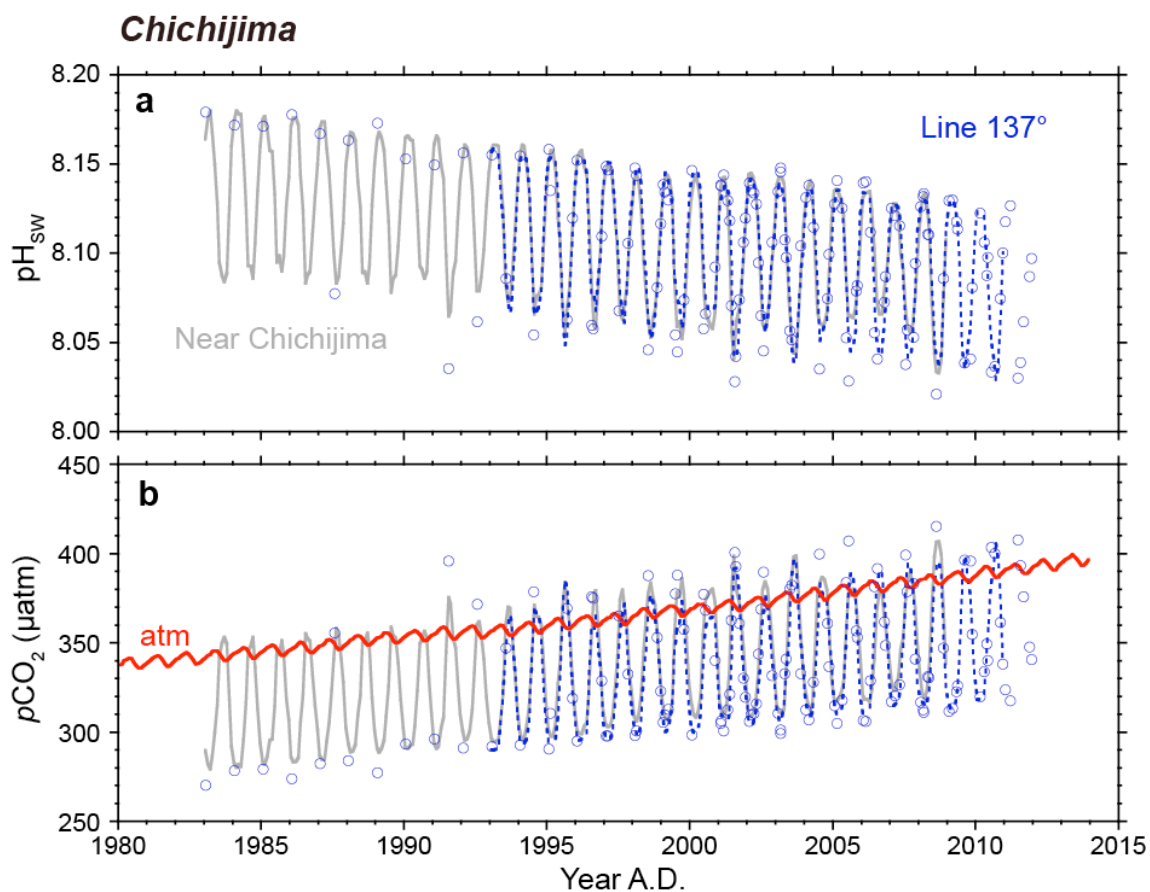


Fig. 2-6. (a,b) Comparison of pH_{sw} and pCO_2 variation during 1980–2015 in the vicinity of Chichijima (time-series; gray line) with those from the 137°E continuous measurements by the JMA (sporadic data, blue circles; monthly time-series, blue dashed line) (Masao Ishii, personal communication). Atmospheric pCO_2 measured at the MLO is also plotted in **b** (a red line) (Tans & Keeling, 2014).

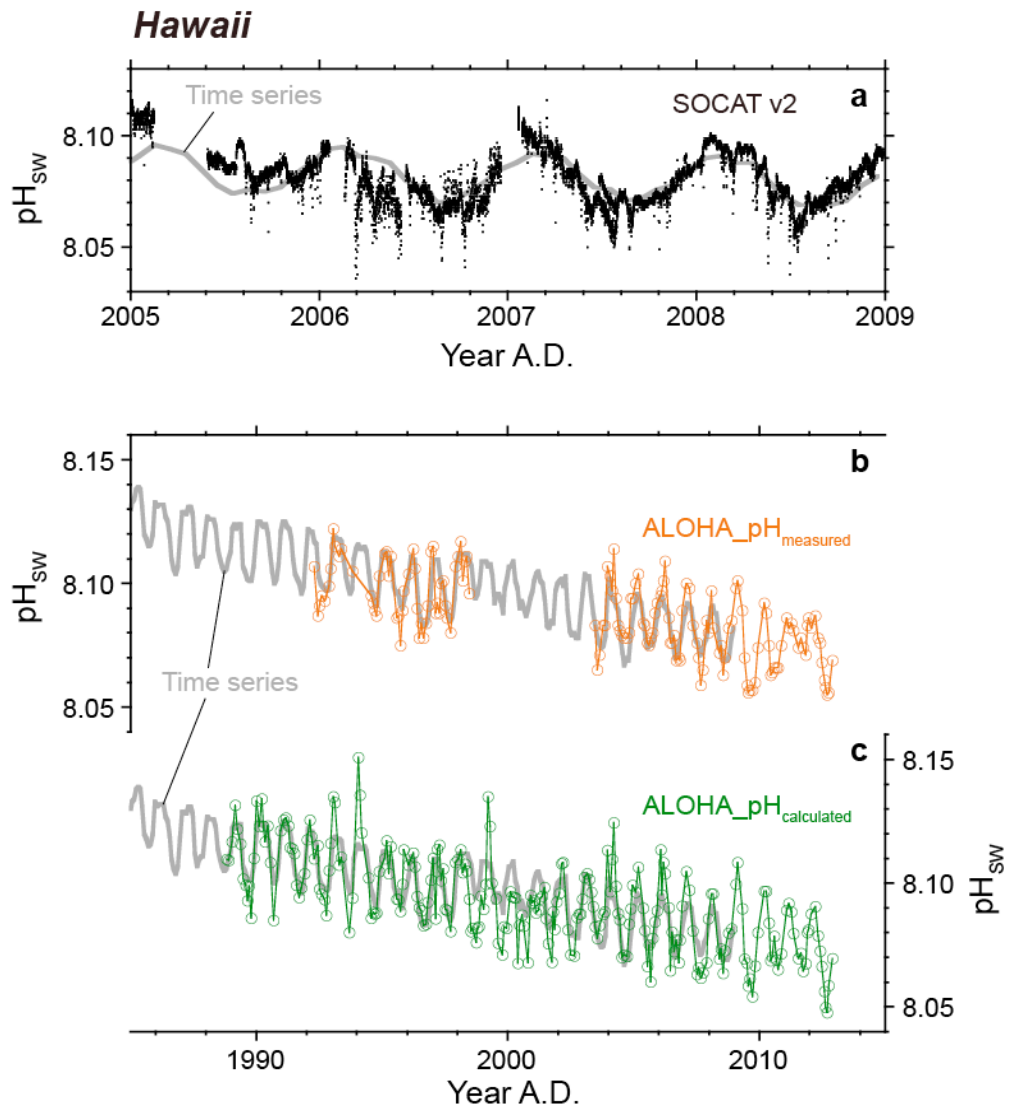


Fig. 2-7. (a) Same as **Fig. 2-5e**, but for years 2005–2009 when data are abundant. Comparison of pH_{sw} time-series with continuous pH_{sw} measurements at the Station ALOHA (directly measured pH_{sw} , orange; calculated from DIC and TA, green) (Dore et al., 2009).

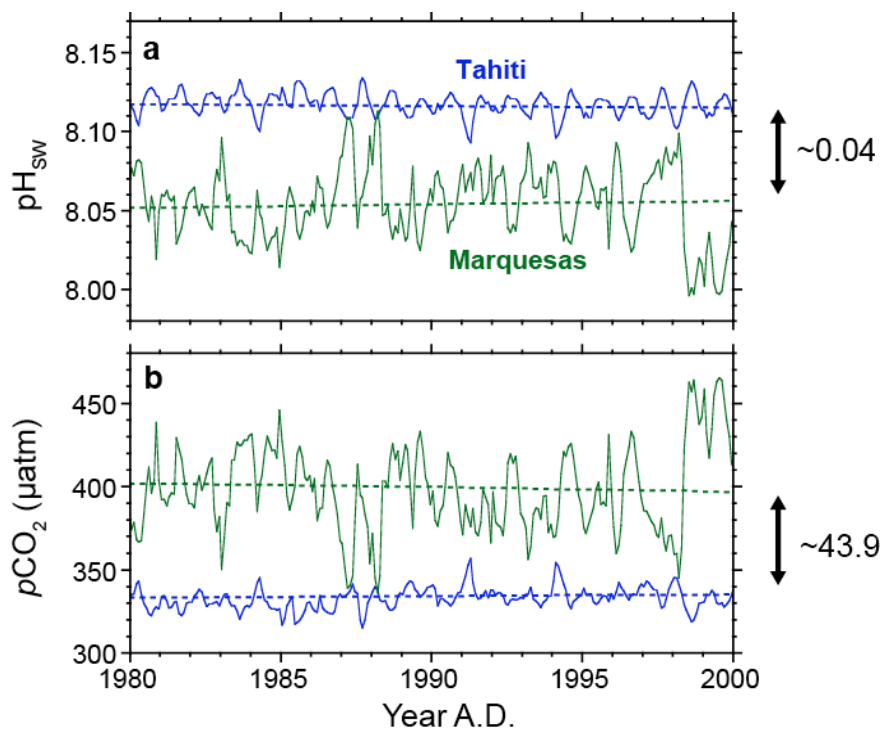


Fig. 2-8. Differences of (a) pH_{sw} and (b) pCO_2 between Tahiti and Marquesas for the years 1980–2000. Linear regressions are shown in dashed line.

2-3-3. pH_{SW} estimation since the Industrial Revolution

We used two boundary conditions of pH_{SW} and atmospheric $p\text{CO}_2$ for 1994 and the Industrial revolution to determine the constant b in Equation (2-5). Firstly we calculated pH_{SW} in 1994 from DIC and TA of GLODAP v1.1 (Key et al., 2004). Secondly, we calculated preindustrial pH_{SW} by subtracting anthropogenic DIC increase of 50 $\mu\text{mol/kg}$ since the Industrial Revolution from present DIC (Key et al., 2004; Sabine et al., 2004, 2002). In this calculation TA was kept constant, because CO_2 invasion against the ocean does not influence TA (e.g., Zeebe & Wolf-Gradlow, 2001). We determined b as 0.7 (Fig. 2-9). Furthermore, we calculated $p\text{CO}_2$ SW from pH_{SW} assuming present SST, SSS, and TA (Fig. 2-9). The estimated $p\text{CO}_2$ SW values in 2000 are 333.1 and 349.5 μatm in Chichijima and Tahiti, respectively (Fig. 2-9). They are consistent with surface $p\text{CO}_2$ distribution (Fig. 2-1) (Takahashi et al., 2009). In addition, their rates of increase since 1970 agree well with those of multiparameter regression (Fig. 2-5). Calculated $p\text{CO}_2$ increases keeping $\Delta p\text{CO}_2$ constant in both Chichijima and Tahiti, suggesting that no significant change in biological productivity occurred since the Industrial Revolution despite global climate change (e.g., ocean acidification, global warming, and deoxygenation; Doney et al., 2014; Gruber, 2011).

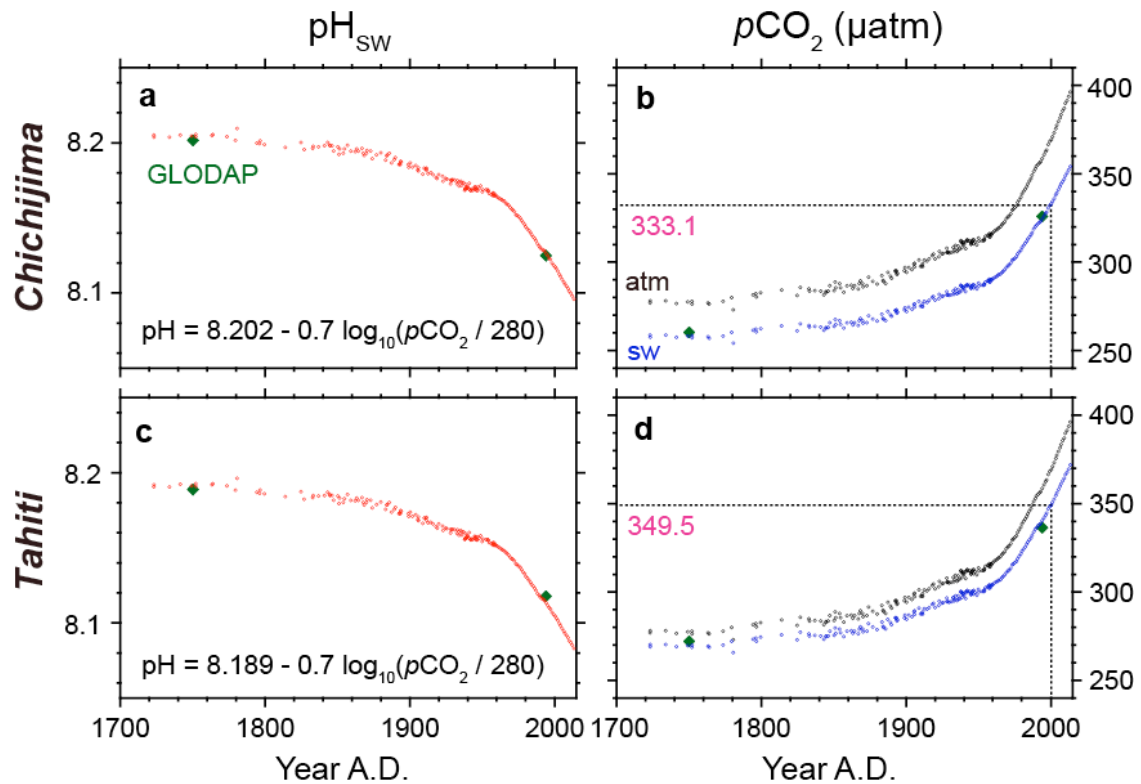


Fig. 2-9. (a-d) Estimated pH_{SW} and pCO₂ SW variation since the Industrial Revolution for the surface water surrounding Chichijima and Tahiti. Black points represent atmospheric pCO₂ records (Tans & Keeling, 2014; Rubino et al., 2013). Time-resolutions are "just 1 year" for observation at the MLO (Tans & Keeling, 2014) and "several years" for Antarctic ice core records depending on a gas smoothing in the surface layer of ice (Rubino et al., 2013). pH_{SW} and pCO₂ SW calculated from GLODAP v1.1 data for the closest grid to each island are plotted in green diamonds (Key et al., 2004).

2-3-4. $\delta^{11}\text{B}$ - pH_{SW} calibration and errors

Based on the empirical calibration by Hönisch *et al.* (2007) outlined in Chapter 1, we determined "offset a " for Chichijima and Tahiti corals through comparing $\delta^{11}\text{B}$ and pH_{SW} (Fig. 2-10). We selected the best-fit offset a that yielded the minimum chi-square values.

$$\chi^2 = \sum_{i=1}^N \left(\frac{\text{pH}_{\text{SW-calculated}} - \text{pH}_{\text{SW-estimated}}}{\sigma_i} \right)^2 \quad (\text{Eq. 2-6})$$

Here N is the number of measurements and σ is the uncertainty of each data point. In the calculation of pH_{SW} using Equation (1-14), we used the fractionation factor from Klochko *et al.* (2006) and $\text{p}K_{\text{B}}$ listed in Table 2-3. As for Marquesas coral, we added 0.04 to the calculated pH_{SW} to compensate for the pH_{SW} difference between Tahiti and Marquesas (Fig. 2-8). Determined a values were -5.07 and -5.92 for Chichijima and Tahiti, respectively (Table 2-3). We will use obtained $\delta^{11}\text{B}$ - pH_{SW} calibration for Tahiti in Chapter 4.

We estimated errors of pH_{SW} estimation derived from the $\delta^{11}\text{B}$ - pH_{SW} fitting as well as analytical uncertainty. We did not estimate the fitting error of Tahiti-Marquesas calibration, because there are only three data points. We estimated the statistical error of offset a (unit is ‰) through finding χ^2 that exhibit ± 1 from the minimum χ^2 . We determined them as +0.04 and -0.04 (-5.07 ± 0.04 , 1σ). We combined errors derived from $\delta^{11}\text{B}$ (± 0.07 , 1σ , $n = 14$) and offset a using Equation (1-14):

$$\sigma_{\text{pH}}(\delta^{11}\text{B} \& a) = \sqrt{\left(\frac{\partial \text{pH}}{\partial \delta^{11}\text{B}} * \sigma(\delta^{11}\text{B}) \right)^2 + \left(\frac{\partial \text{pH}}{\partial a} * \sigma(a) \right)^2} \quad (\text{Eq. 2-7})$$

Here we made the calculation with fractionation factor and $\delta^{11}\text{B}_{\text{SW}}$ as constant (1.0272 and 39.61‰, respectively). When we chose 24.5‰ as a representative value of $\delta^{11}\text{B}$, $\sigma_{\text{pH}}(\delta^{11}\text{B} \& a)$ is ± 0.006 (1σ). However, it does not consider an error derived from $\delta^{11}\text{B}$ - pH_{SW} fitting as seen in deviations from the fitted pH_{SW} curve beyond the analytical uncertainty (Fig. 2-10). Thus we regarded a standard deviation of pH anomalies ($\text{pH}_{\text{SW-calculated}} - \text{pH}_{\text{SW-estimated}}$) as the error derived from the fitting (± 0.020 , 1σ , $n = 15$).

Finally, we calculated a combined error in the pH_{SW} estimation (σ_{pH}):

$$\sigma_{\text{pH}} = \sqrt{\sigma_{\text{pH}}(\delta^{11}\text{B} \& a)^2 + \sigma_{\text{pH}}(\text{fitting})^2} \quad (\text{Eq. 2-8})$$

The finally obtained error was ± 0.021 (1σ). It indicates that the error derived from the fitting dominates the overall error.

Another way to determine the net error of pH_{SW} estimation is to utilize a probabilistic value in the chi-square fitting. In this, we can regard σ_i as a comprehensive error of $\delta^{11}\text{B}$ -pH_{SW} proxy. Choosing σ_i in Equation (2-6) that satisfy 95% significance level, we determined σ_i as ± 0.028 (1σ , $\chi^2 = 6.365$, $df = 14$, $p = 0.96$) (Fig. 2-11). It is slightly higher than the error determined by the aforementioned procedure (i.e., ± 0.021 , 1σ), but it means that there is an only 5% chance that the $\delta^{11}\text{B}$ -pH_{SW} calibration will reconstruct questionable pH_{SW}.

Results of error estimation indicate that even if we adopt a larger error (± 0.028 , 1σ), we can resolve pH_{SW} seasonality (about 0.1 pH unit) with statistical significance from high resolution $\delta^{11}\text{B}$ measurements of Chichijima coral. Similarly, if we can collect fossil *Porites* coral from Chichijima in the future (it has never been documented), we can resolve pH_{SW} difference between glacial to interglacial periods (about 0.1 pH unit) from $\delta^{11}\text{B}$ measurements of them. We should keep in mind the errors in pH_{SW} reconstruction discussed here. However, needless to say, further efforts to reduce errors and to investigate temporal and inter-colonial variation of offset a are necessary to increase applicability of pH_{SW} proxy.

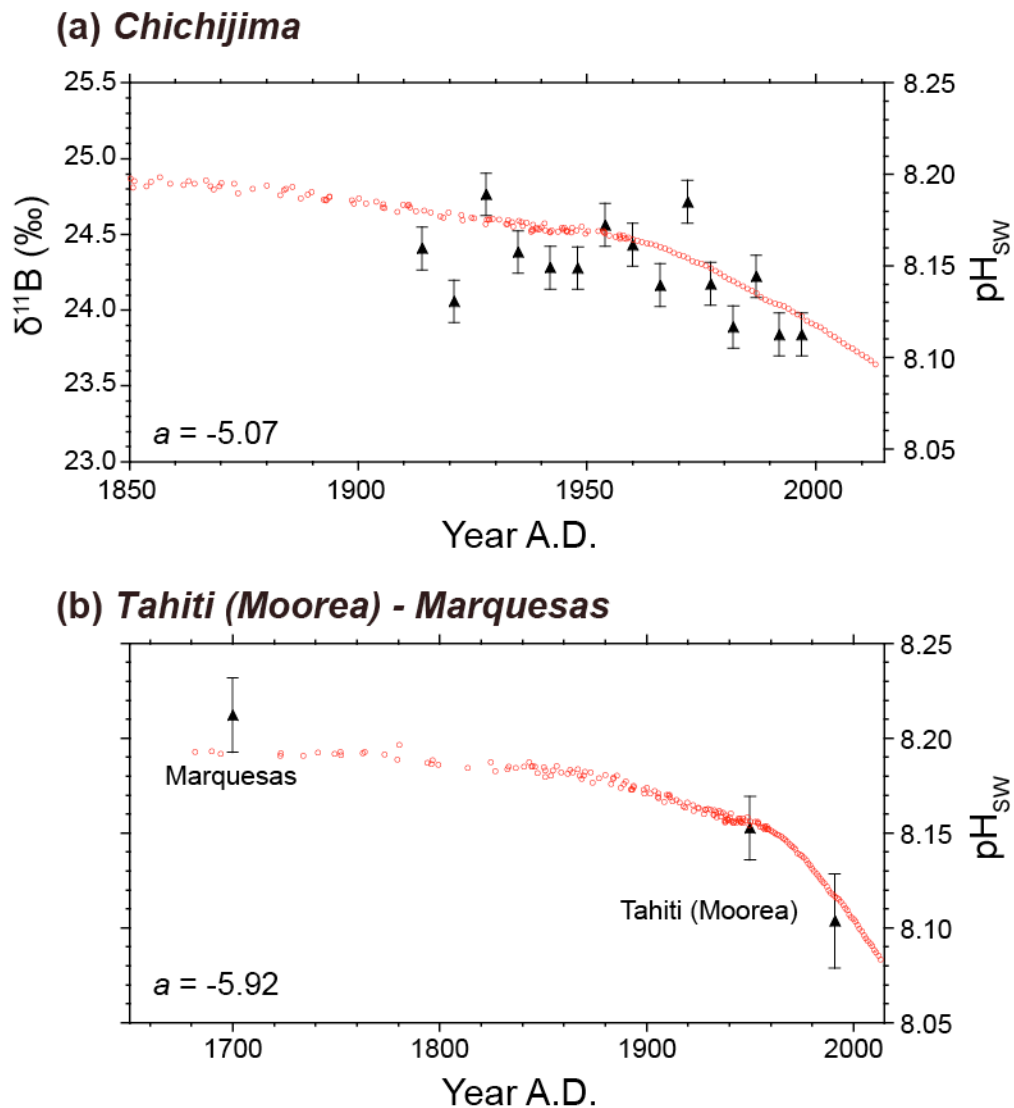


Fig. 2-10. (a) $\delta^{11}\text{B}$ - pH_{SW} calibration using modern *Porites* coral collected at Chichijima. Replicated $\delta^{11}\text{B}$ values during 1914–1997 measured by the P-TIMS is used. Time resolution of each point is three years. Error bars are 2σ of analytical uncertainty. (b) $\delta^{11}\text{B}$ - pH_{SW} calibration using modern and fossil *Porites* corals (Douville et al., 2010; Gaillardet & Allegre, 1995). Modern corals are for the years 1991 and 1950. pH_{SW} calculated from $\delta^{11}\text{B}$ of fossil coral (1700) that was collected at Marquesas is used after a pH_{SW} correction (add +0.04 pH unit). Time resolution of each point is one or two years (Douville et al., 2010). Error bars are 2σ of analytical uncertainty.

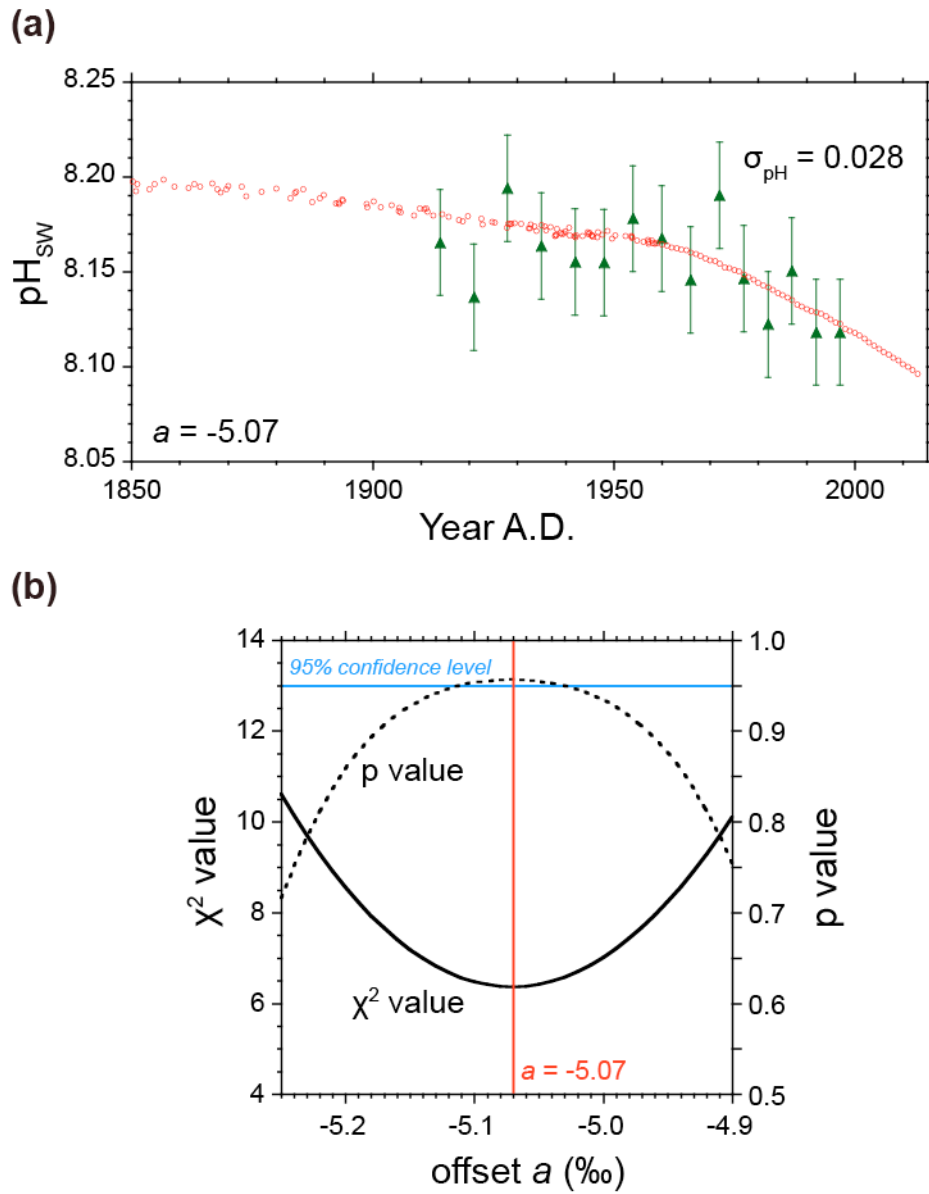


Fig. 2-11. (a) Same as **Fig. 2-10a**, but larger error bars are adopted to satisfy 95% confidence level of the chi-square fitting. (b) χ^2 and p values when σ_i is 0.028. The maximum p value is 0.96, which satisfies 95% confidence level.

Table 2-3. A summary of *Porites* corals and parameters used in the $\delta^{11}\text{B}$ -pH_{SW} calibration.

Location	Resolution (years)	Reference	T (°C)	S	pK_B	offset <i>a</i> (‰)
Chichijima	3	This study	24.7	34.5	8.60	-5.07
Tahiti Marquesas	1 or 2	Douville et al., 2010 ; Gaillardet & Allegre, 1995	27.4 27.9	35.9 35.6	8.57 8.56	-5.92
Hainan	4	Liu et al., 2014	26.9	33.8	8.58	-4.5
Guam	1	Shinjo et al., 2013	28.4	34.4	8.56	-4.0

2-3-5. Location-specific difference of offset a

Using offset a of -5.07 (for Chichijima coral), we recalculated pH_{SW} and $p\text{CO}_2_{\text{SW}}$ from $\delta^{11}\text{B}$ of Hainan and Guam corals (Liu et al., 2014; Shinjo et al., 2013) using present SST, SSS, and TA that were calculated from Equation (2-3). The calculated pH_{SW} and $p\text{CO}_2_{\text{SW}}$ were more reasonable than the values originally calculated using the $\text{pH}_{\text{SW}}\text{-pH}_{\text{CF}}$ relationship of cultured *Porites* corals (Trotter et al., 2011), however most of the calculated $p\text{CO}_2_{\text{SW}}$ still remained higher than the atmospheric $p\text{CO}_2$. This indicates that Hainan and Guam are located in CO_2 "source" region, which obviously contradicts with the observed $p\text{CO}_2$ distributions (Fig. 2-1) (Takahashi et al., 2009; Tseng et al., 2006). Instead, suitable a values appear to be about -4.5 and -4.0 for Hainan and Guam corals, respectively (Fig. 2-12, Table 2-3). If these values are correct, we can reconcile three issues: (1) $p\text{CO}_2$ values in 2000 for Hainan and Guam areas, (2) pH_{SW} decrease since the Industrial Revolution in Hainan area, and (3) pH_{SW} values and its decreasing trend for the last 60 years in Guam area (Fig. 2-12). Larger $p\text{CO}_2_{\text{SW}}$ values than the atmospheric $p\text{CO}_2$ sporadically seen in both Hainan and Guam areas may be due to internal climate variability from interannual to decadal timescales. For instance, monsoonal wind and El Nino - Southern Oscillation (ENSO) can respectively influence CO_2 chemistry in the surface ocean of these areas (Liu et al., 2014; Shinjo et al., 2013).

The difference of offset a among locations (i.e., Chichijima, Tahiti, Guam, and Hainan) indicates that there is no ubiquitous calibration equation and paleo- pH_{SW} reconstruction needs *in situ* calibration using one or more modern corals. The reason why there are differences between field-based and culturing-based calibrations is perhaps related to the fact that culture experiments assume severe acidification that can exert a bad influence on coral physiology. In fact, Krief et al. (2010) found that skeletal growth of cultured massive *Porites* spp. decreased in acidified seawater. Similarly, many culture experiments on massive *Porites* spp. have reported inhibition of calcification under high $p\text{CO}_2$ level (e.g., Iguchi et al., 2014, 2012). This issue will be further discussed in Chapter 3.

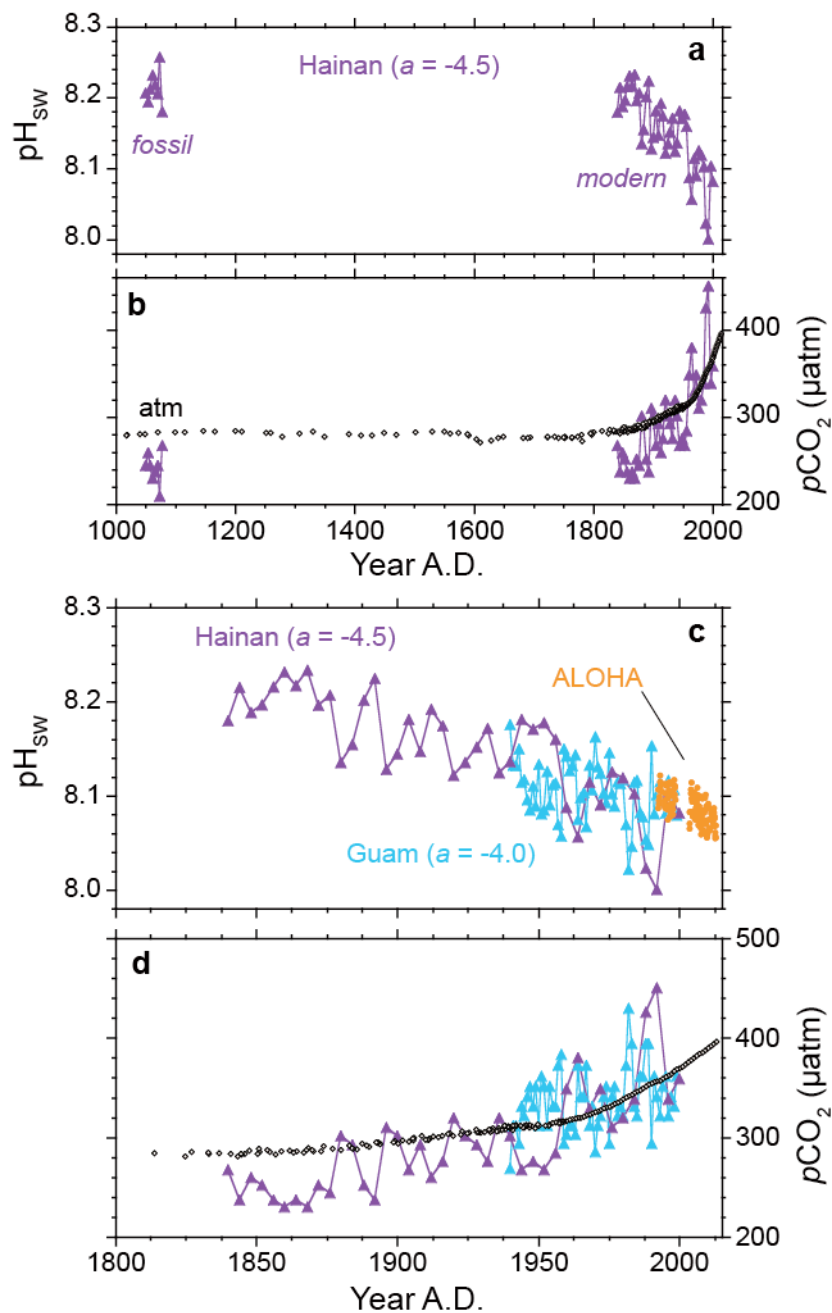


Fig. 2-12. Reconstructed pH_{sw} and pCO₂ sw from δ¹¹B of *Porites* corals that were collected at Hainan (purple, Liu et al., 2014) and Guam (light blue, Shinjo et al., 2013) since (a,b) 1000 and (c,d) 1800 to the present. Time-resolutions are 4 years for Hainan coral and 1 year for Guam coral. Calculations were made using Equation (1-14) with a values of -4.5 and 4.0, respectively. pH_{sw} seasonality measured at the Station ALOHA (Dore et al., 2009) and atmospheric pCO₂ records (Tans & Keeling, 2014; Rubino et al., 2013) are also shown.

2-4. Conclusion

We showed that even though there is no monitoring site, we can estimate not only annual variation but also seasonality of pH_{SW} utilizing abundant open ocean CO_2 chemistry measurements using research vessels since 1970. We confirmed the validity of the estimation of time series through comparison with more abundant and continuous measurements at the Line 137°E and the Station ALOHA. We extended pH_{SW} estimation from the recent ~45 years further back to the preindustrial period utilizing atmospheric $p\text{CO}_2$ measurements at the MLO and reconstructions from Antarctic Ice cores. Measured $\delta^{11}\text{B}$ of *Porites* coral collected at Chichijima showed no statistically significant trend from 1907 to 1960 and then decreased ($-0.17 \pm 0.07\%$ /decade, $p = 0.05$), being consistent with acceleration of pH_{SW} decrease after 1960 (i.e., ocean acidification). A comparison between obtained pH_{SW} and measured $\delta^{11}\text{B}$ variation enabled me to calibrate $\delta^{11}\text{B}$ - pH_{SW} relationship. We found that offset a values of modern corals were different from location to location (i.e., Chichijima, Tahiti, Hainan, and Guam), which means that we must establish the $\delta^{11}\text{B}$ - pH_{SW} calibration where we collect fossil corals. The newly employed calibration reconciled several discrepancies between CO_2 chemistry observations and pH_{SW} and $p\text{CO}_2$ SW reconstructions using culturing-based $\delta^{11}\text{B}$ - pH_{SW} calibrations. The field-based calibration proposed by this chapter will become a new means to reconstruct past pH_{SW} and $p\text{CO}_2$ (both seawater and atmosphere), but it is clear that more works are needed to investigate temporal and inter-colonial variation of offset a .

CHAPTER 3

Effects of recent ocean acidification in the western North Pacific on *Porites* coral calcification

Chapter 3 Abstract

Marine calcifying organisms such as scleractinian corals are being threatened by rapid ocean acidification (OA) due to the oceanic uptake of anthropogenic CO₂. To better understanding how organisms and ecosystems will adapt to or be damaged by the resulting changes in environments, field observations are crucial. Here we show clear evidence, based on $\delta^{11}\text{B}$ measurements, that OA is affecting the pH_{CF} in *Porites* coral collected at Chichijima, one of the Ogasawara Islands, an archipelago located in the western North Pacific Subtropical Gyre. A rapid decline of $\delta^{11}\text{B}$ of coral skeleton since 1960 ($-0.17 \pm 0.07\%$ /decade) was observed and was compared with pH_{SW} near the Chichijima over the 20th century, as estimated from a large number of shipboard measurements of seawater CO₂ chemistry and atmospheric CO₂. The results indicate that pH_{CF} has been changing sensitively to pH_{SW} and suggest that the calcification fluid of coral will become corrosive to aragonite in the future (pH_{CF} = ca. 8.3 when pH_{SW} = ca. 8.0 in 2050) at an earlier point than previously expected, despite the pH_{CF} up-regulation mechanism of coral.

3-1. Introduction

When CO₂ dissolves in seawater, it becomes a carbonic acid and perturbs the weakly alkaline seawater toward an even less alkaline state. Surface pH_{SW} is considered to have declined by about 0.1 since the beginning of the industrial era, and an additional decline of approximately 0.3 is projected by the end of this century (Doney et al., 2014; Gattuso & Hansson, 2011; Feely et al., 2009; Tans et al., 2009; Orr et al., 2005; Sabine et al., 2005; Key et al., 2004; Caldeira & Wickett, 2003). The impact of OA is thought to manifest earlier in polar oceans than in tropical-subtropical ones (Feely et al., 2009), although it has also been suggested that coral reef ecosystems are more susceptible to a decline of pH_{SW} and saturation state with respect to aragonite (Ω_{ar}) (Hoegh-Guildberg et al., 2011; Pandolfi et al., 2011; Gattuso & Hansson, 2011; Kleypas & Yates, 2009; Doney et al., 2009; Kleypas & Langdon, 2007; Kleypas et al., 1999a,b). As relative changes of seawater Ω_{ar} ($\Omega_{ar\ SW}$) in tropical-subtropical oceans are bigger than in polar oceans (Feely et al., 2009), this will lead to severe consequences. A critical threshold below which reef growth will be hampered is still contested, although is often claimed based on field observations to be 3.3 (Hoegh-Guildberg et al., 2011; Kleypas & Langdon, 2007; Kleypas et al., 1999b). In the surface layers of tropical-subtropical oceans, $\Omega_{ar\ SW}$ is projected to decline as low as 3.3 by 2050, when atmospheric CO₂ level will exceed about 480 μ atm (Hoegh-Guildberg et al., 2011; Feely et al., 2009).

To better understand the response of corals under acidified water, we employed long-living corals. As these corals have already been experienced OA over centuries, especially for the last 50 years, after the post-1960s growth of anthropogenic CO₂ emissions. Field-based observations have several advantages compared to culture experiments, since culture experiments often put corals under excessively acidic water (e.g., pH < 7.8) that coral reefs rarely experience in the wild, and will in fact not even experience this century under business as usual CO₂ emissions scenario (e.g., Krief et al., 2010; Hönisch et al., 2004)

To attain the purpose, we chose Chichijima as a study region. The ocean surrounding Chichijima is oligotrophic with limited vertical mixing and low biological productivity (Ishii et al., 2011, 2001). A seasonal change dominates temporal variability in pH_{SW} as is observed as $p\text{CO}_2\ \text{SW}$ (Fig. 3-1), driven mainly by seasonal variation in SST (about 20°C in winter and about 29°C in summer) and in part by variation in the

DIC content (about 1960 $\mu\text{mol/kg}$ in summer and about 1990 $\mu\text{mol/kg}$ in winter at years around 2010 when normalized to salinity of 35). A trend of $p\text{CO}_2\text{sw}$ increase (and pH_{sw} decrease) in the northern subtropical zone of the western North Pacific is nearly tracking the rate of the atmospheric CO_2 increase (Fig. 3-1) (Midorikawa et al., 2012, 2010). These oceanographic characteristics strengthen the reliability of seawater CO_2 chemistry estimation for both seasonal and interannual timescales.

To summarize, objectives of this chapter is to gain insights of effects of OA over the last 100 years on the calcification of Chichijima coral based on pH up-regulation mechanisms (Chapter 1). We regarded $\delta^{11}\text{B}$ of Chichijima coral (Chapter 2) as an indicator of pH_{CF} , and compared it with pH_{sw} that was estimated from CO_2 chemistry observation and atmospheric $p\text{CO}_2$ records (Tans & Keeling, 2014; Rubino et al., 2013). We did not discuss Tahiti-Marquesas corals (Chapter 2), because these records do not consist of a single colony (Douville et al., 2010; Gaillardet & Allegre, 1995) and are not suitable to investigate biological responses to the changing environment.

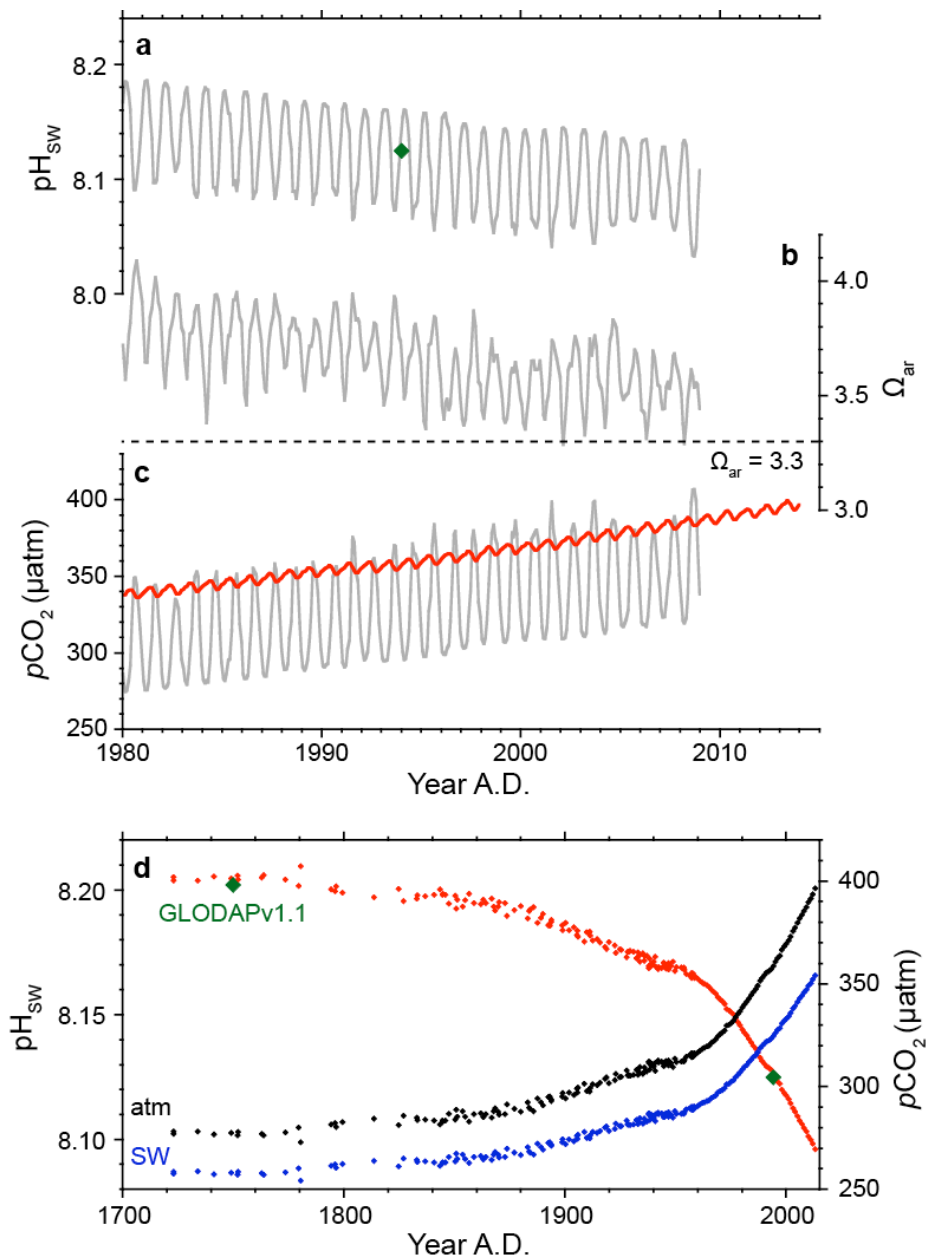


Fig. 3-1. (a-c) Time series of pH_{sw} , Ω_{ar} , and pCO_2 . Monthly atmospheric pCO_2 records measured at the MLO are also shown in red line. Dashed horizontal line indicates threshold Ω_{ar} for coral reef calcification, 3.3. (d) pH_{sw} (red) and pCO_2 (blue, seawater; black, atmosphere) variability since the Industrial Revolution. Atmospheric pCO_2 during 1959–2013 were measured at the MLO (Tans & Keeling, 2014) and those prior to 1959 were reconstructed from trapped air in an Antarctic ice sheet (Rubino et al., 2013). pH_{sw} calculated from GLODAP v1.1 DIC and TA for the year 1994 and 1750 are shown in green diamonds in a and d (Key et al., 2004).

3-2. Material and Methods

3-2-1. $\delta^{11}\text{B}$ and $\delta^{13}\text{C}$ values of Chichijima coral

We used $\delta^{11}\text{B}$ values measured in P-TIMS method. We used $\pm 0.14\text{‰}$, obtained from repeated analysis of JCp-1 (Chapter 2), as the analytical uncertainty of our $\delta^{11}\text{B}$ measurements. We calculated pH_{CF} and ΔpH (that is pH_{CF} minus pH_{SW}) using Equations (1-12) and (1-13). The dissociation constant of boric acid, $\text{p}K_{\text{B}}$, is 8.60 at 24.6 °C and a salinity of 34.8 at Chichijima (Dickson, 1990). We used $\delta^{11}\text{B}_{\text{SW}}$ of 39.61‰ (Foster et al., 2010) and α_{3-4} of 1.0272 (Klochko et al., 2006) for the calculation.

We calculated annually averaged $\delta^{13}\text{C}_{\text{coral}}$ from previously reported monthly records (Felis et al., 2009). We also calculated averages for each 3-year period that corresponded to the same portions of the coral skeleton used for $\delta^{11}\text{B}$ analyses. We could not calculate the 3-year averaged data for 1997 because monthly $\delta^{13}\text{C}_{\text{coral}}$ records were limited until 1994.

3-2-2. Seawater CO_2 chemistry

As we did not observe any significant difference between CO_2 chemistry time series in the vicinity of Chichijima and those for Line 137°E (Chapter 2), we used the former records. We also calculated Ω_{arg} from regressed nDIC records using CO2calc software (Fig. 3-1).

As pH is temperature-dependent, we evaluated SST effects on pH_{SW} estimation since the Industrial Revolution. In all calculations, we kept SSS constant at the present climatological value (34.8), as it had negligible variations less than 0.05 during 1911–1997 (Felis et al., 2009). We calculated past SST from monthly coral Sr/Ca records using equations reported by Felis et al. (2009) for the same coral colony:

$$\text{Sr} / \text{Ca} = \frac{10.33 - 0.051 * \text{SST}}{10^3} \quad (\text{Eq. 3-1})$$

We calculated nDIC from obtained SST and SSS (34.8) using Equation (2-4), where the

term for the linear trend was removed to examine seasonal to inter-annual variations. Then, using CO2calc we calculated de-trended pH_{SW} in combination with assumed TA. We calculated averages for each 3-year period that corresponded to the same portions of the coral skeleton used for $\delta^{11}\text{B}$ analyses. We could not calculate the 3-year averaged data for 1997 for the same reason as $\delta^{13}\text{C}_{\text{coral}}$.

3-3. Results and Discussion

3-3-1. $\delta^{11}\text{B}$ variation

Statistically insignificant $\delta^{11}\text{B}$ variation is recorded for the period between 1914 and 1954 ($p = 0.78$), whereas a rapid decrease in $\delta^{11}\text{B}$ became evident after 1960 ($-0.17 \pm 0.07\text{‰}/\text{decade}$, $p = 0.05$). This trend resembles pH_{SW} evaluated from the atmospheric pCO_2 records (Figs. 3-1 & 3-2). Although we averaged three years of Chichijima coral to minimize effects derived from oceanographic variations that have interannual timescales, we observed some short-term variations that is well beyond the uncertainty of $\delta^{11}\text{B}$ measurements (Figs 3-2 & 3-3). For instance, $\delta^{11}\text{B}$ values for the mean year of 1921 and 1971 showed negatively and positively pronounced values, respectively. We did not find any correlations with SST proxies (Sr/Ca, U/Ca, and $\delta^{18}\text{O}$) that exhibit interannual to decadal variations (Fig. 3-3). (Felis et al., 2011; Felis et al., 2009). The 3-year averaged SST anomaly had a standard deviation of $0.5\text{ }^\circ\text{C}$, and that of the pH_{SW} anomaly was only 0.004 (Fig. 3-4). Therefore, owing to 3-year averaging, we confirmed that effects of past SST changes were negligible in the pH_{SW} calculation. SSS change in the past 100 year is so small (~ 0.05) that it can hardly influence CO_2 chemistry and coral geochemical records. Furthermore, modern CO_2 chemistry observation does not show any short-term variations because the surface ocean is close to equilibrated state to the atmosphere (Figs. 2-5, 2-6 & 3-1). Thus, rather than the environmental factor, issues related to coral skeleton is suspected as the cause of the short-term variability. Heterogeneity of coral subsamples or existence of drivers in addition to pH_{SW} is one of such possibilities (discussed later in Chapter 5). It should be noted that to identify the cause is beyond the scope of this chapter, and it does not affect the conclusion derived from pH_{CF} and pH_{SW} comparison discussed in the subsequent section.

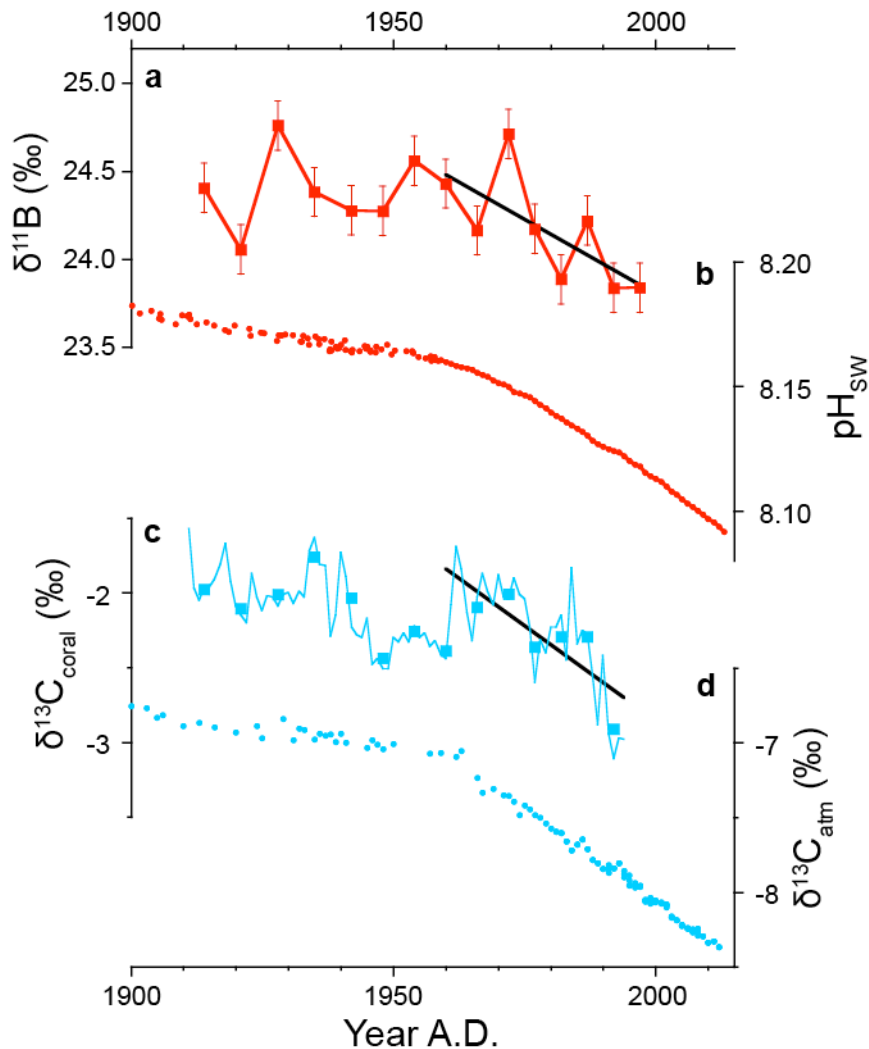


Fig. 3-2. (a) $\delta^{11}\text{B}$ records of Chichijima coral. A regression line after 1960 shown in black suggests an acceleration of $\delta^{11}\text{B}$ decline ($p = 0.05$). (b) as Fig. 3-1d but for the years 1900–2013. (c) as a but for $\delta^{13}\text{C}_{\text{coral}}$ (Felis et al., 2009). Annual (line) and 3 year averaged (rectangles) $\delta^{13}\text{C}_{\text{coral}}$ were calculated from monthly records (Felis et al., 2009). $\delta^{13}\text{C}_{\text{coral}}$ decreases (a black regression line; $p < 0.01$) at equivalent rates to $\delta^{13}\text{C}_{\text{atm}}$ after 1960. (d) $\delta^{13}\text{C}_{\text{atm}}$ during 1981–2012 were measured at the MLO and that prior to 1981 were reconstructed from trapped air in an Antarctic ice sheet (Rubino et al., 2013).

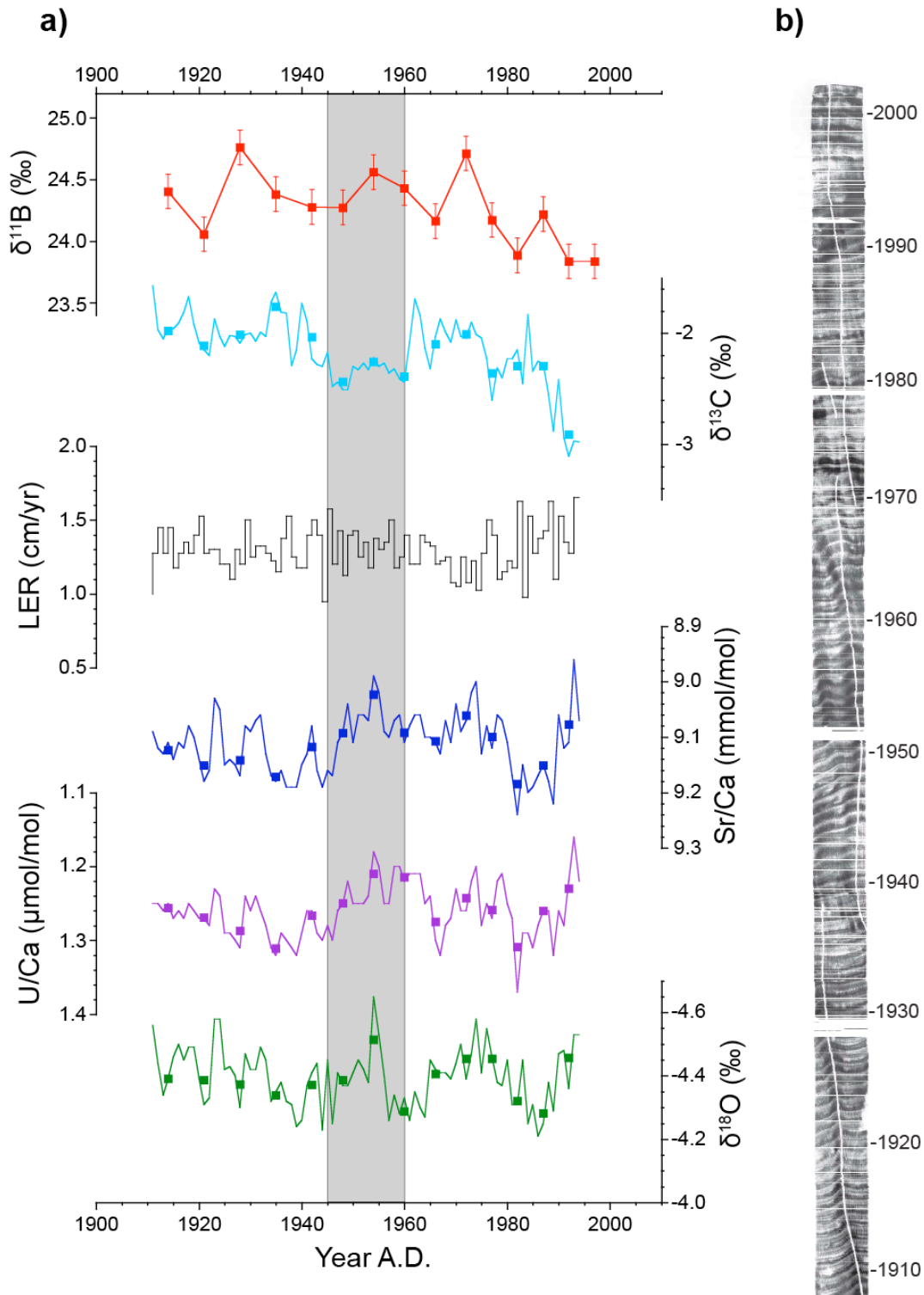


Fig. 3-3. (a) A summary of geochemical records of Chichijima coral ($\delta^{11}\text{B}$, this study; others, Felis et al., 2009). LER, Linear Extension Rate. (b) A photograph of the coral skeleton taken under soft X-ray (Felis et al., 2009).

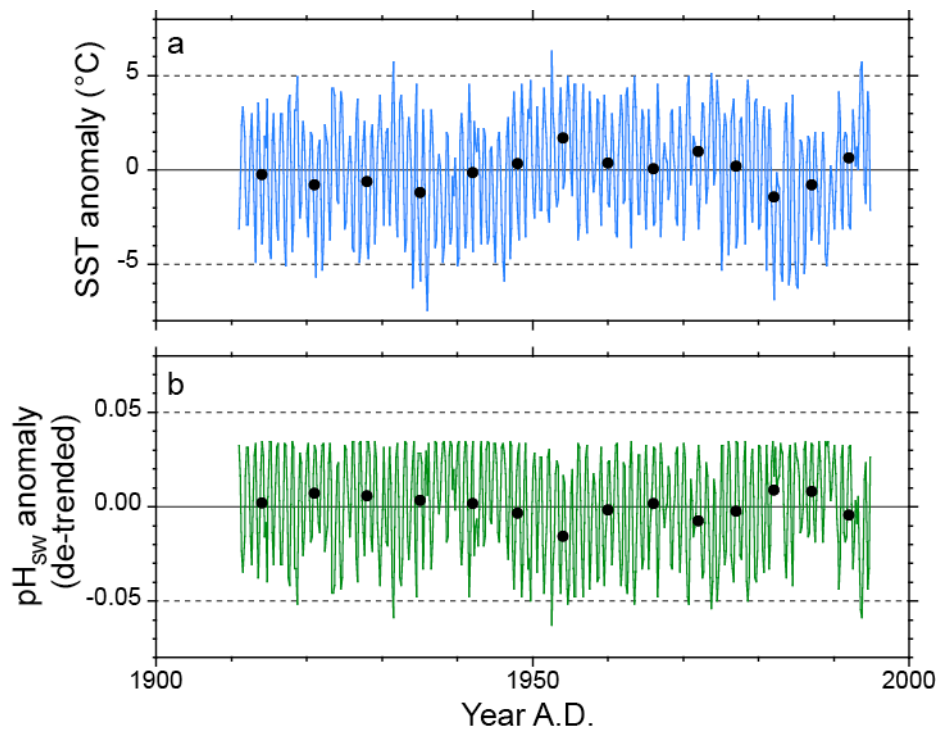


Fig. 3-4. Monthly mean (a) SST ($^{\circ}\text{C}$) and (b) resulting pH_{sw} anomalies estimated from coral Sr/Ca paleo-thermometer for the years 1911–1994 (lines). Black circles represent 3-year averages that correspond to portions of skeletons for which $\delta^{11}\text{B}$ were analyzed.

3-3-2. $\delta^{13}\text{C}$ variation

The stable carbon isotopic ratio ($\delta^{13}\text{C}$) previously reported for the same coral ($\delta^{13}\text{C}_{\text{coral}}$) (Felis et al., 2009) behaves in similar fashion (Fig. 3-2 & 3-3). $\delta^{13}\text{C}_{\text{coral}}$ keeps steady levels until 1960 ($-0.11 \pm 0.02\text{‰}/\text{decade}$, $p < 0.01$) followed by a subsequent sharp decrease ($-0.25 \pm 0.04\text{‰}/\text{decade}$, $p < 0.01$). It is consistent with the $\delta^{13}\text{C}$ of atmospheric CO_2 ($\delta^{13}\text{C}_{\text{atm}}$) records corresponding to $-0.04 \pm 0.01\text{‰}/\text{decade}$ ($p < 0.01$) and $-0.24 \pm 0.01\text{‰}/\text{decade}$ ($p < 0.01$) before and after 1960, respectively (Rubino et al., 2013) (Figs. 3-5).

No statistically significant difference of decreasing trends between $\delta^{13}\text{C}_{\text{coral}}$ and $\delta^{13}\text{C}_{\text{atm}}$ after 1960 was found ($p = 0.82$). The most important driver of long-term $\delta^{13}\text{C}_{\text{coral}}$ decrease is probably a $\delta^{13}\text{C}_{\text{DIC}}$ decrease, that is, the Suess effect (Dassié et al., 2013; Schmittner et al., 2013; Swart et al., 2010; Keeling et al., 2004; Quay & Stutsman, 2003; Quay et al., 2003, 1992; Gruber et al., 1999; Nozaki et al., 1978). Previous studies have estimated that the surface ocean reach to isotopic equilibrium in ~ 10 years (Schmittner et al., 2013; Gruber et al., 1999). As a first order approximation, therefore, $\delta^{13}\text{C}_{\text{coral}}$ must have decreased by 1.01‰ since 1910 if CO_2 is efficiently ventilated (Fig. 3-6). In addition to the Suess effect, previous studies have reported that there are other marginal effects derived from, for example, changes of (1) depth (Dassié et al., 2013; Grottoli, 2002, 1999) and (2) pH_{SW} (Krief et al., 2010).

The depth effect is almost equivalent to a solar irradiance effect, because the light attenuates with depth and photosynthesis partly control $\delta^{13}\text{C}_{\text{coral}}$. When the irradiance is sufficient, coral polyp selectively incorporate isotopically "lighter (^{12}C -rich)" carbon from the calcification fluid, leaving "heavier (^{13}C -rich)" carbon to the fluid from which the corals form the skeleton. Thus, a coral living in shallower (deeper) water tend to have a heavier (lighter) $\delta^{13}\text{C}_{\text{coral}}$. For instance, Dassié et al. (2013) found 0.16‰ - $\delta^{13}\text{C}_{\text{coral}}$ decreases per 1-meter increases of habitat depth ($r = 0.88$, $p < 0.01$) in five colonies of massive *Porites* spp. living in Fiji. Glottoli (1999) reported fairly consistent observation for *Porites lutea* ($p < 0.05$) and *Porites compressa* ($p < 0.01$) living in Hawaiian coral reefs, and Glottoli (2002) further demonstrated the depth effect through irradiance-regulated culturing experiments of *P. compressa* ($p < 0.01$). The fact that horizontally cored skeleton of the same Chichijima coral showed systematically $\sim 1.0\text{‰}$ lighter $\delta^{13}\text{C}_{\text{coral}}$ values than the vertically cored one (Felis et al., 2009) is also in

line with the depth effect, because a side of massive *Porites* coral becomes the shade where low irradiance and resultant less photosynthetic activities are expected. As Chichijima coral grew ~1.1 m vertically since 1910, the depth effect must have increased $\delta^{13}\text{C}_{\text{coral}}$ by 0.17‰ (Fig. 3-6).

On the other hand, through culturing experiment of massive *Porites* spp. Krief *et al.* (2010) found that pH_{SW} change, in addition to $\delta^{13}\text{C}_{\text{DIC}}$ changes, have potential to alter $\delta^{13}\text{C}_{\text{coral}}$ as a result of physiological response of coral-symbiotic systems. This effect is estimated as -0.4‰ per 0.1 pH_{SW} lowering. Because pH_{SW} decreased by 0.06 since 1910, the pH_{SW} effect must have decreased $\delta^{13}\text{C}_{\text{coral}}$ by 0.22‰ (Fig. 3-6). As these two additional drivers (depth and pH_{SW}) almost offset each other, we concluded that the Suess effect is the dominant driver of long-term $\delta^{13}\text{C}_{\text{coral}}$ decrease. Other *Porites* corals collected at the western North Pacific islands such as Ishigakijima, Guam, and Palau also show statistically significant decreasing trends after 1960 ($p < 0.01$) (Fig. 3-5).

However, it is noteworthy that the decreasing trends of $\delta^{13}\text{C}_{\text{coral}}$ are different among corals collected from the western North Pacific (i.e., Chichijima, Guam, Ishigaki and Palau) (Fig. 3-5, Table 3-1). For instance, slopes of Ishigakijima and Palau corals were smaller than those of Chichijima and Guam corals (Table 3-1). We found that the depth effect was insufficient to explain the difference in slopes (Table 3-2). Surface seawater observation using research ships since 1970s suggest that the decreasing trends of $\delta^{13}\text{C}_{\text{DIC}}$ depend on how much anthropogenic CO_2 is incorporated from the atmosphere and pristine seawater is mixed from the subsurface (Gruber *et al.*, 1999). The decreasing trend of $\delta^{13}\text{C}_{\text{DIC}}$ is steeper in the subtropical ocean than the upwelling regions in the high and low latitudes (Quay *et al.*, 2003, 1992; Gruber *et al.*, 1999). Consequently, a slope of global mean $\delta^{13}\text{C}_{\text{DIC}}$ changes in the surface ocean between the 1970s and 1990s ($-0.16 \pm 0.02\text{‰/decade}$, Quay *et al.*, 2003) is smaller than that of the contemporary atmosphere ($-0.24 \pm 0.01\text{‰/decade}$, Rubino *et al.*, 2013). Additionally, through compilation of corals distributed over tropical-subtropical Indo-Pacific regions, Swart *et al.* (2010) confirmed that $\delta^{13}\text{C}_{\text{coral}}$ are decreasing at a lower rate than $\delta^{13}\text{C}_{\text{atm}}$. Therefore, the smaller $\delta^{13}\text{C}_{\text{coral}}$ changes at Ishigaki and Palau are probably due to a stronger mixing with pristine water that originates from the equatorial upwelling and the NEC and Kuroshio transport (Fig. 2-2). Therefore, the fact that (1) trends of $\delta^{13}\text{C}_{\text{coral}}$ changes in Chichijima and Guam are identical to that of $\delta^{13}\text{C}_{\text{atm}}$ (Table. 3-1) and (2) the decreasing trend of $\delta^{13}\text{C}_{\text{DIC}}$ at the Station ALOHA (HOT, Fig. 2-2) approximately

equals that of $\delta^{13}\text{C}_{\text{atm}}$ (Table 3-3) further support the key assumption that surface water around these island lying inside of the subtropical gyre is well ventilated in terms of CO_2 .

Before 1960, we also found a statistically significant difference of decreasing trends between $\delta^{13}\text{C}_{\text{coral}}$ and $\delta^{13}\text{C}_{\text{atm}}$ ($p = 0.01$). It is presumably due to relatively lower $\delta^{13}\text{C}_{\text{coral}}$ values during 1945–1960 (A shaded area in Figs. 3-3 & 3-5). In this interval, a linear extension rate (LER) of the skeleton does not change at all (Fig. 3-3) and it is well above "1 cm/yr" below which kinetic effects matter (Hayashi et al., 2013; McConaughey, 1989). Also, no clear disturbance in the skeleton is visible (Fig. 3-3). This interval corresponds to when temperature proxies (Sr/Ca, U/Ca and $\delta^{18}\text{O}$) suggest relatively warmer condition, however previous studies do not observe any influence of temperature on $\delta^{13}\text{C}_{\text{coral}}$ (e.g., Hayashi et al., 2013; Suzuki et al., 2005). Another possibility is regionally lowered $\delta^{13}\text{C}_{\text{DIC}}$ over the western equatorial Pacific during this interval, but no synchronized variation is observed in *Porites* corals collected at Guam, Ishigakijima and Palau (a shaded area in Fig. 3-5) (Osborne et al., 2014; Mishima et al., 2010; Asami et al., 2005). Thus, it might be related to a reduced photosynthetic activity due to some local reason such as temporally increased turbidity. This hypothesis will be tested in future research through analyzing Ba/Ca ratio that is a proxy of terrigenous materials and/or suspended particles (e.g., Alibert et al., 2003). It should be noted that identification of a single mechanism of interannual to decadal scale $\delta^{13}\text{C}_{\text{coral}}$ variation is challenging, because they do not always agree among colonies even in the same region (e.g., Fiji, Dassié et al., 2013; Palau, Osborne et al., 2014).

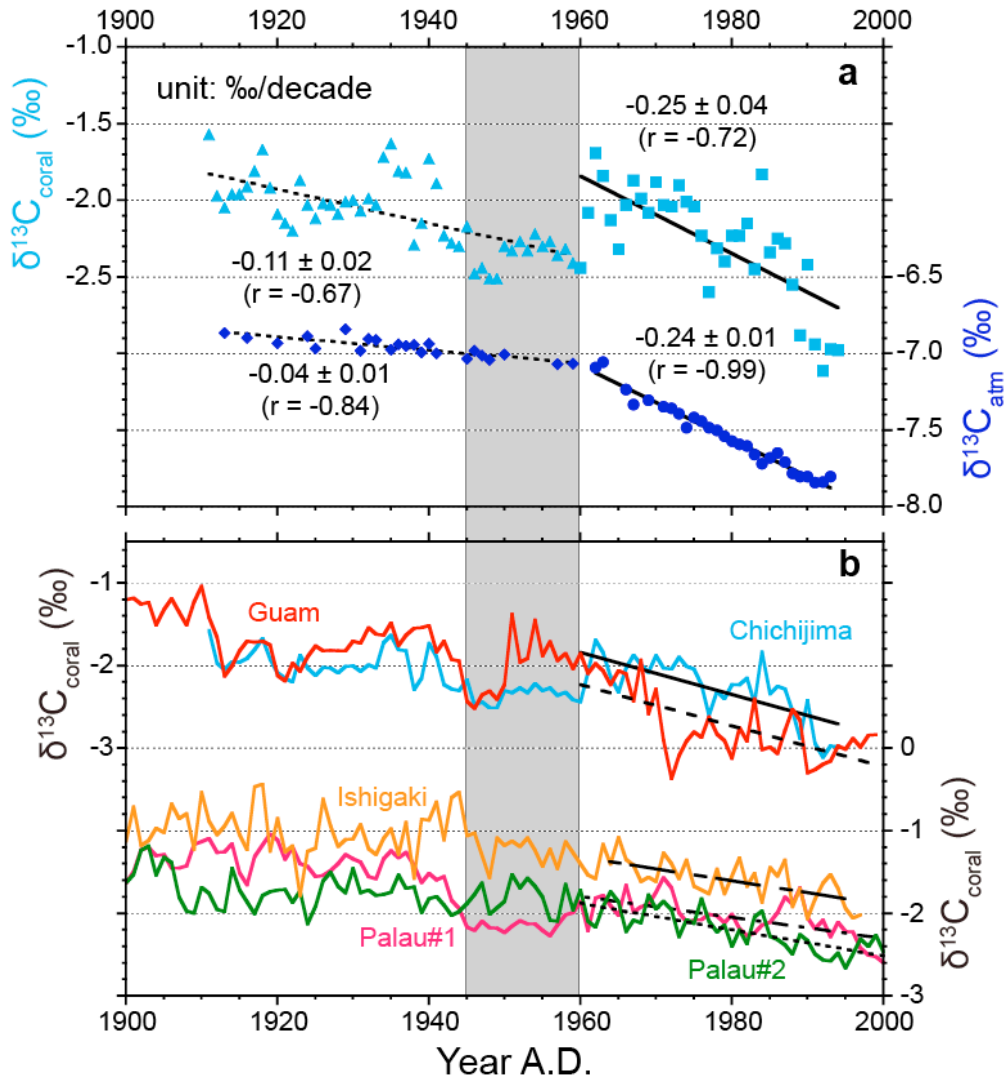


Fig. 3-5. (a) Comparison of Chichijima $\delta^{13}\text{C}_{\text{coral}}$ and $\delta^{13}\text{C}_{\text{atm}}$ records during 1911–1994 (Felis et al., 2009; Rubino et al., 2013). Linear regressions before and after 1960 are shown in black lines. All decreasing trends are statistically significant ($p < 0.01$). (b) Compiled $\delta^{13}\text{C}_{\text{coral}}$ records from the western North Pacific (Chichijima, Felis et al., 2009; Guam, Asami et al., 2005; Ishigakijima, Mishima et al., 2010; Palau, Osborne et al., 2014). Black lines indicate linear regressions of each record during 1960–2000. Slopes of Chichijima and Guam corals are identical to that of $\delta^{13}\text{C}_{\text{atm}}$, but those of Ishigakijima and Palau are not (Table 3-1).

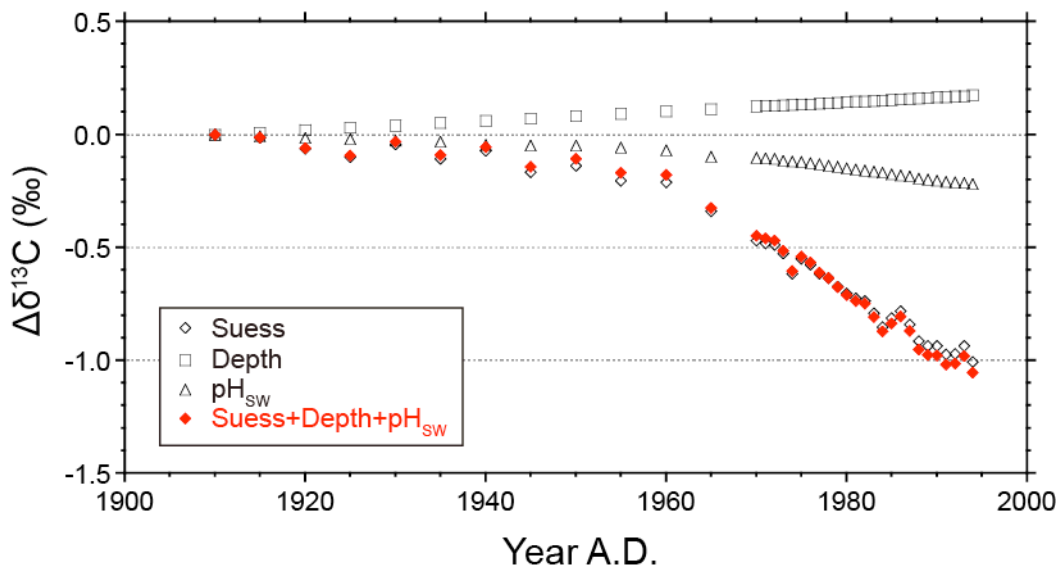


Fig. 3-6. A simulation of effects of long-term changes of pH_{SW} (Krief et al., 2010), depth (Dassié et al., 2013), and $\delta^{13}\text{C}_{\text{DIC}}$ (the Suess effect) (Rubino et al., 2013) on $\delta^{13}\text{C}_{\text{coral}}$. Δ denotes changes relative to a value of the year 1910. The pH_{SW} effect and the depth effect offset each other, consequently the Suess effect dominates net $\delta^{13}\text{C}_{\text{coral}}$ decreases.

Table 3-1. A summary of $\delta^{13}\text{C}$ slopes after 1960 of *Porites* corals collected in the western North Pacific.

	$\delta^{13}\text{C}$ slopes (‰/decade)	error (1se)	df	r	p-values		Reference
					(1)	(2)	
$\delta^{13}\text{C}_{\text{coral}}$							
Chichijima	-0.25	0.04	33	-0.72	< 0.01	0.80	Felis et al., 2009
Guam	-0.25	0.04	38	-0.70	< 0.01	0.89	Asami et al., 2005
Ishigakijima	-0.14	0.03	33	-0.65	< 0.01	< 0.01	* Mishima et al., 2010
Palau#1	-0.13	0.02	39	-0.64	< 0.01	< 0.01	Osborne et al., 2014
Palau#2	-0.16	0.02	39	-0.78	< 0.01	< 0.01	Osborne et al., 2014
$\delta^{13}\text{C}_{\text{atm}}$							
	-0.24	0.01	26	-0.99	< 0.01	–	Rubino et al., 2013

(1) Statistical significance of $\delta^{13}\text{C}$ trends after 1960 (Fig. 3-5).

(2) The null hypothesis is "there are no statistically significant difference of decreasing trends between $\delta^{13}\text{C}_{\text{coral}}$ and $\delta^{13}\text{C}_{\text{atm}}$ ".

* Unpublished data.

Table 3-2. A summary of *Porites* corals collected in the western North Pacific and expected $\delta^{13}\text{C}$ changes during 1960–2000.

Island (Location)	Depth (m)	LER (cm/yr)	$^{(1)}\Delta\delta^{13}\text{C}_{\text{Coral}}$ (‰)	$^{(2)}\Delta\delta^{13}\text{C}_{\text{Depth}}$ (‰)	Reference
Chichijima (Northern side)	5.6	1.29	-1.00	0.08	Felis et al., 2012
Guam (Double Reef)	5.8	1.60	-1.00	0.10	Asami et al., 2005
Ishigakijima (Yasurazaki)	5.0	1.65	-0.56	0.11	* Mishima et al., 2010
Palau#1 (Rock Islands)	2.0	2.05	-0.52	0.13	Osborne et al., 2014
Palau#2 (Ulong Channel)	12.0	1.36	-0.64	0.09	Osborne et al., 2014

(1) $\delta^{13}\text{C}_{\text{coral}}$ change during 1960–2000 calculated from a slope of linear regression of each coral record (Table 3-1).

(2) An predicted $\delta^{13}\text{C}$ increase due to a vertical coral growth for 40 years. A reported sensitivity of 0.16‰/m is used for the calculation ([Dassié et al., 2013](#)).

* Unpublished data.

Table 3-3. A summary of reported $\delta^{13}\text{C}_{\text{DIC}}$ changes measured at the Station ALOHA.

Interval	⁽¹⁾ $\Delta\delta^{13}\text{C}_{\text{atm}}$ (‰/yr)	$\Delta\delta^{13}\text{C}_{\text{DIC}}$ (‰/yr)	Reference
1988–2002	-0.024	-0.023	Keeling et al., 2004
1990–1999	-0.026	-0.024	Quay et al., 2003
1982–1996	-0.022	-0.025	Gruber et al., 1999

(1) $\delta^{13}\text{C}_{\text{atm}}$ changes calculated from a slope of linear regression of ice core data ([Rubino et al., 2013](#)).

3-3-3. Relationships between $\delta^{11}\text{B}$ and $\delta^{13}\text{C}$

We observed a significant positive correlation between $\delta^{11}\text{B}$ (and pH_{CF}) and $\delta^{13}\text{C}_{\text{coral}}$ ($r = 0.55$, $p = 0.04$). Long-term $\delta^{11}\text{B}$ and $\delta^{13}\text{C}_{\text{coral}}$ decreases are clearly as a result of ocean acidification and the Suess effect, respectively. On the other hand, short-term variability of them is not always correlated (Figs. 3-2 & 3-3). Similarly, those of *Porites* coral collected at Guam do not show any correlated variation in these isotopes annually during 1940–1999, although the long-term decrease trends are apparent (Shinjo et al., 2013; Asami et al., 2005). Therefore, it indicates that short-term $\delta^{11}\text{B}$ and $\delta^{13}\text{C}_{\text{coral}}$ variations are not necessarily controlled by the same mechanism. For instance, Hönisch et al. (2004) reports that $\delta^{13}\text{C}$ of *P. compressa* depends on the irradiance but $\delta^{11}\text{B}$ of it does not. The reason why $\delta^{11}\text{B}$ varies in interannual timescales is still unknown, thus further investigations of drivers of short-term $\delta^{11}\text{B}$ variability is needed (this issue will be discussed in Chapter 5). Again, we emphasize that short-term variability of $\delta^{11}\text{B}$ and $\delta^{13}\text{C}_{\text{coral}}$ do not affect the conclusion derived from pH_{CF} and pH_{SW} comparison discussed in the subsequent section.

3-3-4. Sensitivity of pH_{CF} to pH_{SW} decrease

We found large differences between pH_{SW} (8.12 to 8.18) and pH_{CF} (8.47 to 8.53) derived from $\delta^{11}\text{B}$ of corals and a theoretical curve of $\delta^{11}\text{B}$ of borate ion (Fig. 3-7, Table 3-4). One plausible explanation for the fact that pH_{CF} was higher than pH_{SW} is the proposed “pH up-regulation mechanism” (Venn et al., 2013, 2011; McCulloch et al., 2012a,b; Trotter et al., 2011; Cohen & Holcomb, 2009; Al-Horani et al., 2003). Calcification fluid exists between the coral polyp and the underlying skeleton (extracellular), being semi-isolated from the ambient seawater. Corals spontaneously elevate their pH_{CF} to promote calcification processes in which the function of Ca^{2+} -ATPase is playing a key role for pumping H^{+} out of and Ca^{2+} into the calcification fluid, which in turn increase pH_{CF} and Ω_{ar} ($\Omega_{\text{ar CF}}$). *In situ* pH_{CF} measurements using micro-pH electrodes, visualization using pH-sensitive dye, and observation of mineralogy between biologically precipitated and inorganically synthesized aragonite all support the idea of pH up-regulation (Venn et al., 2013, 2011; Cohen & Holcomb, 2009; Al-Horani et al., 2003). It has been anticipated from this mechanism that *Porites*

corals as well as other scleractinian coral genera can maintain their pH_{CF} under ongoing OA (Venn et al., 2013; McCulloch et al., 2012a,b). Therefore, corals are able to raise ΔpH to keep pH_{CF} as high as possible, due perhaps to homeostasis in calcification in their body (Fig. 3-7). The observation that deep-sea corals have larger ΔpH value than reef-building coral is in line with this idea that the system need to overcome to the stress from more corrosive abyssal seawater than the over-saturated surface sea waters (McCulloch et al., 2012b).

The relationship between pH_{SW} and pH_{CF} for two cultured *Porites* corals (Krief et al., 2010; Hönisch et al., 2004) predict a 0.03 and 0.05 pH_{CF} decline, respectively, per 0.1 pH_{SW} (Fig. 3-7), which suggests that coral $\delta^{11}\text{B}$ may not be sensitive enough to detect anthropogenic OA. However, we discovered clear indication of rapid decline in pH_{CF} of the Chichijima coral with the decline of pH_{SW} , which was not found in cultured corals (Fig. 3-7). Although ΔpH values are similar (0.3–0.5) in the present pH_{SW} range of 8.09–8.17 among corals in the field and cultured environments, rates of ΔpH change for both cases are significantly different ($p < 0.01$) (Fig. 3-7). Furthermore, we found that pH_{CF} change of Chichijima coral is more sensitive than any other previously available scleractinian corals (e.g., *Acropora*, *Stylophora*, and *Cladocora*; $p < 0.03$) cultured to date, and their pH_{CF} were estimated from $\delta^{11}\text{B}$ (Fig. 3-8) (Holcomb et al., 2014; Trotter et al., 2011; Krief et al., 2010; Raynaud et al., 2004; Hönisch et al., 2004). If the relationships between pH_{SW} and pH_{CF} in Chichijima coral are used to project future response to OA, pH_{CF} is about 8.3 and about 7.9 when $\Omega_{\text{ar SW}}$ is 3.3 ($\text{pH}_{\text{SW}} = \text{c.a. } 8.04$) and 2 ($\text{pH}_{\text{SW}} = \text{c.a. } 7.78$), respectively (Fig. 3-7). The magnitude of pH_{CF} decrease is dramatically higher in Chichijima coral than in that predicted from cultured corals (i.e., 8.4–8.5 when $\Omega_{\text{ar SW}} = 3.3$ and 8.3–8.4 when $\Omega_{\text{ar SW}} = 2$).

Because pH up-regulation demands significant energy for calcification, keeping constant ΔpH (Fig. 3-7) seems reasonable from a biological adaptation point of view (McCulloch et al., 2012a,b; Kleypas & Yates, 2009; Cohen & Holcomb, 2009). However, lower pH_{CF} under OA leads to slower calcification of corals, which will make their skeletons more susceptible to bio-erosions, leading to disadvantages in competition with other organisms such as grazers, burrowers, and macroalgae (Crook et al., 2013; Pandolfi et al., 2011). Given that Ca^{2+} concentration in calcification fluid is almost same as that in seawater (< 10% change, Cohen & Holcomb, 2009), sensitive pH_{CF} decrease will lead to faster $\Omega_{\text{ar CF}}$ decrease, as it is pH_{CF} that regulates $\Omega_{\text{ar CF}}$. Thus, it is

reasonable to believe that OA overwhelms or disables their pH_{CF} homeostasis rather than the coral spontaneously regulate their pH_{CF} (Hoegh-Guldberg et al., 2007). The observation of one-to-one relationship between pH_{CF} and pH_{SW} suggests the relationship in current pH ranges (8.1–8.2) is more straightforward than previously thought (Chapter 2). Therefore, it not only strengthens the reliability of coral $\delta^{11}\text{B}$ as pH_{SW} proxy (Chapter 4; Kubota et al., 2014), but also will pave the way for studying OA using coral $\delta^{11}\text{B}$ in diverse coral reef settings.

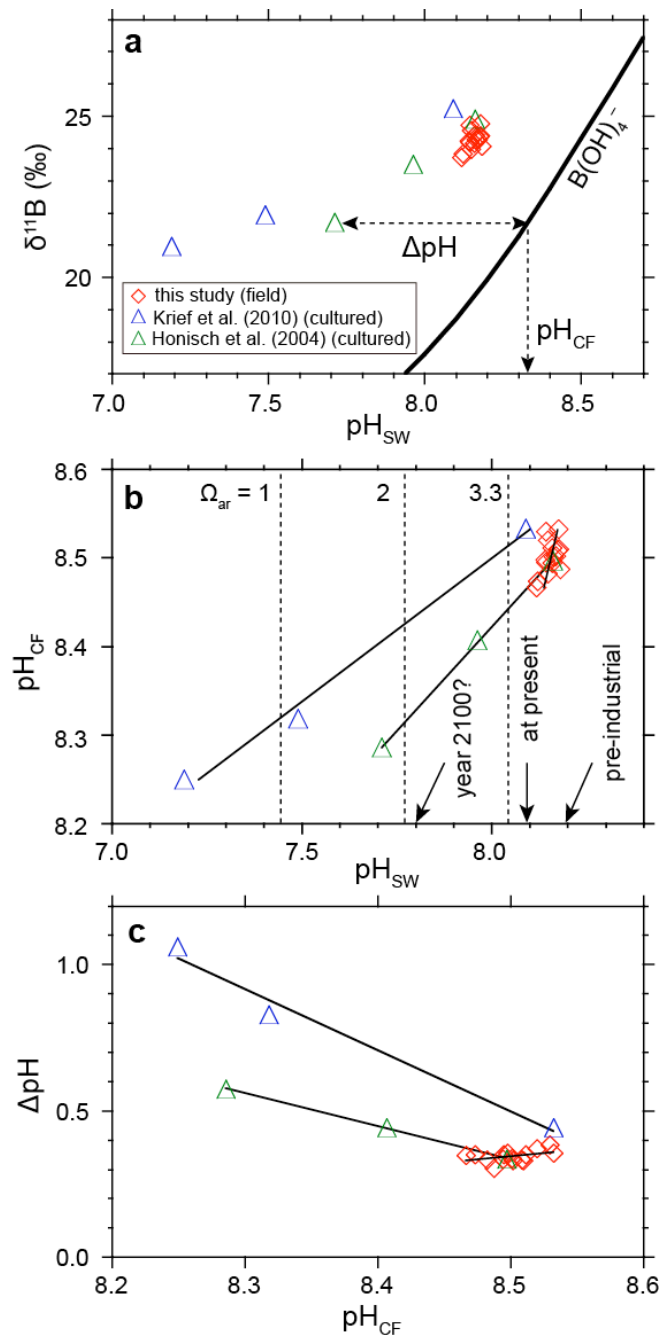
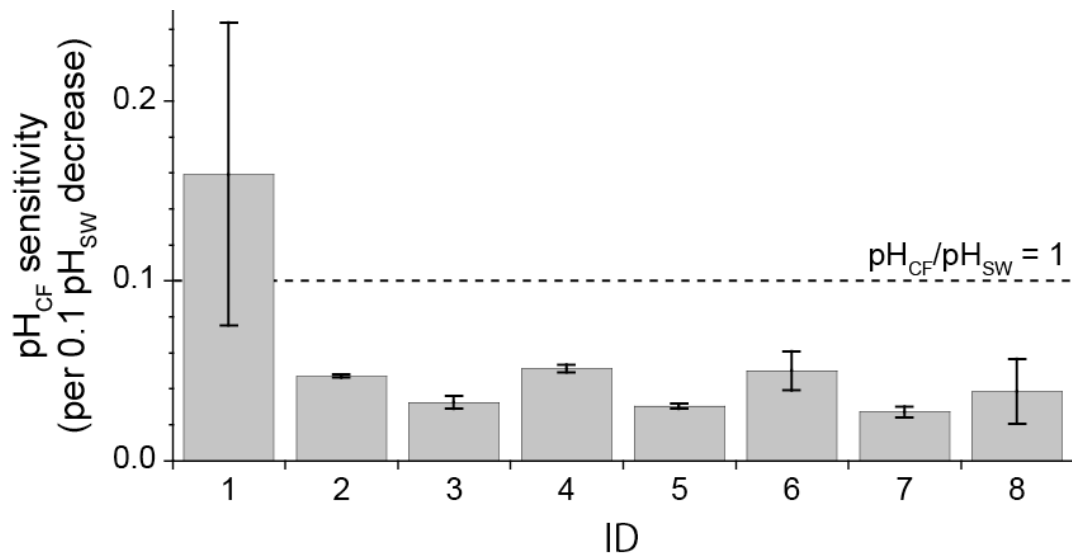


Fig. 3-7. (a) $\delta^{11}\text{B}$ values of Chichijima *Porites* spp., cultured *Porites* spp. (Krief et al., 2010), and cultured *Porites cylindrica* (Hönisch et al., 2004) with the theoretical curve of $\delta^{11}\text{B}$ of borate ion in the seawater (Klochko et al., 2006). (b) A cross plot of pH_{CF} versus pH_{SW} . Regression lines are shown for each coral record. Dashed vertical lines indicate pH_{SW} when $\Omega_{\text{ar SW}}$ become 3.3, 2, and 1 that were calculated using present SST, SSS, and TA. (c) as **b** but for pH_{CF} versus ΔpH .



1. <i>Porites</i> spp.	(This study)	5. <i>Stylophora pistillata</i>	(Krief et al., 2010)
2. <i>Porites cylindrica</i>	(Honisch et al., 2004)	6. <i>Acropora</i> spp.	(Reynaud et al., 2004)
3. <i>Porites</i> spp.	(Krief et al., 2010)	7. <i>Stylophora pistillata</i>	(Holcomb et al., 2014)
4. <i>Acropora nobilis</i>	(Honisch et al., 2004)	8. <i>Cladocora caespitosa</i>	(Trotter et al., 2011)

Fig. 3-8. Sensitivities of pH_{CF} against "0.1 pH_{SW} decrease" for Chichijima coral and the cultured scleractinian corals. Error bars are 1 se.

Table 3-4. Measured $\delta^{11}\text{B}$ values of Chichijima coral, estimated pH_{SW} , and calculated pH_{CF} from $\delta^{11}\text{B}$ values.

Sample name	$\delta^{11}\text{B}_{\text{P-TIMS}}$ ave.	pH_{SW}	pH_{CF}	ΔpH
OGA02_3Y_1997	23.84	8.118	8.47	0.36
OGA02_3Y_1992	23.84	8.124	8.47	0.35
OGA02_3Y_1987	24.22	8.130	8.50	0.37
OGA02_3Y_1982	23.89	8.137	8.48	0.34
OGA02_3Y_1977	24.17	8.144	8.49	0.35
OGA02_3Y_1972	24.71	8.150	8.53	0.38
OGA02_3Y_1966	24.16	8.155	8.49	0.34
OGA02_3Y_1960	24.43	8.160	8.51	0.35
OGA02_3Y_1954	24.56	8.162	8.52	0.36
OGA02_3Y_1948	24.28	8.164	8.50	0.34
OGA02_3Y_1942	24.28	8.167	8.50	0.33
OGA02_3Y_1935	24.38	8.168	8.51	0.34
OGA02_3Y_1928	24.76	8.170	8.53	0.36
OGA02_3Y_1921	24.06	8.173	8.49	0.31
OGA02_3Y_1914	24.41	8.175	8.51	0.33

3-3-5. Environmental stressors for Chichijima corals and implications for future coral reefs

Future pH_{SW} and pH_{CF} levels will likely decrease until CO_2 emission ceases completely, since the residence time of anthropogenic CO_2 in the surface seawater is on a century-long scale (Zeebe, 2012; Gattuso & Hansson, 2011; Feely et al., 2009; Tans, 2009; Orr et al., 2005; Caldeira & Wickett, 2003). In the western North Pacific, $\Omega_{\text{ar SW}}$ has already reached the threshold value of 3.3 in winter and annual average $\Omega_{\text{ar SW}}$ will also reach 3.3 by the year 2035, given linear extrapolation of the current trend (-0.01/year, Ishii et al., 2011) (Fig. 3-1). In addition to pH_{SW} and $\Omega_{\text{ar SW}}$, temperature is another important factor for corals since coral-dinoflagellate symbiosis is strongly temperature-dependent. Coral bleaching will occur upon dinoflagellate release if temperature exceeds corals' thermal tolerance, which sometimes leads to mortality as corals heavily depend on organic carbon supplied by symbiotic organisms (Pandolfi et al., 2011; Kleypas & Yates, 2009). The coral reefs of the Ogasawara Islands are being threatened by regional warming. Recently, mass bleaching events struck coral reef communities in summer of 2003 and 2009 (Biodiversity Center of Japan, 2009). Moreover, the core top—the most recent portion of the coral skeleton—analyzed in this study (1998–2002) showed unsystematic behaviors of its trace element based paleo-thermometer (Sr/Ca and U/Ca ratios) (Felis et al., 2009). These phenomena are likely related to thermal stresses due to regional warming (Yamano et al., 2011), yet we also speculate that ongoing OA is another potential stressor, as $\Omega_{\text{ar SW}}$ is already close to its threshold value of 3.3 (Fig. 3-7). One modeling study predicts that coral reefs will disappear from the coastal regions of Japan earlier than the mid-21st century due to simultaneous degradation of living conditions in higher and lower latitudes, that is, acidification in the north and warming in the south, although there is the possibility of northward migration and adaptation (or even eventual evolution) of corals as well as uncertainties in the threshold of their responses to temperature and $\Omega_{\text{ar SW}}$ (Yara et al., 2012).

Most coral reefs, including those at Chichijima, receive good circulation from open ocean seawater. Open oceans will acidify more rapidly than isolated reefs, which are characterized by a long residence time of seawater that is buffered by dissolution of reef sediments, mitigating acidification (Eyre et al., 2014; Andersson et al., 2014; Kleypas &

Yates, 2009). If the sensitivity of Chichijima coral to OA can be regarded as representative of that of other corals, it follows that many coral reefs surrounding oceanic islands in the wider subtropics might be in more danger than originally thought. Thermal stratification of seawater projected in a high-CO₂ scenario will also deteriorate nutrient availability for corals, which likely increases coral vulnerability since poorly nourished corals are more susceptible to OA (Pandolfi et al., 2011). Ecological regime shifts, such as from coral- to macroalgae- or soft coral- dominated reefs, are possible when environmental stresses exceed a given threshold (Inoue et al., 2013; Fabricius et al., 2011; Kleypas & Yates, 2009; Hall-Spencer et al., 2008).

However, we note that there are large uncertainties in predicting the thresholds for each coral colony and each coral reef community on both global and regional scales. This is because global and local stressors interact with each other in a highly complex fashion (e.g., OA, global warming, destructive fishing, sediment influx) and coral response can vary within and among coral species (Pandolfi et al., 2011; Hoegh-Guldberg et al., 2007). For example, *Porites* coral from Guam (Shinjo et al., 2013) display high sensitivity to the Suess effect (a large $\delta^{13}\text{C}_{\text{coral}}$ decrease) but little sensitivity to OA (a slight $\delta^{11}\text{B}$ decrease), and opposite trends are seen in *Porites* coral from Hainan Island (Liu et al., 2014). To date, many studies have attempted to learn how massive *Porites* corals respond to OA, but results contradict significantly each other (e.g., Iguchi et al., 2014, 2012; Comeau et al., 2014; Crook et al., 2013; Déath et al., 2012, 2009; Cooper et al., 2012; Fabricius et al., 2011). Through culturing experiments under artificially acidified seawater, it is shown that the corals had different responses to OA: Comeau et al. (2014) found no evidence of negative effects of OA on *Porites* spp., whereas Iguchi et al. (2014, 2012) found a significant calcification rate decrease of *Porites australiensis* even under a modest acidification, that is ~ 0.1 pH_{SW} decrease after industrialization. From a field observation on naturally acidified CO₂ seep sites in Mexico, Crook et al. (2013) reports that *Porites asteroides* living in $\Omega_{\text{ar SW}}$ of less than ~ 2 have low-density skeletons and are prone to biological erosion in spite of ample time for acclimation. Similarly, Fabricius et al. (2011) found that massive *Porites* corals living in the CO₂ seep sites in Papua New Guinea have lower calcification rates compared with those living in the natural seawater over the Indo-Pacific region. Past 400-years reconstructions using massive *Porites* corals living in the Great Barrier Reef, the northeastern Australia suggest recent steep decreases of calcification rates, densities,

and growth rates of the corals after 1960s (Déath et al., 2012, 2009). On the contrary, however, calcification rate of massive *Porites* corals living in the western Australia (17–28°S) have increased recently, which may relate to global warming's positive effect (Cooper et al., 2012).

These observations suggest that corals living in natural environments may have different responses to OA depending on the environmental factors of individual reefs. Therefore, more field-based studies using the $\delta^{11}\text{B}$ technique are needed to understand how corals have adapted to OA, before corals disappear due to physical, chemical, and biological erosions (Pandolfi et al., 2011; Hoegh-Guldberg et al., 2007).

3-4. Conclusion

We used $\delta^{11}\text{B}$ values of *Porites* coral collected at Chichijima (Ogasawara Archipelago) to estimate pH_{CF} changes for the last 100 years. $\delta^{11}\text{B}$ values showed a decline and its rate of decrease was accelerated after 1960 ($-0.17 \pm 0.07\text{‰}/\text{decade}$, $p = 0.05$). The observation was in line with pH_{SW} decrease (i.e., OA) estimated from atmospheric $p\text{CO}_2$ increase. ΔpH remained almost constant values, suggesting pH_{CF} has decreased overcoming homeostasis of calcification fluid. Importantly, a rate of pH_{CF} decrease was significantly faster (ca. $0.2 \text{ pH}_{\text{CF}} / 0.1 \text{ pH}_{\text{SW}}$ decrease) than those of two *Porites* corals that have cultured under the artificially acidified seawater (ca. $0.03\text{--}0.05 \text{ pH}_{\text{CF}} / 0.1 \text{ pH}_{\text{SW}}$ decrease). We also found a significant positive relationship between coral $\delta^{13}\text{C}$ and $\delta^{11}\text{B}$, indicating these phenomena were originated from anthropogenic sources. In association with global warming, OA will perhaps lead to significant consequences because a pH_{CF} decrease and a resultant $\Omega_{\text{ar CF}}$ decrease will likely make coral's calcium carbonate skeletons more vulnerable to erosions. As winter $\Omega_{\text{ar SW}}$ is already below a threshold value of 3.3 in the western North Pacific, it suggests that many coral reefs including Chichijima's are more in danger than we thought.

CHAPTER 4

Marine carbon cycle at the equatorial Pacific during the last deglaciation

Chapter 4 Abstract

While physical and biogeochemical processes in the Southern Ocean are thought to be central to atmospheric CO₂ increases during the last deglaciation, the roles of the equatorial Pacific, where the largest CO₂ source currently exists, remains largely unconstrained. In this chapter we present pH_{SW} and pCO_{2 SW} variations from fossil *Porites* corals collected from Tahiti based on a newly calibrated δ¹¹B-pH_{SW} proxy. The new data, together with recalibrated existing data, indicate that significant pCO_{2 SW} increases (pH_{SW} decreases), accompanied by anomalously large marine ¹⁴C reservoir ages, happened following not only the Younger Dryas, but also Heinrich Stadial 1. These findings indicate an expanded zone of equatorial upwelling and resultant CO₂ emission, which may be caused by higher subsurface DIC concentration.

4-1. Introduction

Atmospheric $p\text{CO}_2$ increased by ~ 80 μatm during the last deglaciation, with ~ 50 μatm released during Heinrich Stadial 1 (HS1, from 17.5 to 14.6 kyr), followed by an additional ~ 30 μatm during the Younger Dryas (YD, from 12.9 to 11.7 kyr) (Lourantou et al., 2010). While the Southern Ocean is generally considered to be central to the deglacial CO_2 rise (e.g., Siani et al., 2013; Matsumoto & Yokoyama, 2013; Burke & Robinson, 2012; Yokoyama & Esat, 2011; Skinner et al., 2010; Rose et al., 2010; Anderson et al., 2009; Toggweiler et al., 2006), the contribution from other oceanic regions remains largely uninvestigated (Foster & Sexton, 2014; Henehan et al., 2013; Yu et al., 2013; Douville et al., 2010; Foster, 2008; Palmer & Pearson, 2003). Information on $p\text{CO}_2$ $_{\text{sw}}$ is needed to directly constrain past air-sea CO_2 exchange. It can be reconstructed from $\delta^{11}\text{B}$ of marine carbonates, pH_{sw} proxy (Hönisch et al., 2007). Regions where surface seawater CO_2 is out of equilibrium with the atmosphere are ideal for such studies. Thus, the equatorial Pacific is particularly well suited because it represents the largest global CO_2 source at present (e.g., Sutton et al., 2014; Takahashi et al., 2009; Gruber et al., 2009; Feely et al., 2006, 2002). Corals living in tropical to subtropical regions are good archives for paleo- CO_2 studies because they can be dated precisely using U-series radiogenic isotopes (Yokoyama & Esat, 2011; Deschamps et al., 2012), unlike foraminifers that may be affected by ^{14}C marine reservoir ages (R).

Two previous studies have attempted to reconstruct equatorial Pacific pH_{sw} and $p\text{CO}_2$ $_{\text{sw}}$ changes. Palmer & Pearson (2003) showed increased CO_2 emission during the last deglaciation in the western equatorial Pacific (WEP) from $\delta^{11}\text{B}$ measurements on the planktonic foraminifer (*Globigerinoides sacculifer*) in a sediment core recovered from offshore Papua New Guinea (ERDC-92, Fig. 4-1). Douville et al. (2010) performed $\delta^{11}\text{B}$ on fossil corals collected from the Marquesas (9.5°S 139.4°W, Fig. 4-1). They also demonstrated that CO_2 emission increased at the end of the YD. However they did not observe a significant CO_2 release during HS1. It complicates interpretation of the equatorial Pacific's contribution to deglacial atmospheric CO_2 rise. Integrated Ocean Drilling Program Expedition 310 (IODP Exp. 310, Camoin et al., 2007) drilled the outer reef slope at Tahiti (17.6°S 149.5°W, Fig. 4-1) recovering fossil corals from an open ocean environment spanning HS1. Therefore, we can assess the issue. Furthermore,

previous estimation was based on out-of-date fractionation factor between boric acid and borate ions reported by Kakihana *et al.* (1977). Thus we refined the calibration (Chapter 2) and obtained the new pH_{SW} and $\text{pCO}_{2\text{ SW}}$ estimations since the last glacial maximum (LGM).

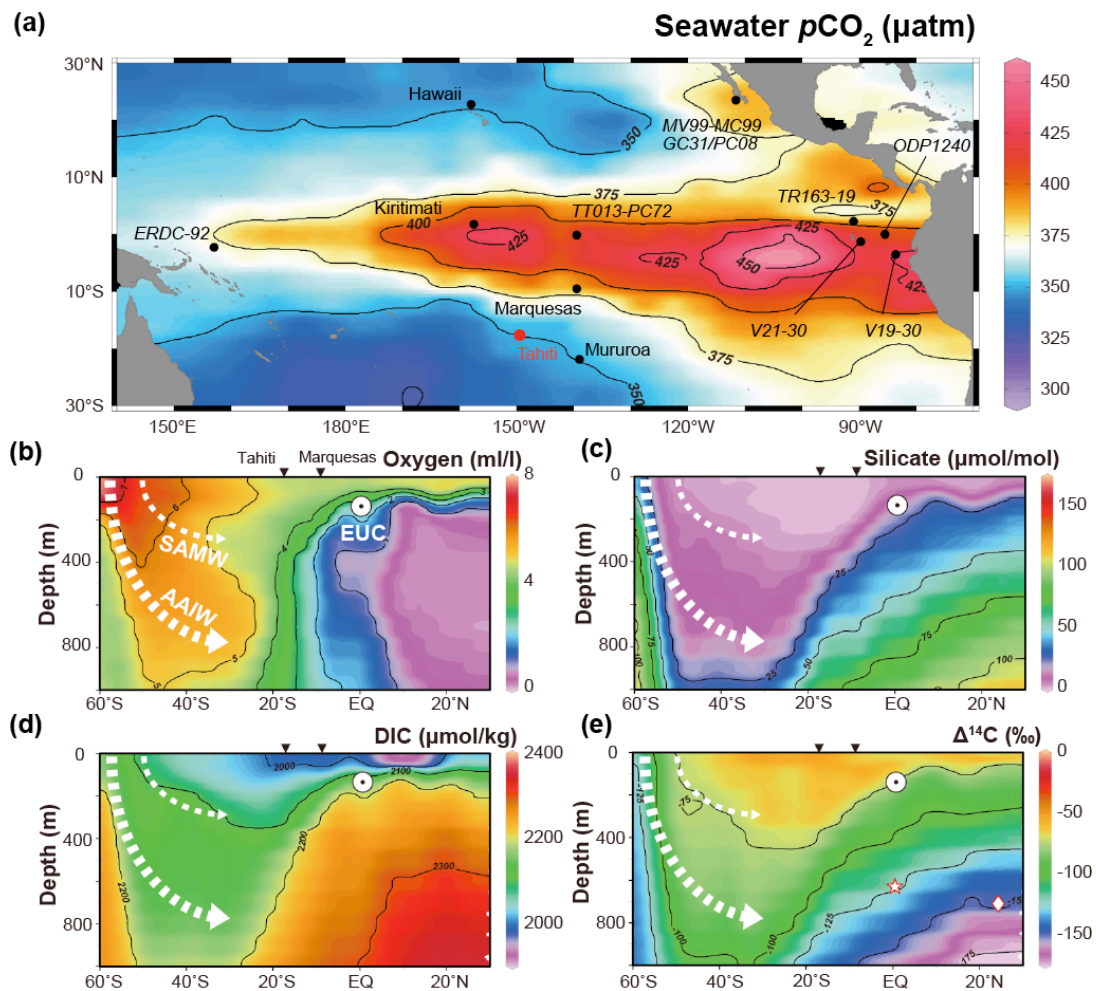


Fig. 4-1. $p\text{CO}_2$ sw in the equatorial Pacific and vertical sections from 60 °S to 30 °N of the South Pacific. (a) $p\text{CO}_2$ sw for the reference year AD 2000 in which red and blue colours represent CO_2 sources and sinks, respectively (Takahashi et al., 2009). Vertical sections of (b) oxygen, (c) silicate, (d) DIC, and (e) $\Delta^{14}\text{C}$. Data source is “World Ocean Atlas 2009 > annual” for oxygen and silicate, “Global Alkalinity & TCO_2 > annual” for DIC (Goyet et al., 2000), and “GLODAP Gridded Data” for $\Delta^{14}\text{C}$ (Key et al., 2004). All data were downloaded via <http://odv.awi.de/en/data/> and plotted using Ocean Data View software version 4.6.2 (Schlitzer, 2014). Inverted black triangles represent locations of Tahiti and Marquesas. The star and diamond indicate the locations of cores MV99-MC99/GC31/PC08 (Basak et al., 2010; Marchitto et al., 2007) and V21-31 (Stott et al., 2009), respectively. SAMW, Subantarctic Mode Water; AAIW, Antarctic Intermediate Water; EUC, Equatorial Undercurrent.

4-2. Material and Methods

4-2-1. $\delta^{11}\text{B}$ -pH_{SW} calibration

The way of $\delta^{11}\text{B}$ -pH_{SW} calibration used for Tahiti and Marquesas areas is described in Chapter 2. Using the new calibration methodology we calculated pH_{SW} from both previously reported and newly obtained $\delta^{11}\text{B}$ values considering a local difference of pH_{SW} between Tahiti and Marquesas (Fig. 2-8). We further calculated $p\text{CO}_2$ from obtained pH_{SW} values from $\delta^{11}\text{B}$ using CO2calc software under assumptions of constant SST, SSS, and TA. We did not include the $\delta^{11}\text{B}$ values of *G. sacclifer* (Palmer & Pearson, 2003) here due to large uncertainties in the $\delta^{11}\text{B}$ -pH_{SW} calibration (e.g., Henehan et al., 2013; Foster, 2008).

4-2-2. $\delta^{11}\text{B}$ analysis of Tahitian fossil corals

The $\delta^{11}\text{B}$ values of fossil *Porites* spp. that were obtained under the program of IODP Exp. 310 were measured using the P-TIMS method according to the protocol of Ishikawa and Nagaishi (2011). Fossil corals were screened for diagenetic alteration with X-ray diffraction (XRD) and geochemical analyses (e.g., Mg/Ca, Hathorne et al., 2011), and visual using a Scanning Electron Microscope (SEM) (Inoue et al., 2010). We conducted bulk sampling along the growth axis, and time resolution of each sample is several years (1 - 8 years) depending on growth rate of each coral (Inoue et al., 2010). We used typically 6 mg of carbonate for the $\delta^{11}\text{B}$ measurement. After removals of organic matter using 30% H₂O₂ for ~12 hours, we purified boron by cation and anion exchange and then $\delta^{11}\text{B}$ were measured using the P-TIMS (Thermo Finnigan TRITON) at Kochi Institute for Core Sample Research. All reported $\delta^{11}\text{B}$ values are the mean of duplicate analyses (Table 4-1). Repeated analysis of the JCp-1 yielded 24.21 ± 0.18 ‰ (2 σ , n = 18) (Okai et al., 2004). We used ± 0.14 ‰ as the analytical uncertainty of $\delta^{11}\text{B}$ measurements.

Table 4-1. The $\delta^{11}\text{B}$ values of *Porites* corals and calculated pH_{sw} and $p\text{CO}_2$ (after Kubota *et al.* (2014)).

Location	'Sample ID	^{14}C -age (Years BP)		$\delta^{11}\text{B}$ values (‰)		pH		$p\text{CO}_2$ (μatm)		$\Delta p\text{CO}_2$ (μatm)	
		1 σ	Reference	'mean	2 σ	Reference	2 σ	2 σ	2 σ		
Fossil											
Tahiti	310-M0005B-3R-1W_58-67 (3116500)	10387	Inoue <i>et al.</i> , 2010	26.29	0.18	This study	8.213	0.013	251	11	-12
Tahiti	310-M0005C-8R-2W_0-5 (3116758)	10608	Inoue <i>et al.</i> , 2010	26.13	0.18	This study	8.200	0.014	261	10	-7
Tahiti	310-M0007A-18R-1W_76-90 (3113922)	10030	Deschamps <i>et al.</i> , 2012; Durand <i>et al.</i> , 2013	26.04	0.18	This study	8.191	0.014	268	11	8
Tahiti	310-M0007A-18R-1W_28-58 (3113876)	10030	Deschamps <i>et al.</i> , 2012; Durand <i>et al.</i> , 2013	25.64	0.18	This study	8.163	0.014	292	13	32
Tahiti	310-M0007B-21R-1W_0-20 (3114984)	11035	Deschamps <i>et al.</i> , 2012; Hathorne <i>et al.</i> , 2011	25.49	0.18	This study	8.149	0.014	304	13	42
Tahiti	310-M0018A-18R-1W_40-50 (3125580)	14273	Durand <i>et al.</i> , 2013	26.39	0.18	This study	8.214	0.013	250	10	11
Tahiti	310-M0018A-18R-1W_50-63 (3125582)	14273	Durand <i>et al.</i> , 2013	25.51	0.18	This study	8.154	0.014	300	12	61
Tahiti	310-M0009D-7R-1W_11-28 (3105506)	14217	Deschamps <i>et al.</i> , 2012; Durand <i>et al.</i> , 2013; Asami <i>et al.</i> , 2009	25.73	0.18	This study	8.166	0.014	289	12	50
Tahiti	310-M0023A-6R-1W_48-62 (3101822)	12404	Asami <i>et al.</i> , 2009	25.58	0.18	This study	8.166	0.014	289	12	43
Tahiti	310-M0024A-11R-1W_77-90 (3111904)	14994	Deschamps <i>et al.</i> , 2012; Durand <i>et al.</i> , 2013	26.20	0.18	This study	8.206	0.014	256	11	28
Tahiti	310-M0024A-11R-1W_60-75 (3111884)	14994	Deschamps <i>et al.</i> , 2012; Durand <i>et al.</i> , 2013	24.82	0.18	This study	8.093	0.015	359	15	131
Tahiti	310-M0024A-11R-2W_25-61 (3111958)	14997	Felis <i>et al.</i> , 2012; Durand <i>et al.</i> , 2013; Dechamps <i>et al.</i> , 2012	25.82	0.18	This study	8.173	0.014	283	12	55
Tahiti	310-M0024A-12R-2W_140-150 (3112030)	15080	Deschamps <i>et al.</i> , 2012	26.10	0.18	This study	8.187	0.014	271	11	43

<i>Continued</i>													
Tahiti	310-M0024A-12R-2W_62-80 (3112024)	15075	29	Deschamps et al., 2012	26.04	26.07	0.18	This study	8.195	0.014	265	11	37
Tahiti	310-M0024A-13R-1W_32-41 (3112052)	15149	15.5	Deschamps et al., 2012; Durand et al., 2013	26.09 25.14	25.18	0.18	This study	8.125	0.015	327	13	99
Tahiti	Ta P8-348	12910	30	Bard et al., 1996	25.21	25.9	0.25	Douville et al., 2010	8.149	0.020	304	18	66
Tahiti	Ta P8-353	13335	30	Bard et al., 1996	25.21	26.6	0.25	Douville et al., 2010	8.203	0.019	259	15	21
Marquesas	Eiao DR16(3)	8990	130	Cabioch et al., 2008	25.21	26.0	0.25	Douville et al., 2010	8.179	0.020	267	18	11
Marquesas	Eiao DR16(5)	9110	130	Cabioch et al., 2008	25.21	26.3	0.25	Douville et al., 2010	8.203	0.019	245	16	-11
Marquesas	Eiao DR12(1)	9590	180	Cabioch et al., 2008	25.21	26.2	0.25	Douville et al., 2010	8.195	0.019	253	16	-6
Marquesas	DW1281 75a2	11470	90	Pateme et al., 2004	25.21	24.8	0.25	Douville et al., 2010	8.077	0.022	375	27	112
Marquesas	DW1281 75a2	11470	90	Pateme et al., 2004	25.21	24.5	0.25	Douville et al., 2010	8.050	0.023	408	29	145
Marquesas	Hiva Oa DR10(2)	12420	100	Cabioch et al., 2008	25.21	26.2	0.25	Douville et al., 2010	8.195	0.019	253	16	8
Marquesas	Eiao DR11bis(4)	13410	190	Cabioch et al., 2008	25.21	25.6	0.25	Douville et al., 2010	8.147	0.021	298	20	60
Marquesas	Eiao DR8(1)	14560	180	Cabioch et al., 2008	25.21	26.1	0.25	Douville et al., 2010	8.187	0.020	260	18	21
Marquesas	Hiva Oa DR14bis(1)	15450	150	Cabioch et al., 2008	25.21	26.1	0.25	Douville et al., 2010	8.187	0.020	260	18	35
Marquesas	Hiva Oa DR8bis(1)	15460	110	Cabioch et al., 2008	25.21	26.4	0.25	Douville et al., 2010	8.211	0.019	239	16	14
Marquesas	Hiva OaDR5	20720	200	Cabioch et al., 2008	25.21	27.1	0.25	Douville et al., 2010	8.263	0.018	197	14	10
Modern													
Moorea	COM2	(1991)				25.3	0.30	Gaillardet & Allegre, 1995	8.096	0.025	356	25	-15
Moorea	MOO 3A-1-02	(1950)				25.8	0.25	Douville et al., 2010	8.145	0.023	308	20	-10
Marquesas	Niuku Hiva DR6(1)	250	30	Cabioch et al., 2008		26.2	0.25	Douville et al., 2010	8.205	0.022	244	18	-17
		(1700)											

- (1) Original sample code of IODP Exp. 310 and sample code in individual laboratories.
- (2) Calendar age of fossil corals. For 310-M0005B-3R-1W_58-67 and 310-M0005C-8R-2W_0-5, dating was conducted by ^{14}C dating method (Inoue et al., 2010).
- (3) Boron isotope values for this study are average values of duplicate analysis. Those for Douville et al. (2010) are mainly of replicate analysis.
- (4) pH for Marquesas were added by 0.04 after calculation for comparison. pK_B for Tahiti-Moorea and Marquesas are listed in Table 2-3.

4-2-3. Marine ^{14}C reservoir age compilation

We compiled published ^{14}C (radiocarbon years) and U/Th ages of fossil corals obtained during IODP Exp. 310 in order to calculate residual radiocarbon activities ($\Delta^{14}\text{C}$) and R. We verified that the exact same samples were selected via sample ID and core photographs (Camoin et al., 2007). In some cases different part of the skeleton of the same coral was dated. Given that coral lifetimes are generally less than several decades, temporal gaps derived from sub-sampling are negligible in the calculations of $\Delta^{14}\text{C}$ and R. We did not use ^{14}C ages from either microbialite or encrusting coralline algae (Seard et al., 2010). We made calculation using an original radiocarbon data ($^{14}\text{C}_{\text{age}}$) before a local R correction (Burr et al., 2009; Adkins & Boyle, 1997).

$$\Delta^{14}\text{C}_{\text{marine}} = \left(\frac{e^{-\frac{^{14}\text{C}_{\text{age}}}{8033}}}{e^{-\frac{(\text{U/Th})_{\text{age}}}{8266}}} - 1 \right) * 10^3 \quad (\text{‰}) \quad (\text{Eq. 4-1})$$

$$\begin{aligned} R &= 8033 * \ln \left(\frac{\Delta^{14}\text{C}_{\text{atm}} + 10^3}{\Delta^{14}\text{C}_{\text{marine}} + 10^3} \right) \\ &= {}^{14}\text{C}_{\text{age(marine)}} - {}^{14}\text{C}_{\text{age(atm)}} \end{aligned} \quad (\text{Eq. 4-2})$$

Atmospheric $\Delta^{14}\text{C}$ ($\Delta^{14}\text{C}_{\text{atm}}$) from IntCal13 (Reimer et al., 2013a) was used to calculate R.

In order to calculate R, we also used other ^{14}C and U/Th datasets for fossil corals from the equatorial Pacific islands that include Tahiti (Bard et al., 1998), Marquesas (Paterne et al., 2004), Kiritimati (Fairbanks et al., 2005) and Mururoa (Bard et al., 1998) (Fig. 4-1). R_{diff} denotes differences between calculated R and modern R (235 ± 110 for Tahiti, Reimer et al., 2009; 390 ± 60 for Marquesas, Paterne et al., 2004; 335 ± 100 for Kiritimati, Fairbanks et al., 2005; 300 ± 100 for Mururoa, Bard et al., 1998). We estimated that accumulated R_{diff} uncertainties are the sum of errors in ^{14}C dating, U/Th dating, and modern R estimation.

4-3. Results and Discussion

4-3-1. pH_{SW} and pCO_2_{SW} reconstructions

Using the revised calibration, we reconstructed pH_{SW} from new $\delta^{11}\text{B}$ measurements on Tahitian corals, as well as from previously reported data from both the Marquesas and Tahiti (Douville et al., 2010), and the overall result is consistent with the WEP foraminifer $\delta^{11}\text{B}$ variations (Palmer & Pearson, 2003) (Fig. 4-2). The oldest coral sample, dated to 20.7 ka BP during the LGM, exhibits a relatively high pH (8.26). From 15.5 to 9.0 ka BP, pH_{SW} is generally constant within uncertainty (8.15 - 8.22) and consistent with the preindustrial value of 8.20. Four notable pH excursions are associated with HS1 and the YD. Two of IODP Exp. 310 samples exhibit anomalously low pH at the end of HS1 (8.13 at 15.15 ka and 8.09 at 14.99 ka BP), in addition to those at end of the YD at the Marquesas (Douville et al., 2010). The low pH_{SW} following HS1 had been previously undetected at this location. Calculation of pCO_2_{SW} reveals deglacial values significantly above those of the atmosphere (Fig. 4-2). Conversely, ΔpCO_2 during last glacial and the early Holocene was nearly zero.

Results from a different portion of the same 14.99 ka BP coral sample deviate by as much as 1.4 ‰, which corresponds to 0.11 in pH_{SW} and 100 μatm in pCO_2_{SW} (310-M0024A-11R-1W_77-90 and 310-M0024A-11R-1W_60-75, Table 4-1). Considering the average ~4 year temporal resolution of each sample, these excursions occurred abruptly and persisted for several years, which differs from modern observations that show no clear interannual or decadal variability (Fig. 2-5). This enhanced variability, which is also observed in Sr/Ca derived SST results from another *Porites* colony recovered from IODP Exp. 310 (Felis et al., 2012), may relate to Tahiti's location at the rim of equatorial upwelling cell (Fig. 4-1). Taken together, pCO_2_{SW} records indicate that the equatorial Pacific became a larger CO_2 source during the last deglaciation with excursions at the end of HS1 and the YD.

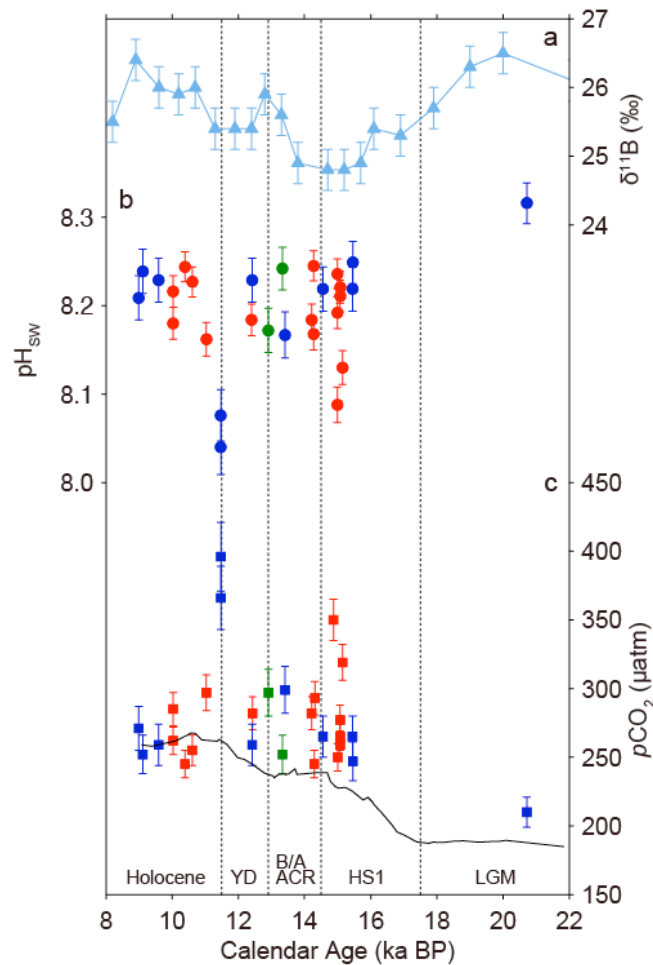


Fig. 4-2. Deglacial $\delta^{11}\text{B}$, pH_{sw} and $p\text{CO}_2$ variations in the equatorial Pacific. (a) Reported $\delta^{11}\text{B}$ values of planktonic foraminifera from ERDC-92 core (Palmer & Pearson, 2003). Age model is from the original publication. (b) pH_{sw} reconstructed from $\delta^{11}\text{B}$ of fossil *Porites* spp. Green and red circles are from Tahiti by Douville *et al.* (2010) and this study, respectively. Blue circles are from Marquesas by Douville *et al.* (2010) after correction by +0.04 pH units. (c) $p\text{CO}_2$ around the equatorial South Pacific Ocean (same colors as b). Atmospheric $p\text{CO}_2$ are also shown on the GICC05 timescale (Lourantou *et al.*, 2010). All error bars are 2σ . LGM, Last Glacial Maximum; HS1, Heinrich Stadial 1; ACR, Antarctic Cold Reversal; B/A, Bølling/Allerød; YD, Younger Dryas.

4-3-2. Marine ^{14}C reservoir ages

Compiled R throughout the equatorial Pacific resembles $p\text{CO}_2$ variability (Figs. 4-3 and 4-4). Larger and more variable values of R are evident in Tahiti during HS1 and the YD, and enhanced R variability is also seen in the Marquesas (Figs. 4-3 and 4-4). Paterne *et al.* (2004) sub-sampled different parts in the same fossil coral skeleton and analyzed both ^{14}C and U/Th. They observed no difference in U/Th dates, but a much larger difference in ^{14}C . Possibilities of either a diagenetic alteration or a change in R were suggested. The latter is more probable because a large variation in R is also suggested from Vanuatu coral at 11.7 - 12.4 ka (~ 400 years; during the YD, Burr *et al.*, 1998).

R_{diff} during the Holocene suggests no substantial change (Fig. 4-3 & 4-4). Reported R_{diff} data around the upwelling zone during the LGM are so sparse that it is unclear if R_{diff} during that period was same as present. However, the above-mentioned observation that $\Delta p\text{CO}_2$ is essentially equivalent to zero during the Holocene and the LGM suggests R_{diff} during the LGM is also near zero due to good ventilation. Large scatters seen in the last glacial corals of Mururoa and Tahiti may relate to Heinrich events 2 and 3 (Reimer *et al.*, 2013a).

There are large differences between IntCal09 and IntCal13 $\Delta^{14}\text{C}_{\text{atm}}$ data sets prior to 15.5 ka BP. This is partly because the previous version of Intcal09 curve heavily relied on Cariaco Basin varve sediment records in the equatorial Atlantic, whose assumption that local R was kept constant is highly questionable (Reimer *et al.*, 2013a, b; Southon *et al.*, 2012). The latest version of Intcal13 curve omitted a part of Cariaco Basin records, and instead adopted Lake Suigetu ^{14}C records whose chronology is anchored by Hulu Cave calendar ages through ^{14}C wiggle-matching (Reimer *et al.*, 2013a, b; Bronk-Ramsey *et al.*, 2012). Therefore, we must keep in mind that if the IntCal curve is updated in the future, estimation of R prior to 15.5 ka BP may change, too (this issue will be further discussed in Chapter 5).

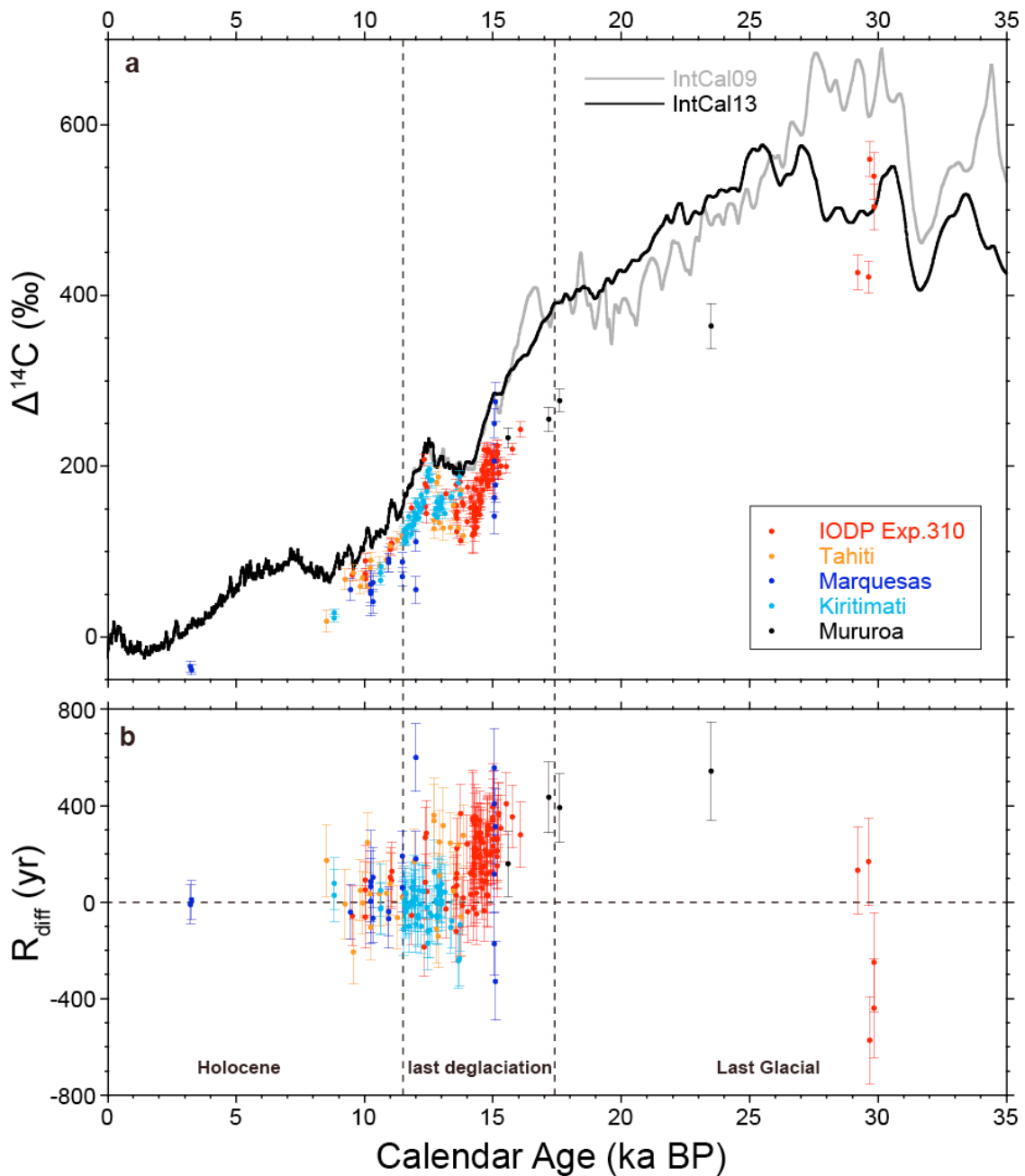


Fig. 4-3. (a) Time series of atmospheric $\Delta^{14}\text{C}$ (black line: IntCal13 (Reimer et al., 2013a); gray line: Intcal09 (Reimer et al., 2009)). (b) Differences between modern and past R around the equatorial Pacific Ocean. All data are from fossil corals (red: offshore Tahiti (this study); orange: reef crest of Tahiti barrier reef (Bard et al., 1998), blue: Marquesas (Paterne et al., 2004); light blue: Kiritimati (Fairbanks et al., 2005); black: Mururoa (Bard et al., 1998)). Horizontal gray dashed line represents ' $R_{\text{diff}} = 0$ '. All error bars are 1σ .

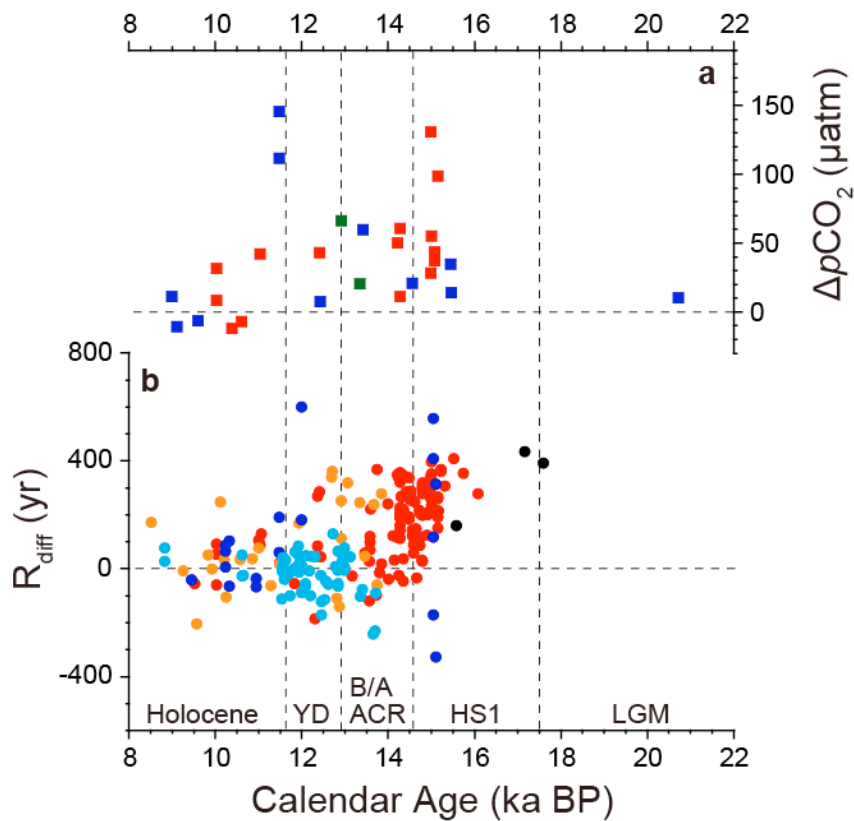


Fig. 4-4. Differences between modern and deglacial $p\text{CO}_2$ and R ($\Delta p\text{CO}_2$ and R_{diff}). The last deglaciation is characterized by larger and more variable $p\text{CO}_2$ and R values. (a) Atmosphere-ocean $\Delta p\text{CO}_2$ based on Tahiti and Marquesas corals and Antarctic ice core (Lourantou et al., 2010). Figure legend is same as Fig. 4-2. (b) R_{diff} around the equatorial Pacific Ocean calculated from fossil corals (legends are same as Fig. 4-3). Horizontal dashed lines represent $\Delta p\text{CO}_2 = 0$ and $R_{\text{diff}} = 0$.

4-3-3. SSS effects on TA and $p\text{CO}_2$ sw calculations

Reduced sea level during the last glacial is thought to have increased global salinity by ~ 1.2 g/kg (Adkins et al., 2002). During the LGM, which likely exhibited the largest magnitude change in TA relative to present, if the local TA-SSS relationship remained unchanged, TA at Tahiti would have increased by 79.6 mmol/kg (Eq. 2-3, Kutchinke et al., 2014). This would only result in a 0.007 reduction in pH_{sw} and a 12.1 μatm increase in $p\text{CO}_2$ sw (Table 4-2). Therefore, we neglected SSS changes during the last deglaciation throughout this chapter.

Table 4-2. Evaluation of SSS and TA changes on $p\text{CO}_2\text{sw}$ calculation.

	SSS	pK_B	$\delta^{11}\text{B}$ (‰)	$^{(1)}p\text{H}_{\text{sw}}$	TA ($\mu\text{mol/kg}$)	$p\text{CO}_2\text{sw}$ (μatm)
Present SSS	35.9	8.562	26	8.192	2359.7	268.7
LGM SSS & TA	37.1	8.556	26	8.185	2439.2	280.8
Differences	1.2	-0.007	0	-0.007	79.6	12.1

(1) Calculated from $\delta^{11}\text{B}$ value of fossil coral.

4-3-4. SST effects on $p\text{CO}_2$ sw reconstructions

Determination of past pH_{sw} and $p\text{CO}_2$ sw requires knowledge of paleo-SST because these parameters, as well as the dissociation constant of boric acid ($\text{p}K_{\text{B}}$), are temperature dependent (Robins et al., 2010; Hönisch et al., 2007; Zeebe & Wolf-Gladrow, 2001; Dickson, 1990) such that a 10 °C decrease in temperature corresponds to an approximate 0.1 unit increase in pH_{sw} . Temperature reconstructions (MARGO Project Members, 2009; Kiefer & Kienast, 2005) from the tropical and subtropical Pacific indicate relatively little change from modern values within the temporal range of our data. A compilation of SST records obtained from marine sediments indicates an overall increase from LGM to present, without major reversals during the YD or HS1, and with a total change of 2 °C from 15 ka (Kiefer & Kienast, 2005).

However, coral SST reconstructions indicate lower temperatures (2 - 4 °C) during the last deglaciation and early Holocene at Tahiti (Felis et al., 2012; DeLong et al., 2010; Asami et al., 2009). Therefore, we recalculated $p\text{CO}_2$ sw considering the coldest reported SST to estimate the maximum range of $p\text{CO}_2$ sw change. For this, we used SST results from IODP Exp. 310 corals that indicate SST was cooler by 3.5 °C at 15.0 ka BP (HS1) (Felis et al., 2012), 2.1°C at 14.2 ka BP Bølling/Allerød (B/A) (Asami et al., 2009), 3.4°C at 12.4 ka BP (YD) (Asami et al., 2009), 3.2 °C at 9.5 ka BP during the Holocene (DeLong et al., 2010) (Fig. 4-5). Because there are no LGM SST data from this region, we employed a 5 °C LGM change (Stute et al., 1995; Guilderson et al., 1994) (Fig. 4-5). Note that this does not consider the possibility of changes in either seawater Sr/Ca through time or Sr/Ca-SST sensitivity as discussed in previous studies (Gagan et al., 2012; Felis et al., 2012; DeLong et al., 2010; Asami et al., 2009) and therefore represents maximum potential SST change.

Positive $\Delta p\text{CO}_2$ during the last deglaciation (Fig. 4-5) is clearly insensitive to a large potential SST decrease. Carbon dioxide emission from the equatorial Pacific, as well as anomalously higher $p\text{CO}_2$ at ends of HS1 and the YD, persist (Fig. 4-5). we also note that only a slight lowering of LGM SST (1 – 3°C), the accepted equatorial Pacific range (MARGO Project Members, 2009; Kiefer & Kienast, 2005), results in an estimated LGM $\Delta p\text{CO}_2$ that is nearly identical to that of the Holocene (under modern

SST conditions, [Kiefer & Kienast, 2005](#)) (Fig. 4-5). This implies the surface seawater was in near CO₂ equilibrium state during these periods.

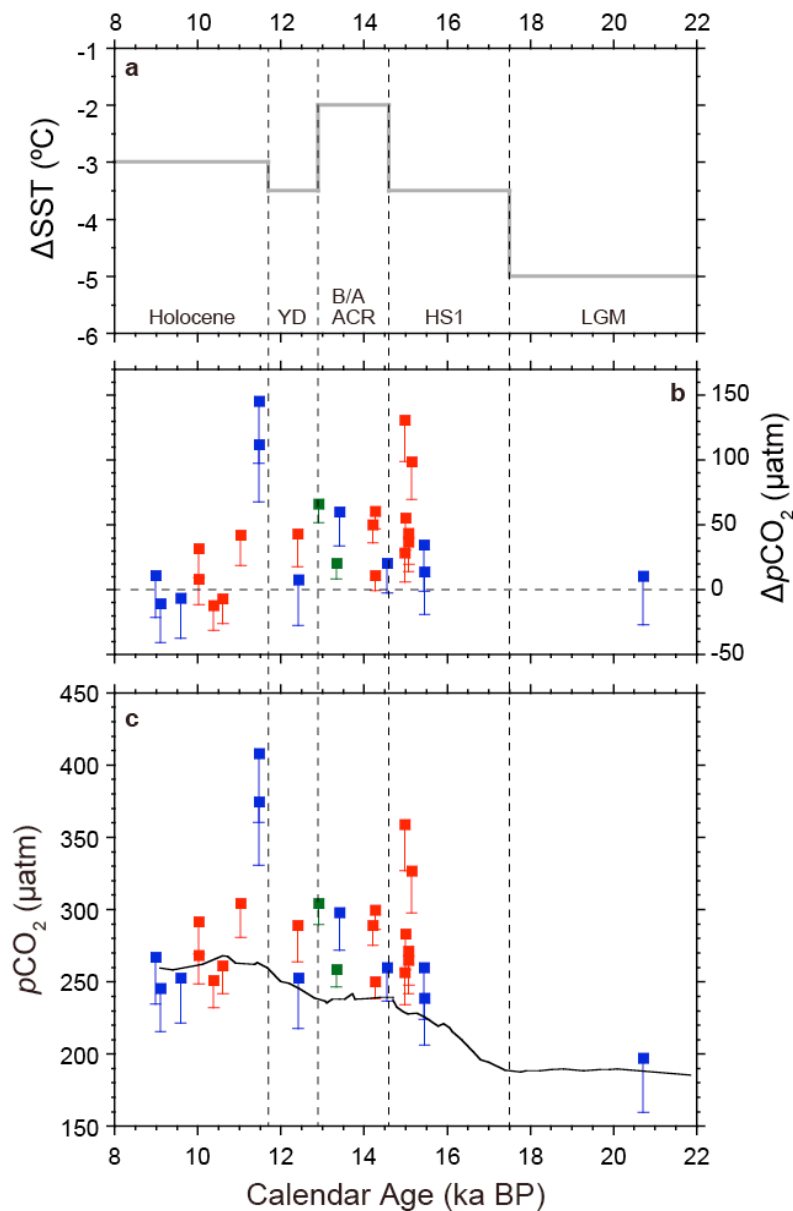


Fig. 4-5. Evaluation of influence of SST change on $p\text{CO}_2$ estimation. **(a)** Estimated SST differences compared to the preindustrial era using the most extreme potential decrease. The absolute minimum reported SST values from the equatorial Pacific were used for calculation of lower limits of uncertainty in **b** and **c**. **(b)** $p\text{CO}_2$ difference between the surface water at Tahiti and Marquesas and the atmosphere. Horizontal dashed line represents ' $\Delta p\text{CO}_2 = 0$ '. **(c)** Calculated $p\text{CO}_2$ of the surface water around the equatorial South Pacific Ocean assuming the same SST to the present (legends are same as **Figs. 4-2 and 4-4**) and atmospheric $p\text{CO}_2$ on the GICC05 timescale (black line) (Lourantou et al., 2010).

4-3-5. Mechanisms to explain higher $\Delta p\text{CO}_2$ during the last deglaciation

$p\text{CO}_2$ variability in subtropical oligotrophic water can be explained by mixing of water masses that exhibit distinctly different DIC concentrations. A southward migration of the ITCZ that partly controls thermocline depth is hypothesized during Heinrich Events including HS1 and the YD (e.g., [Deplazes et al., 2014](#); [Broccoli et al., 2006](#); [Zhang & Delworth, 2005](#)). At present, the ITCZ does not seem to directly affect surface $p\text{CO}_2$ variability (Fig. 4-1) because there is no indication of a latitudinal migration of the $p\text{CO}_2$ maxima in accordance with the ITCZ migration ([Feely et al., 2006, 2002](#)), and if it is displaced southward, the locus of equatorial upwelling remains at the equator due to the influence of inter-hemispheric asymmetry of Coriolis force (e.g., [Talley et al., 2011](#); [Gruber & Sarmiento, 2011](#)). Enhanced upwelling (shallower thermocline, La Niña-like conditions) or increased subsurface DIC (and TA?) concentration are more likely to drive $p\text{CO}_2$ variability based on sedimentary evidence from the equatorial Pacific for higher nutrient content, e.g., enhanced biogenic opal export production and lower $\delta^{13}\text{C}$ (TT013-PC72, ODP Site 1240 and TR163-19; Fig. 4-1) ([Pena et al., 2013, 2008](#); [Hayes et al., 2011](#); [Spero & Lea, 2002](#)). Semi-conservative radiogenic neodymium isotopes (ϵNd) from sediment cores at the eastern equatorial Pacific (EEP) (ODP Site 1240) and off Baja California (MV99-MC99-GC31/PC08) indicate stronger subsurface water transport from the south ([Pena et al., 2013](#); [Basak et al., 2010](#)) (Fig. 4-1). Covariation of geochemical properties between the Southern Ocean and the equatorial Pacific suggest a subsurface connection during the last deglaciation (e.g., [Pena et al., 2013, 2008](#); [Hayes et al., 2011](#); [Basak et al., 2010](#); [Loubere & Bennet, 2008](#); [Bostock et al., 2004](#); [Spero & Lea, 2002](#)). Thus, $p\text{CO}_2$ variability may be explained by an increase in DIC in the upwelled, subsurface water masses as opposed to physical processes alone.

4-3-6. A similarity between R_{diff} and $p\text{CO}_2$ variability

Water mass subduction along the subantarctic front, mainly off Chile (Bostock et al., 2013), forms Subantarctic Mode Water (SAMW) and Antarctic Intermediate Water (AAIW) that upwells at the equatorial Pacific via the Equatorial Undercurrent (EUC) (Fig. 4-1). SAMW and AAIW are characterized by higher/lower concentrations of oxygen/silicic acid (Fig. 4-1). It is suggested that the abyssal DIC reservoir around the Southern Ocean increased during the last glacial period (Burke & Robinson, 2012; Skinner et al., 2010; Rose et al., 2010; Sikes et al., 2000), which would have contributed to lower atmospheric $p\text{CO}_2$. Carbon dioxide was released to the surface through deep ocean ventilation during HS1 and the YD (Siani et al., 2013; Matsumoto & Yokoyama, 2013; Burke & Robinson, 2012; Yokoyama & Esat, 2011; Skinner et al., 2010; Rose et al., 2010; Anderson et al., 2009; Toggweiler et al., 2006), however export production was insufficient to fully compensate the increased carbon flux (Foster & Sexton, 2014; Horn et al., 2011). This is consistent with residual radiocarbon content ($\Delta^{14}\text{C}$) of intermediate water at the EEP (V21-30, Stott et al., 2009) and off Baja California (MV99-MC99-GC31/PC08, Marchitto et al., 2007) that indicates anomalously older water was incorporated into SAMW/AAIW (Fig. 4-1), as well as with depleted $\delta^{13}\text{C}$ of surface and lower thermocline dwelling foraminifers from sediment cores at both equatorial (TT013-PC72, ODP Site 1240 and TR163-19) and South Pacific sites (Pena et al., 2013, 2008; Hayes et al., 2011; Loubere & Bennet, 2008; Bostock et al., 2004; Spero & Lea, 2002). Moreover, enhanced export production of biogenic opal suggest more silicic acid was transported via the EUC to thermocline water at the equatorial Pacific (V19-30 and TT013-PC72) without being consumed completely within the Southern Ocean (Horn et al., 2011; Hayes et al., 2011; Anderson et al., 2009). Stronger Ekman transport in association with sea ice retreat and a poleward shift of southern westerlies is suggested to be a driver (Anderson et al., 2009; Toggweiler et al., 2006).

A similarity between R_{diff} and $p\text{CO}_2$ variability during the last deglaciation supports an interpretation that older DIC was incorporated to subtropical surface water through mixing with SAMW/AAIW (Siani et al., 2013). Yet, further work is still needed to fully understand both the physical and biogeochemical dynamics in the Southern Ocean and the equatorial Pacific (Matsumoto & Yokoyama, 2013).

4-3-7. Did the equatorial Pacific contribute to the deglacial CO₂ rise?

Positive $\Delta p\text{CO}_2$ indicates CO₂ flux from the ocean to the atmosphere (e.g., Takahashi et al., 2009). Previous studies (Douville et al., 2010; Palmer & Pearson, 2003) indicated that the equatorial Pacific contributed to deglacial CO₂ rise, however the timing of anomalously higher $p\text{CO}_2$ events recorded in radiogenically dated fossil corals do not systematically correspond to those of atmospheric CO₂ rise recovered from Antarctic ice core on the GICC05 timescale (Lourantou et al., 2010) (Fig 4-2). Moreover the new calibration reveals a modest CO₂ emission continued through the Bølling/Allerød/Antarctic Cold Reversal when no atmospheric CO₂ increase is observed (Figs. 4-2, 4-3, and 4-5). Though we demonstrate that the equatorial Pacific became a larger CO₂ source during the last deglaciation, it is too early to conclude its exact contribution to atmospheric CO₂ rise. The Southern Ocean is suggested to be central in CO₂ degassing due to its connectivity with the deep seawater, vast surface areas, and strong wind (Siani et al., 2013; Matsumoto & Yokoyama, 2013; Burke & Robinson, 2012; Yokoyama & Esat, 2011; Skinner et al., 2010; Rose et al., 2010; Anderson et al., 2009; Toggweiler et al., 2006). Furthermore, the contribution of other oceanic basins and the terrestrial biosphere should be further evaluated (Ciais et al., 2012; Yu et al., 2010). More evidence spanning the YD and the early part of HS1, in particular the sharp rise in atmospheric CO₂ and the sudden drop of $\delta^{13}\text{C}$ of CO₂ (Schmitt et al., 2012; Lourantou et al., 2010), as well as more spatial coverage is needed.

4-4. Conclusion

In order to assess equatorial Pacific's contribution to deglacial CO₂ rise, we measured $\delta^{11}\text{B}$ of fossil corals that were obtained at Tahiti. After procedure-specific isotopic corrections and location-specific pH_{SW} and $p\text{CO}_2_{\text{SW}}$ difference corrections, $p\text{CO}_2_{\text{SW}}$ were calculated from $\delta^{11}\text{B}$ values of both newly obtained and previously reported fossil corals using the new calibration established in Chapter 2. Reconstructed $p\text{CO}_2_{\text{SW}}$ showed larger values than the atmospheric $p\text{CO}_2$ during the last deglaciation and near equilibrium condition during the LGM and the Holocene. These observations indicate that during the last deglaciation the equatorial Pacific became larger CO₂ source than the present. A compilation of marine ¹⁴C reservoir ages in the surface seawater also

became larger during the last deglaciation, suggesting that a mixing with subsurface seawater characterized as higher DIC and older ages was stronger. More $p\text{CO}_2$ sw reconstructions using fossil corals as well as marine sediment cores will reveal how glacial abyssal carbon had escaped to the atmosphere.

CHAPTER 5

General conclusion and future perspectives

5-1. General conclusion

In this thesis, a new approach of the $\delta^{11}\text{B}$ - pH_{SW} calibration using massive *Porites* corals living in the natural environment was shown (Chichijima and Tahiti) (Chapter 2), and two application studies through $\delta^{11}\text{B}$ measurements of modern and fossil corals collected from Chichijima (Chapter 3) and Tahiti (Chapter 4). The key findings of this thesis are summarized as follows.

(1) *pH_{SW} estimations are possible when CO_2 ventilation is good and abundant CO_2 chemistry data is available.*

Even if seawater CO_2 chemistry measurements are limited or do not exist at all, in some cases we can calculate past variations of pH_{SW} and pCO_2 SW by utilizing atmospheric CO_2 records. Thus it is critical to check whether a study region is near the air-sea CO_2 equilibrium state or not. Additionally, we should not neglect international efforts that quantified the ocean's anthropogenic CO_2 absorption by ship based measurements and model simulations.

(2) *The $\delta^{11}\text{B}$ - pH_{SW} calibration using cultured corals is not feasible to reconstruct reasonable pH_{SW} variations.*

The pH_{SW} reconstructions should be conducted using field-based $\delta^{11}\text{B}$ - pH_{SW} calibration. It may be related to the fact that culturing experiments are basically conducted under heavily acidified seawater causing physiological stresses on corals. In addition, empirical equations are different depending on the sites in question (i.e., Chichijima, Tahiti, Guam, and Hainan), which means that the equation that can be ubiquitously applicable does not exist, and a regional calibration using one or more modern corals must be conducted. Thus, further $\delta^{11}\text{B}$ measurements of corals living in the natural environment are required to achieve more accurate pH_{SW} reconstructions.

(3) *Past 100 years' ocean acidification has been negatively influencing calcification of *Porites* coral living in Chichijima through pH_{CF} decreases.*

It can be highlighted that a rapid decrease of pH_{CF} after 1960 is clearly seen. It was found that pH_{CF} decreases of the Chichijima coral are significantly more sensitive to pH_{SW} decreases than the other scleractinian corals cultured under the artificially

acidified seawater. These findings suggest that even 0.1 pH unit acidification has potential to cause substantial impacts on coral calcifications. This is the controversial view that corals can keep homeostasis in calcification fluids. The $\delta^{13}\text{C}_{\text{coral}}$ has been decreasing at a consistent rate with $\delta^{13}\text{C}_{\text{atm}}$ since 1960 (the Suess effect). A significant positive relationship between $\delta^{13}\text{C}$ and $\delta^{11}\text{B}$ indicates that these phenomena are from anthropogenic origin.

(4) *The equatorial Pacific became a larger CO_2 source during the last deglaciation.*

The CO_2 purging events at Tahiti at 15.15 and 14.99 ka BP were discovered. These were analogous to the previously reported event found from Marquesas at 11.5 ka BP. The ^{14}C marine reservoir ages in the equatorial Pacific showed larger values during the last deglaciation than the present values, and a reasonable explanation for this is a stronger mixing with subsurface seawater characterized by higher DIC and older ages. A part of glacial carbon reservoir emerged in the Southern Ocean might have been incorporated into SAMW and AAIW, and then appeared in the equatorial Pacific.

5-2. Future perspectives

5-2-1. Perspectives on $\delta^{11}\text{B}$ -pH systematics

A part of the $\delta^{11}\text{B}$ interannual variabilities over analytical uncertainties from the Chichijima coral (Fig. 2-10) may be due to “heterogeneity of subsamples of coral skeleton” or “interannual variation of offset a ”, because such a large variation is unexpected from the $\delta^{11}\text{B}$ theoretical curve and seawater CO_2 chemistry (Figs. 2-5 & 2-9). The quantities of subsamples for $\delta^{11}\text{B}$ measurements were only a fraction ($\sim 0.1\%$, preliminary result) of the entire skeleton drilled to obtain three-year averages of environmental records. The heterogeneity of subsamples potentially biases $\delta^{11}\text{B}$ values, because pH_{SW} changes by 0.1 seasonally at Chichijima ($\delta^{11}\text{B}$ seasonalities are perhaps $\sim 1\%$). Relatively smaller seasonalities of pH_{SW} at Tahiti (and Marquesas) may partly explain why the fitting of coral $\delta^{11}\text{B}$ values and pH_{SW} are better than that of Chichijima (Fig. 2-10). Thus, methodologies to drill the carbonate skeleton and to mix coarse grain subsamples are important to be developed. Another possible explanation of the large interannual $\delta^{11}\text{B}$ variabilities found in the Chichijima coral is the annual variation in offset a (measured $\delta^{11}\text{B}$ - theoretical $\delta^{11}\text{B}$), more correctly ΔpH ($= \text{pH}_{\text{CF}} - \text{pH}_{\text{SW}}$). Given the fact that not only *Porites* corals but also other genus of corals have different offset a and ΔpH (Figs. 1-4, 3-5 & 5-1), it is reasonable to assume that these parameters can vary from seasonal to decadal timescales. For instance, Dissald *et al.* (2012) found that light intensity could influence $\delta^{11}\text{B}$ of *Acropora* spp. through modifications of pH_{CF} . As for branching *P. cylindrica* and *P. compressa*, Hönisch *et al.* (2004) did not find any effect of water depths, nutrient levels, and temperatures on $\delta^{11}\text{B}$. Strictly speaking, however, potential environmental factors (e.g., irradiance, temperature, salinity, and growth rate) that may control $\delta^{11}\text{B}$ of massive *Porites* corals have not been fully investigated yet. Hence through culturing experiments of massive *Porites* corals, effects of these environmental factors must be evaluated further to better understandings of $\delta^{11}\text{B}$ -pH systematics. There seem other controlling factors in addition to pH_{SW} , because not only the Chichijima coral but also *Porites* spp. collected in Guam showed interannual variabilities over analytical uncertainties (Fig. 5-1). Shinjo *et al.* (2013) did not find any correlations between $\delta^{11}\text{B}$ and ENSO index. Furthermore, these large interannual pH_{SW} variations are unrealistic considering good ventilation of CO_2 in this

region. It is proposed that future works should quantify relative importance of pH_{SW} and other factors.

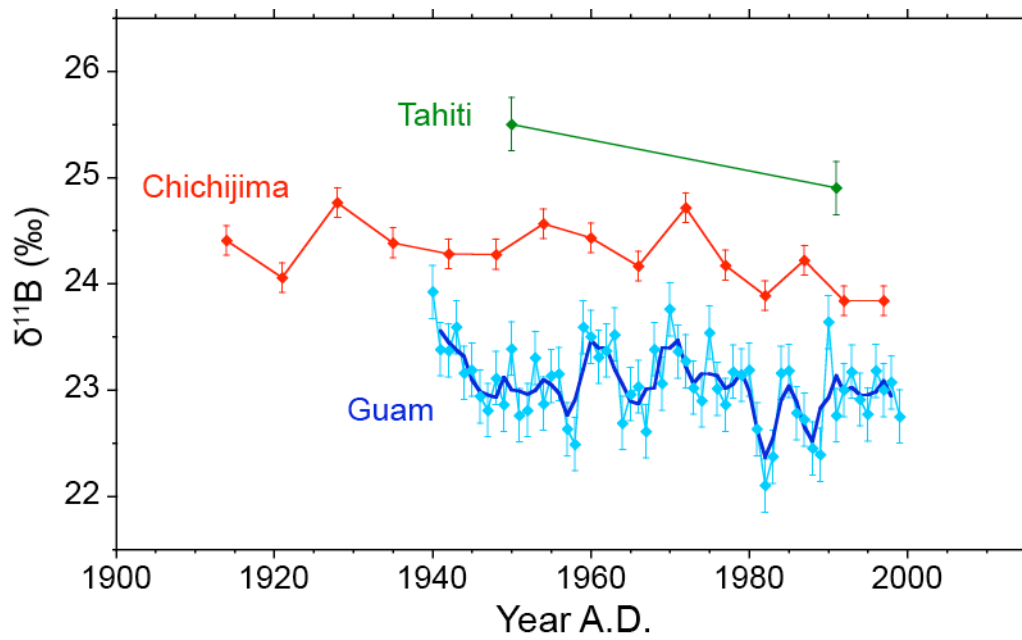


Fig. 5-1. Comparison of $\delta^{11}\text{B}$ records of *Porites* spp. collected from Chichijima, Tahiti (Gaillardet & Allegre, 1995; Douville et al., 2010), and Guam (Shinjo et al., 2013). In Guam coral records, blue line represents three-year moving averages of annual records (light blue). Error bars are analytical uncertainties (2σ).

5-2-2. Direction of $\delta^{11}\text{B}$ -pH_{SW} calibration using long-lived calcifying organisms

For future research, the new calibration procedures proposed by this thesis should further be applied to massive *Porites* corals from other areas for more comprehensive understanding of $\delta^{11}\text{B}$ -pH systematics. In this section, points needed to be addressed will be briefly described, and then near-future directions of our studies will be introduced.

(1) *Corals that are more than ~50 years old should be used.*

It is after 1960 when ocean acidification accelerated, thus $\delta^{11}\text{B}$ of corals that were more than 50 years old could record pH_{SW} decreases. To date, only massive *Porites* spp. has been studied but other long-lived scleractinian corals such as *Favia* spp., *Diploria* spp., and *Siderastrea* spp. are also candidates for this research. In addition, potential of other surface living calcifiers such as coralline algae, sclerosponges, and mollusks should be investigated.

(2) *A well-ventilated area should be selected as a study region.*

The field-based $\delta^{11}\text{B}$ -pH_{SW} calibration requires independent pH_{SW} estimations. Open ocean seawater is well equilibrated with the overlying atmosphere in terms of CO₂. Thus, even around the coast of large continents, a region where seawater is well mixed with open ocean seawater should be selected as a study area. Ocean acidification occurs at a similar rate in the global surface ocean as far as CO₂ is well ventilated (e.g., [Takahashi et al., 2014](#); [Midorikawa et al., 2010](#); [Lenton et al., 2010](#); [Tans, 2009](#); [Dore et al., 2009](#); [Bates, 2007](#)). It should be noted that there are many locations such as coastal regions, marginal seas, upwelling regions, and large coral reefs where CO₂ chemistry is far from the air-sea CO₂ equilibrium (e.g., [Hendriks et al., 2015](#); [Gruber et al., 2012](#); [Hofmann et al., 2011](#)). Such regions are not suitable for the calibration work.

Although long-lived massive *Porites* corals are very rare, inter-colonial variability often exist in coral skeletal geochemistry. Thus, we are going to measure two colonies *Porites* spp. collected from Kikaijima in 2009 (28.32°N 129.97°E). One coral is ~230 years old and the other coral is ~430 years old. Importantly the latter records preindustrial oceanic environments ([Kawakubo et al., 2013](#)). We believe that Kikaijima is one of the best study regions because these corals were collected from the environment that satisfies aforementioned prerequisites. Furthermore, as the island is close to Chichijima, we can evaluate the location-specific difference between two islands.

5-2-3. Paleoclimatological perspectives

Several important issues have been unsolved in paleoceanography since the last glacial period. First, even though pH_{SW} and pCO_2_{SW} reconstructions require past sea temperature changes, SST in the equatorial region during the LGM are in disagreement among proxies from myriad studies. Therefore, much more works are needed to constrain the LGM SST, as well as to estimate SST in less explored area such as the central Pacific. The second issue is a scarcity of R reconstructions at the equatorial Pacific during the LGM (Fig. 4-3). One critical reason is little evidence of coral reef growth during the LGM (Marshall & McCulloch, 2002). It substantially limits our knowledge about R. What is worse, there is no promising marine sediment cores that enables R estimation from ^{14}C measurements of planktonic foraminifer in association with independent age models (e.g., Reimer et al., 2013b). Recent success of coral reef drilling by IODP Exp. 325 at the world heritage site of the Great Barrier Reef, the northeastern Australia, must improve our understandings of past R variabilities, because it recovered many fossil corals dated to the LGM (Yokoyama et al., 2011). The third issue is about the IntCal curve (atmospheric $\Delta^{14}\text{C}$ records) during the glacial period. The IntCal curve is defined as "*the result of a community effort to produce the best calibration sets from the currently available data*" (Reimer et al., 2013a), thus there is the possibility of future revisions. The latest version of IntCal13 (especially, Lake Suigetu sediments and Hulu Cave speleothem data sets) are based on the hypothesis that dead carbon fraction (DCF) of Hulu Cave speleothem, a dilution effect by ^{14}C -depleted carbon derived from CaCO_3 bedrock, is absolutely constant through times. Whereas the DCF is constant from 12.55 ka BP to the present (Southon et al., 2012), it still remains unknown if it applies prior to 12.55 ka BP. In fact, a growth rate of Hulu Cave speleothem changes before and after ~ 19 ka BP (Southon et al., 2012), which is perhaps due to changes of a residence time of fresh water flowing through the bedrock. Residence time changes can influence the DCF estimation (Reimer et al., 2013b). Therefore, further efforts are necessary to establish the robust IntCal curve that does not require the reservoir corrections (i.e., R and DCF).

In terms of atmospheric CO_2 reconstructions, ice cores have provided invaluable records since 800 ka BP. Recently Marcott *et al.* (2014) published the highest resolution

CO₂ records so far during the last deglaciation through the analyses of West Antarctica Divide ice core (WDC) (Fig. 5-2). Intriguingly it revealed, for the first time, sudden CO₂ purge events (10–15 μatm increase in 200 years) beginning at 16.3 ka BP (during HS1), as well as previously reported events at 14.6 ka BP (the end of HS1) and 11.7 ka BP (the end of the YD) (Fig. 5-2). In marine CO₂ purge events found at the equatorial Pacific, one in Marquesas happened 230 years after 11.7 ka event (11.47 ± 0.09 ka BP, [Douville et al., 2010](#)). The other marine CO₂ events found at Tahiti (15.15 and 14.99 ka BP, this study) do not coincide with any major atmospheric CO₂ events, but it happened 350–510 years after slight $p\text{CO}_{2\text{atm}}$ increases at 15.5 ka BP (Fig. 5-2). One hypothesis to explain these observations is; it takes several hundred years for the upwelling of DIC-rich water in the Southern Ocean to emerge in the equatorial Pacific via SAMW and AAIW transport. However, this hypothesis should be tested with more spatial coverage of $p\text{CO}_{2\text{sw}}$ reconstructions around the equatorial Pacific region.

As seen in different reconstructions of the timing and the duration of these atmospheric CO₂ events from different Antarctic ice cores (e.g., WDC, EDC, Byrd, and Siple Dome) (Fig. 5-2), ice cores suffer from smoothing of the atmospheric CO₂ signal in the firn and large uncertainties in age determinations of gas trapped in the ice (e.g., [Marcott et al., 2014](#); [Pedro et al., 2012](#); [Lourantou et al., 2010](#)). Hence, modern and fossil corals, which are dated very accurately using U-series and preserve high-resolution records, have great potential to reveal fine structures of CO₂ events that might have occurred in a short period of time (decade to centuries): such as rapid CO₂ increases during the last deglaciation ([Marcott et al., 2014](#)) and during Heinrich events in the glacial period (e.g., [Ahn & Brook, 2014](#)), and rapid CO₂ decreases at ~1600 AD (e.g., [Rubino et al., 2013](#)).

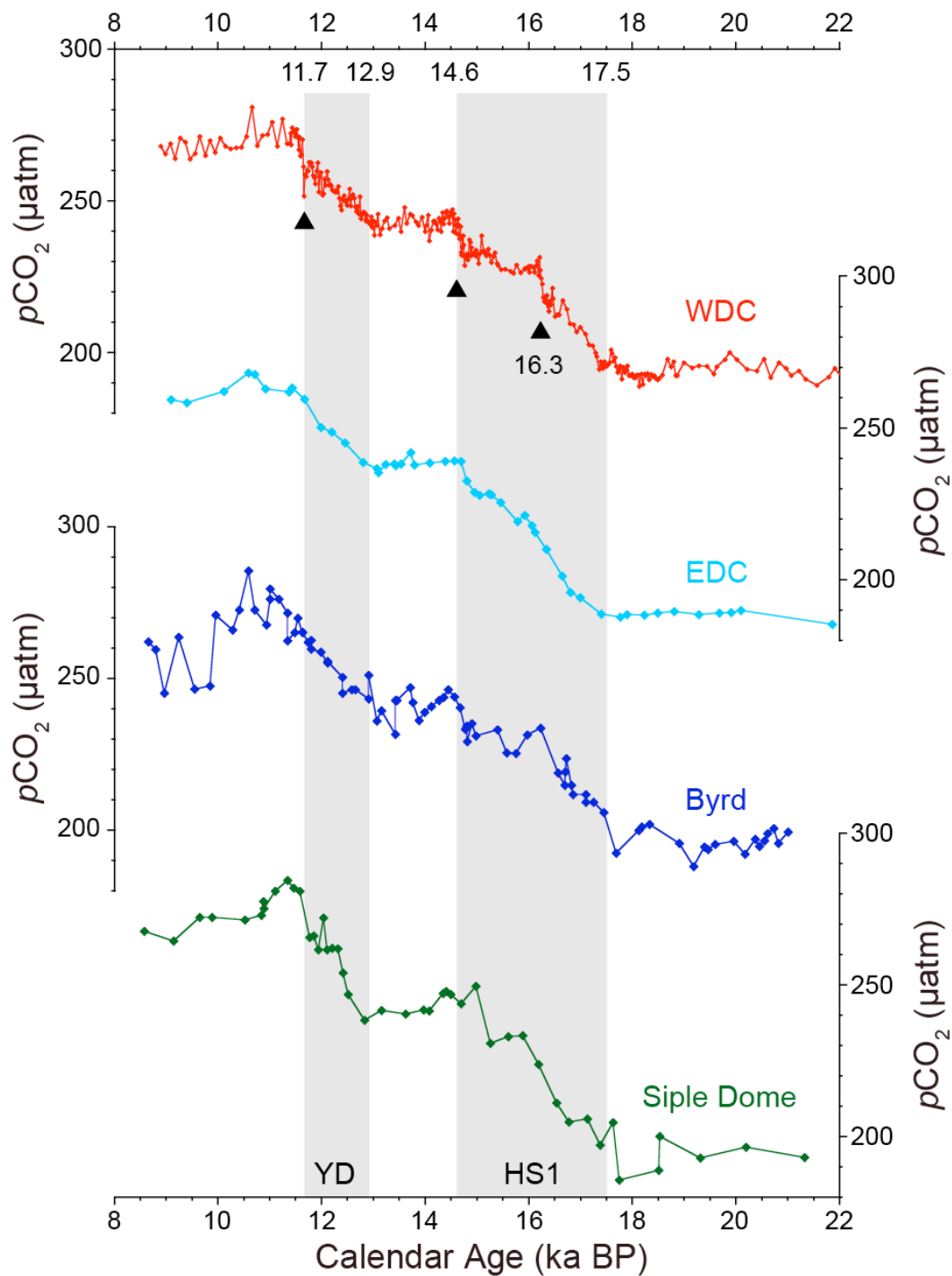


Fig. 5-2. Atmospheric $p\text{CO}_2$ records of Antarctic ice cores. Gass-ice age models are WDC06A–7 for WDC (Marcott et al., 2014); GICC05 for EDC (Lourantou et al., 2010), Byrd (Pedro et al., 2012), and Siple Dome (Pedro et al., 2012) ice cores. All replicated analyses are averaged. YD, Younger Dryas; HS1, Heinrich Stadial 1; WDC, West Antarctica Divide ice core; EDC, EPICA Dome C.

Acknowledgements

First of all, I would like to thank Dr. Yusuke Yokoyama for being my advisor and mentor. He gave me not only a lot of advices, encourages, and suggestions but also plentiful opportunities to learn how to become a critical and an international scientist. I am also grateful to Dr. Tsuyoshi Ishikawa as a second supervisor in Kochi Core Center. He taught me to be objective to my own results and gave me plenty of advices and suggestions in the experimental plan of boron isotope analysis and a lot of opportunities to use a variety of machines. I also thank Dr. Jun Matsuoka and Dr. Kazuya Nagaishi for helping me analyze coral samples and keeping machines always in the best condition. I thank Dr. Mayuri Inoue for helping and teaching me the experiment and providing a lot of knowledge of the coral skeletal climatology. I thank Dr. Atsushi Suzuki for preparing coral samples and teaching me a lot about skeletogenesis, culturing experiments, seawater CO₂ chemistry, and geochemical analyses of corals. I thank Masao Ishii for teaching me a lot about seawater CO₂ chemistry and offering valuable dataset of CO₂ chemistry measured by research vessels. I thank Dr. Sumiko Tsukamoto and IODP Exp. 310 members for obtaining coral samples of Chichijima and Tahiti used in this thesis. I thank Dr. Stephen P. Obrochta, Dr. Christelle Not, and Tomoko Bell for discussing with me and spending a lot of time to correct my poor English. I thank M. Harada, Y. Yoshinaga, K. Tsuzuki, M. Becchaku, K. Machida, A. Okada, and Ms. Namba for helping me prepare coral samples and the experiment. My thesis was substantially improved through the discussions with Dr. Katsumi Matsumoto, Dr. Axel Timmermann, Dr. Takashi Toyohuku, Dr. Akihisa Kitamura, Dr. Kentaro Tanaka, Dr. Kotaro Shirai, Dr. Yusuke Okazaki, Dr. Takuya Sagawa, and Dr. Osamu Seki. The Members in Yusuke Yokoyama Laboratory, Earth Environmental Seminar, and OFGS Seminar of Atmosphere and Ocean Research Institute gave a lot of constructive suggestions and criticisms. A part of my study was supported by the Grant-in-Aid of Japan Society for the Promotion of Science Fellows DC1. I cannot be too thankful for my families, especially my parents for giving me emotional and financial supports.

References

- Adkins, J. F., Boyle, E. A. Changing atmospheric $\Delta^{14}\text{C}$ and the record of deepwater paleoventilation ages. *Paleoceanography* **12**, 337-344 (1997).
- Adkins, J. F., McIntyre, K., Schrag, D. P. The Salinity, Temperature, and $\delta^{18}\text{O}$ of the Glacial Deep Ocean. *Science* **298**, 1769-1773 (2002).
- Ahn, J., Brook, E. J. Siple Dome ice reveals two modes of millennial CO_2 change during the last ice age. *Nature Communications*, doi:10.1038/ncomms4723 (2014).
- Al-Horani, F. A., Al-Moghrabi, S. M., de Beer, D. The mechanism of calcification and its relation to photosynthesis and respiration in the scleractinian coral *Galaxea fascicularis*. *Marine Biology* **142**, 419–426 (2003).
- Alibert, C., Kinsley, L., Fallon, S. J., McCulloch, M. T., Berkelmans, R., Mcallister, F. Source of trace element variability in Great Barrier Reef corals affected by the Burdekin flood plumes. *Geochimica et Cosmochimica Acta* **67**, 231–246 (2003).
- Allison, N., Cohen, I., Finch, A. A., Erez, J., Tudhope, A. W., Edinburgh Ion Microprobe Facility. Corals concentrate dissolved inorganic carbon to facilitate calcification. *Nature Communications*, doi:10.1038/ncomms6741 (2014).
- Allison, N., Finch, A. A., EIMF. $\delta^{11}\text{B}$, Sr, Mg and B in a modern *Porites* coral: the relationship between calcification site pH and skeletal chemistry. *Geochimica et Cosmochimica Acta* **74**, 1790–1800 (2010).
- Anagnostou, E., Huang, K.-F., You, C.-F., Sikes, E. L., Sherrell, R. M. Evaluation of boron isotope ratio as a pH proxy in the deep sea coral *Desmophyllum dianthus*: Evidence of physiological pH adjustment. *Earth and Planetary Science Letters* **349–350**, 251–260 (2012).
- Anderson, R. F., Ali, S., Bradtmiller, L. I., Nielsen, S. H. H., Fleisher, M. Q., Anderson, B. E., Burckle, L. H. Wind-Driven Upwelling in the Southern Ocean and the Deglacial Rise in Atmospheric CO_2 . *Science* **323**, 1443–1448 (2009).
- Andersson, A. J., Yeakel, K. L., Bates, N. R., de Putron, S. J. Partial offsets in ocean acidification from changing coral reef biogeochemistry. *Nature Climate Change* **4**, 56–61 (2014).
- Archer, D., Winguth, A., Lea, D., Mahowald, N. What Caused The Glacial/Interglacial Atmospheric $p\text{CO}_2$ Cycles? *Reviews of Geophysics* **38**, 159–189 (2000).
- Asami, R., Felis, T., Deschamps, P., Hanawa, K., Iryu, Y., Bard, E., Durand, N., Murayama, M. Evidence for tropical South Pacific climate change during the Younger Dryas and the Bølling-Allerød from geochemical records of fossil Tahiti corals. *Earth and Planetary Science Letters* **288**, 96–107 (2009).
- Asami, R., Yamada, T., Iryu, Y., Quinn, T. M., Meyer, C. P., Paulay, G. Interannual and decadal variability of the western Pacific sea surface condition for the years 1787–2000: Reconstruction based on stable isotope record from a Guam coral. *Journal of Geophysical Research* **110**, doi:10.1029/2004JC002555 (2005).

- Bakker, D. C. E., Pfeil, B., Smith, K., Hankin, S., Olsen, A., Alin, S. R., Cosca, C. E., Harasawa, S., Kozyr, A., Nojiri, Y., O'Brien, K. M., Schuster, U., Telszewski, M., Tilbrook, B., Wada, C., Akl, J., Barbero, L., Bates, N. R., Bozec, Y., Boutin, J., Cai, W.-J., Castle, R. D., Chavez, F. P., Chen, L., Chierici, M., Currie, K. I., de Baar, H. J. W., Evans, W., Feely, R. A., Fransson, A., Gao, Z., Hardman-Mountford, N., Hoppema, M., Huang, W.-J., Hunt, C. W., Huss, B., Ichikawa, T., Jacobson, A. R., Johannessen, T., Jones, E., Jones, S. D., Jutterstrøm, S., Kitidis, V., Körtzinger, A., Landschützer, P., Lauvset, S. K., Lefèvre, N., Manke, Ansley., Mathis, J. T., Merlivat, L., Metzl, N., Monteiro, P. M. S., Murata, A., Newberger, T., Ono, T., Park, G.-H., Paterson, K., Pierrot, D., Ríos, A. F., Sabine, C. L., Saito, S., Salisbury, J., Sarma, V. V. S. S., Schlitzer, R., Sieger, R., Skjelvan, I., Steinhoff, T., Sullivan, K., Sun, H., Sutton, A., Suzuki, T., Sweeney, C., Takahashi, T., Tjiputra, J., Tsurushima, N., van Heuven, S., Vandemark, D., Vlahos, P., Wallace, D. W. R., Wanninkhof, R., Watson, A. J. An update to the Surface Ocean CO₂ Atlas (SOCAT version 2). *Earth System Science Data* **6**, 69–90 (2014).
- Bard, E., Hamelin, B., Arnold, M., Montaggioni, L., Cabioch, G., Faure, G., Rougerie, F. Deglacial sea-level record from Tahiti corals and the timing of global melt water discharge. *Nature* **382**, 241–244 (1996).
- Bard, E., Arnold, M., Hamelin, B., Tisnerat, L. N., Cabioch, G. Radiocarbon calibration by means of mass spectrometric ²³⁰Th/²³⁴U and ¹⁴C ages of corals: an updated database including samples from Barbados, Mururoa and Tahiti. *Radiocarbon* **40**, 1085–1092 (1998).
- Basak, C., Martin, E. E., Horikawa, K., Marchitto, T. M. Southern Ocean source of ¹⁴C-depleted carbon in the North Pacific Ocean during the last deglaciation. *Nature Geoscience* **3**, 770–773 (2010).
- Bates, N. R. Interannual variability of the oceanic CO₂ sink in the subtropical gyre of the North Atlantic Ocean over the last 2 decades. *Journal of Geophysical Research* **112**, JC003759 (2007).
- Beerling, D. J., Royer, D. L. Convergent Cenozoic CO₂ history. *Nature Geoscience* **4**, 418–420 (2011).
- Biodiversity Center of Japan. Monitoring Site 1000. <<http://www.biodic.go.jp/moni1000/index.html>>, (2009).
- Bostock, H. C., Opdyke, B. N., Gagan, M. K., Fifield, L. K. Carbon isotope evidence for changes in Antarctic Intermediate Water circulation and ocean ventilation in the southwest Pacific during the last deglaciation. *Paleoceanography*, doi:10.1029/2004PA001047 (2004).
- Bostock, H. C., Sutton, P. J., Williams, M. J. M., Opdyke, B. N. Reviewing the circulation and mixing of Antarctic Intermediate Water in the South Pacific using evidence from geochemical tracers and Argo float trajectories. *Deep-Sea Research I* **73**, 84–98 (2013).
- Bouttes, N., Paillard, D., Roche, D. M., Brovkin, V., Bopp, L. Last Glacial Maximum CO₂ and δ¹³C successfully reconciled. *Geophysical Research Letters*, doi:10.1029/2010GL044499 (2011).
- Bouttes, N., Paillard, D., Roche, D. M. Impact of brine-induced stratification on the

- glacial carbon cycle. *Climate of the Past* **6**, 575–589 (2010).
- Broccoli, A. J., Dahl, K. A., Stouffer, R. J. Response of the ITCZ to Northern Hemisphere cooling. *Geophysical Research Letters*, doi:10.1029/2005GL024546 (2006).
- Broecker, W. S., Peng, T.-H. Interhemispheric Transport of carbon dioxide by ocean circulation. *Nature* **356**, 587–589 (1992).
- Bronk-Ramsey, C., Staff, R. A., Bryant, C. L., Brock, F., Kitagawa H., van der Plicht, J., Schlolaut, G., Marshall, M. H., Brauer, A., Lamb, H. F., Payne, R. L., Tarasov, P. E., Haraguchi, T., Gotanda, K., Yonenobu, H., Yokoyama, Y., Tada, R., Nakagawa, T. A Complete Terrestrial Radiocarbon Record for 11.2 to 52.8 kyr B.P. *Science* **338**, 370–374 (2012).
- Brzezinski, M. A., Pride, C. J., Franck, V. M., Sigman, D. M., Sarmiento, J. L., Matsumoto, K., Gruber, N., Rau, G. H., Coale, K. H. A switch from Si(OH)₄ to NO₃ depletion in the glacial Southern Ocean. *Geophysical Research Letters*, doi:10.1029/2001GL014349 (2002).
- Burke, A., Robinson, L. F. The Southern Ocean's Role in Carbon Exchange During the Last Deglaciation. *Science* **335**, 557–561 (2012).
- Burr, G. S., Beck, J. W., Taylor, F. W., Recy, J., Edwards, R.L., Cabioch, G., Corrège, T., Donahue, D. J., Malley, M. O. A high-resolution radiocarbon calibration between 11,700 and 12,400 calendar years BP derived from ²³⁰Th ages of corals from Espiritu Santo island, Vanuatu. *Radiocarbon* **40**, 1093–1105 (1998).
- Burr, G. S., Beck, J. W., Corrège, T., Cabioch, G., Taylor, F. W., Donahue, D. J. Modern and Pleistocene reservoir ages inferred from South Pacific Corals. *Radiocarbon* **51**, 319–335 (2009).
- Cabioch, G., Montaggioni, L., Frank, N., Seard, C., Sallé, E., Payri, C., Pelletier, B., Paterne, M. Successive reef depositional events along the Marquesas foreslopes (French Polynesia) since 26 ka. *Marine Geology* **254**, 18–34 (2008).
- Cahyarini, S. Y., Pfeiffer, M., Dullo, W.-C. Improving SST reconstructions from coral Sr/Ca records: multiple corals from Tahiti (French Polynesia). *International Journal of Earth Sciences* **98**, 31–40 (2009).
- Caldeira, K., Wickett, M. E. Anthropogenic carbon and ocean pH. *Nature* **425**, 365 (2003).
- Camoin, G. F., Iryu, Y., McInroy, D. B., Asami, R., Braaksma, H., Cabioch, G., Castillo, P., Cohen, A., Cole, J. E., Deschamps, P., Fairbanks, R. G., Felis, T., Fujita, K., Hathorne, E., Lund, S., Machiyama, H., Matsuda, H., Quinn, T. M., Sugihara, K., Thomas, A., Vasconcelos, C., Verwer, K., Warthmann, R., Webster, J. M., Westphal, H., Woo, K. S., Yamada, T., Yokoyama, Y. IODP Expedition 310 Reconstructs Sea Level, Climatic, and Environmental Changes in the South Pacific during the Last Deglaciation. *Scientific Drilling* **5**, 4–12 (2007).
- Carton, J. A., Giese, B. S. A Reanalysis of Ocean Climate Using Simple Ocean Data Assimilation (SODA). *Monthly Weather Review* **136**, 2999–3017 (2008).
- Ciais, P., Gasser, T., Paris, J. D., Caldeira, K., Raupach, M. R., Canadell, J. G., Patwardhan, A., Friedlingstein, P., Piao, S. L., Gitz, V. Attributing the increase in

- atmospheric CO₂ to emitters and absorbers. *Nature Climate Change* **3**, 926–930 (2013).
- Ciais, P., Tagliabue, A., Cuntz, M., Bopp, L., Scholze, M., Hoffmann, G., Lourantou, A., Harrison, S. P., Prentice, I. C., Kelley, D. I., Koven, C., Piao, S. L. Large inert carbon pool in the terrestrial biosphere during the Last Glacial Maximum. *Nature Geoscience* **5**, 74–79 (2012).
- Cohen, A. L., Holcomb, M. Why Corals Care About Ocean Acidification Uncovering the Mechanism. *Oceanography* **22**, 118–127 (2009).
- Comeau, S., Carpenter, R. C., Nojiri, Y., Putnam, H. M., Sakai, K., Edmunds, P. J. Pacific-wide contrast highlights resistance of reef calcifiers to ocean acidification. *Proceedings of the Royal Society B*, doi:10.1098/rspb.2014.1339 (2014).
- Cooper, T. F., O’Leary, R. A, Lough, J. M. Growth of Western Australian Corals in the Anthropocene. *Science* **335**, 593-596 (2012).
- Crook, E. D., Cohen, A. L., Rebolledo-Vieyra, M., Hernandez, L., Paytan, A. Reduced calcification and lack of acclimatization by coral colonies growing in areas of persistent natural acidification. *Proceedings of the National Academy of Sciences* **110**, 11044–11049 (2013).
- Dassié, E. P., Lemley, G. M., Linsley, B. K. The Suess effect in Fiji coral $\delta^{13}\text{C}$ and its potential as a tracer of anthropogenic CO₂ uptake. *Palaeogeography, Palaeoclimatology, Palaeoecology* **370**, 30–40 (2013).
- De Pol-Holz, R., Keigwin, L., Southon, J., Hebbeln, D., Mohtadi, M. No signature of abyssal carbon in intermediate waters off Chile during deglaciation. *Nature Geoscience* **3**, 192–195 (2010).
- DeLong, K. L., Quinn, T. M., Shen, C.-C., Lin, K. A snapshot of climate variability at Tahiti 9.5 ka using a fossil coral from IODP expedition 310, *Geochemistry, Geophysics, Geosystems*, doi:10.1029/2009GC002758 (2010).
- Deplazes, G., Lückge, A., Peterson, L. C., Timmermann, A., Hamann, Y., Hughen, K. A., Röhl, U., Laj, C., Cane, M. A., Sigman, D. M., Haug, G. H. Links between tropical rainfall and North Atlantic climate during the last glacial period. *Nature Geoscience* **6**, 213–217 (2013).
- Deschamps, P., Durand, N., Bard, E., Hamelin, B., Camoin, G., Thomas, A. L., Henderson, G. M., Okuno, J., Yokoyama, Y. Ice-sheet collapse and sea-level rise at the Bølling warming 14,600 years ago. *Nature* **483**, 559–564 (2012).
- Déath, G., Fabricius, K. E., Sweatman, H., Puotinen, M. The 27–year decline of coral cover on the Great Barrier Reef and its causes. *Proceedings of the National Academy of Sciences* **109**, 17995–17999 (2012).
- Déath, G., Lough, J. M., Fabricius, K. E. Declining Coral Calcification on the Great Barrier Reef. *Science* **323**, 116–119 (2009).
- Dickson, A. G. Thermodynamics of the dissociation of boric acid in synthetic seawater from 273.15 to 318.15 K. *Deep-Sea Research* **37**, 755–766 (1990).
- Dissard, D., Douville, E., Reynaud, S., Juillet-Leclerc, A., Montagna, P., Louvat, P., McCulloch, M. Light and temperature effects on $\delta^{11}\text{B}$ and B/Ca ratios of the

- zooxanthellate coral *Acropora* sp.: results from culturing experiments. *Biogeosciences* **9**, 4589–4605 (2012).
- Doney, S. C., Balch, W. M., Fabry, V. J., Feely, R. A. Ocean Acidification: A Critical Emerging Problem for the Ocean Sciences. *Oceanography* **22**, 16–25 (2009).
- Doney, S. C., Bopp, L., Long, M. C. Historical and Future Trends in Ocean Climate and Biogeochemistry. *Oceanography* **27**, 108–119 (2014).
- Dore, J. E., Lukas, R., Sadler, D. W., Church, M. J., Karl, D. M. Physical and biogeochemical modulation of ocean acidification in the central North Pacific. *Proceedings of the National Academy of Sciences* **106**, 12235–12240 (2009).
- Douville, E., Paterne, M., Cabioch, G., Louvat, P., Gaillardet, J., Juillet-Leclerc, A., Ayliffe, L. Abrupt sea surface pH change at the end of the Younger Dryas in the central sub-equatorial Pacific inferred from boron isotope abundance in corals (*Porites*). *Biogeosciences* **7**, 2445–2459 (2010).
- Durand, N., Deschamps, P., Bard, E., Hamelin, B., Camoin, G., Thomas, A. L., Henderson, G. M., Yokoyama, Y., Matsuzaki, H. Comparison of ^{14}C and U-Th ages in corals from IODP #310 cores offshore Tahiti. *Radiocarbon* **55**, 1–26 (2013).
- Etheridge, D. M., Steele, L. P., Langenfelds, R. L., Francey, R. J., Barnola, J.-M., Morgan, V. I. Natural and anthropogenic changes in atmospheric CO_2 over the last 1000 years from air in Antarctic ice and firn. *Journal of Geophysical Research* **101**, 4115–4128 (1996).
- Eyre, B. D., Andersson, A. J., Cyronak, T. Benthic coral reef calcium carbonate dissolution in an acidifying ocean. *Nature Climate Change* **4**, 969–976 (2014).
- Fabricius, K. E., Langdon, C., Uthicke, S., Humphrey, C., Noonan, S., Déath, G., Okazaki, R., Muehllehner, N., Glas, M. S., Lough, J. M. Losers and winners in coral reefs acclimatized to elevated carbon dioxide concentrations. *Nature Climate Change* **1**, 165–169 (2011).
- Fabry, V. J., Seibel, B. A., Feely, R. A., Orr, J. C. Impacts of ocean acidification on marine fauna and ecosystem processes. *ICES Journal of Marine Science* **65**, 414–432 (2008).
- Fairbanks, R. G., Mortlock, R. A., Chiu, T.-C., Cao, L., Kaplan, A., Guilderson, T. P., Fairbanks, T. W., Bloom, A. L., Grootes, P. M., Nadeau, M.-J. Radiocarbon calibration curve spanning 0 to 50,000 years BP based on paired $^{230}\text{Th}/^{234}\text{U}/^{238}\text{U}$ and ^{14}C dates on pristine corals. *Quaternary Science Reviews* **24**, 1781–1796 (2005).
- Fallon, S. J., McCulloch, M. T., van Woesik, R., Sinclair, D. J. Corals at their latitudinal limits: laser ablation trace element systematics in *Porites* from Shirigai Bay, Japan. *Earth and Planetary Science Letters* **172**, 221–238 (1999).
- Farmer, J. R., Hönisch, B., Robinson, L. F., Hill, T. M. Effects of seawater-pH and biomineralization on the boron isotopic composition of deep-sea bamboo corals. *Geochimica et Cosmochimica Acta* (in press).
- Feely, R. A., Takahashi, T., Wanninkhof, R., McPhaden, M. J., Cosca, C. E., Sutherland, S. C., Carr, M.-E. Decadal variability of the air-sea CO_2 fluxes in the equatorial Pacific Ocean. *Journal Of Geophysical Research* **111**, doi:10.1029/2005JC003129 (2006).

- Feely, R. A., Boutin, J., Cosca, C. E., Dandonneau, Y., Etcheto, J., Inoue, H. Y., Ishii, M., Le Quere, C., Mackey, D. J., McPhaden, M., Metzl, N., Poisson, A., Wanninkhof, R. Seasonal and interannual variability of CO₂ in the equatorial Pacific. *Deep-Sea Research II* **49**, 2443–2469 (2002).
- Feely, R. A., Doney, S. C., Cooley, S. R. Ocean Acidification: Present Conditions and Future Changes in a High-CO₂ World. *Oceanography* **22**, 36–47 (2009).
- Felis, T., Suzuki, A., Kuhnert, H., Rimbu, N., Kawahata, H. Pacific Decadal Oscillation documented in a coral record of North Pacific winter temperature since 1873. *Geophysical Research Letters*, doi:10.1029/2010GL043572 (2010).
- Felis, T., Merkel, U., Asami, R., Deschamps, P., Hathorne, E. C., Kölling, M., Bard, E., Cabioch, G., Durand, N., Prange, M., Schulz, M., Cahyarini, S. Y., Pfeiffer, M. Pronounced interannual variability in tropical South Pacific temperatures during Heinrich Stadial 1. *Nature Communications*, doi:10.1038/ncomms1973 (2012).
- Felis, T., Suzuki, A., Kuhnert, H., Dima, M., Lohmann, G., Kawahata, H. Subtropical coral reveals abrupt early-twentieth-century freshening in the western North Pacific Ocean. *Geology* **37**, 527–530 (2009).
- Foster, G. L., Sexton, P. F. Enhanced carbon dioxide outgassing from the eastern equatorial Atlantic during the last glacial. *Geology*, doi: 10.1130/G35806.1 (2014).
- Foster, G. L. Seawater pH, pCO₂ and [CO₃²⁻] variations in the Caribbean Sea over the last 130 kyr: A boron isotope and B/Ca study of planktic foraminifera. *Earth and Planetary Science Letters* **271**, 254–266 (2008).
- Foster, G. L., Pogge von Strandmann, P. A. E., Rae, J. W. B. Boron and magnesium isotopic composition of seawater. *Geochemistry Geophysics Geosystems*, doi:10.1029/2010GC003201 (2010).
- Francey, R. J., Allison, C. E., Etheridge, D. M., Trudinger, C. M., Enting, I. G., Leuenberger, M., Langenfelds, R. L., Michel, E., Steele, L. P. A 1000-year high precision record of δ¹³C in atmospheric CO₂. *Tellus* **51B**, 170–193 (1999).
- Francey, R. J., Trudinger, C. M., van der Schoot, M., Law, R. M., Krummel, P. B., Langenfelds, R. L., Steele, L. P., Allison, C. E., Stavert, A. R., Andres, R. J., Rödenbeck, C. Atmospheric verification of anthropogenic CO₂ emission trends. *Nature Climate Change* **3**, 520–524 (2013).
- Fujjeki, L. A. HOT : the Hawaii Ocean Time-Series. <http://hahana.soest.hawaii.edu/hot/hot_jgofs.html>, (2012).
- Gagan, M., Dunber, G. B., Suzuki, A. The effect of skeletal mass accumulation in *Porites* on coral Sr/Ca and δ¹⁸O paleothermometry. *Paleoceanography*, doi:10.1029/2011PA002215 (2012).
- Gaillardet, J., Allègre, C. J. Boron isotopic compositions of corals: seawater or diagenesis record? *Earth and Planetary Science Letters* **136**, 665–676 (1995).
- Gattuso, J.-P., Hansson, L. in *Ocean Acidification*. (Oxford University Press, 2011).
- Goyet, C., Healy, R., Ryan, J. Global distribution of total inorganic carbon and total alkalinity below the deepest winter mixed layer depths. *Technical report NPD-076. Carbon Dioxide Information and Analysis Center, Oak Ridge National Laboratory*,

- Oak Ridge Tennessee* (2000).
- Grottoli, A. G. Effect of light and brine shrimp on skeletal $\delta^{13}\text{C}$ in the Hawaiian coral *Porites compressa*: A tank experiment. *Geochimica et Cosmochimica Acta* **66**, 1955–1967 (2002).
- Grottoli, A. G. Variability of stable isotopes and maximum linear extension in reef-coral skeletons at Kaneohe Bay, Hawaii. *Marine Biology* **135**, 437–449 (1999).
- Gruber, N. Warming up, turning sour, losing breath: ocean biogeochemistry under global change. *The Philosophical Transactions of the Royal Society A* **369**, 1980–1996 (2011).
- Gruber, N., Gloor, M., Mikaloff Fletcher, S. E., Doney, S. C., Dutkiewicz, S., Follows, M. J., Gerber, M., Jacobson, A. R., Joos, F., Lindsay, K., Menemenlis, D., Mouchet, A., Muller, S. A., Sarmiento, J. L., Takahashi, T. Oceanic sources, sinks, and transport of atmospheric CO_2 . *Global Biogeochemical Cycles*, doi:10.1029/2008GB003349 (2009).
- Gruber, N., Hauri, C., Lachkar, Z., Loher, D., Frölicher, T. L., Plattner, G.-K. Rapid Progression of Ocean Acidification in the California Current System. *Science* **337**, 220–223 (2012).
- Gruber, N., Keeling, C. D., Bacastow, R. B., Guenther, P. R., Lueker, T. J., Wahlen, M., Meijer, H. A. J., Mook, W. G., Stocker, T. F. Spatiotemporal patterns of carbon-13 in the global surface oceans and the oceanic Suess effect. *Global Biogeochemical Cycles* **13**, 307–335 (1999).
- Guilderson, T. P., Fairbanks, R. G., Rubenstone, J. L. Tropical Temperature Variations Since 20,000 Years Ago: Modulating Interhemispheric Climate Change. *Science* **263**, 663–665 (1994).
- Hall-Spencer, J. M., Rodolfo-Metalpa, R., Martin, S., Ransome, E., Fine, M., Turner, S. M., Rowley, S. J., Tedesco, D., Buia, M.-C. Volcanic carbon dioxide vents show ecosystem effects of ocean acidification. *Nature* **454**, 96–99 (2008).
- Hathorne, E. C., Felis, T., James, R. H., Thomas, A. Laser ablation ICP-MS screening of corals for diagenetically affected areas applied to Tahiti corals from the last deglaciation. *Geochimica et Cosmochimica Acta* **75**, 1490–1506 (2011).
- Hayashi, E., Suzuki, A., Nakamura, T., Iwase, A., Ishimura, T., Iguchi, A., Sakai, K., Okai, T., Inoue, M., Araoka, D., Murayama, S., Kawahata, H. Growth-rate influences on coral climate proxies tested by a multiple colony culture experiment. *Earth and Planetary Science Letters* **362**, 198–206 (2013).
- Hayes, C. T., Anderson, R. F., Fleisher, M. Q. Opal accumulation rates in the equatorial Pacific and mechanisms of deglaciation. *Paleoceanography*, doi: 10.1029/2010PA002008 (2011).
- Heindel, K., Wisshak, M., Westphal, H. Microbioerosion in Tahitian reefs: a record of environmental change during the last deglacial sea-level rise (IODP 310). *Lethaia* **42**, 322–340 (2009).
- Hemming, N. G., Hanson, G. N. Boron isotopic composition and concentration in modern marine carbonates. *Geochimica et Cosmochimica Acta* **56**, 537–543 (1992).

- Hemming, N. G., Guilderson, T. P., Fairbanks, R. G. Seasonal variations in the boron isotopic composition of coral: A productivity signal? *Global Biogeochemical Dynamics* **12**, 581–586 (1998).
- Hendriks, I. E., Duarte, C. M., Olsen, Y. S., Steckbauer, A., Ramajo, L., Moore, T. S., Trotter, J. A., McCulloch, M. Biological mechanisms supporting adaptation to ocean acidification in coastal ecosystems. *Estuarine, Coastal and Shelf Science* **152**, A1–A8 (2015).
- Henehan, M. J., Rae, J. W. B., Foster, G. L., Erez, J., Prentice, K. C., Kucera, M., Bostock, H. C., Martinez-Boti, M. A., Milton, J. A., Wilson, P. A., Marshall, B. J., Elliott, T. Calibration of the boron isotope proxy in the planktonic foraminifera *Globigerinoides ruber* for use in palaeo-CO₂ reconstruction. *Earth and Planetary Science Letters* **364**, 111–122 (2013).
- Heumann, K. G. Isotopic analyses of inorganic and organic substances by mass spectrometry. *International Journal of Mass Spectrometry and Ion Processes* **1**, 87–110 (1982).
- Hoegh-Guldberg, O., Mumby, P. J., Hooten, A. J., Steneck, R. S., Greenfield, P., Gomez, E., Harvell, C. D., Sale, P. F., Edwards, A. J., Caldeira, K., Knowlton, N., Eakin, C. M., Iglesias-Prieto, R., Muthiga, N., Bradbury, R. H., Dubi, A., Hatziolos, M. E. Coral Reefs Under Rapid Climate Change and Ocean Acidification. *Science* **318**, 173–175 (2007).
- Hofmann, G. E., Smith, J. E., Johnson, K. S., Send, U., Levin, L. A., Micheli, F., Paytan, A., Price, N. N., Peterson, B., Takeshita, Y., Matson, P. G., Crook, E. D., Kroeker, K. J., Gambi, M. C., Rivest, E. B., Frieder, C. A., Yu, P. C., Martz, T. R. High-Frequency Dynamics of Ocean pH: A Multi-Ecosystem Comparison. *PLoS ONE*, doi:10.1371/journal.pone.0028983 (2011).
- Holcomb, M., Venn, A. A., Tambutte, E., Tambutte, S., Allemand, D., Trotter, J., McCulloch, M. Coral calcifying fluid pH dictates response to ocean acidification. *Scientific Reports*, doi:10.1038/srep05207 (2014).
- Horn, M. G., Beucher, C. P., Robinson, R. S., Brzezinski, M. A. Southern ocean nitrogen and silicon dynamics during the last deglaciation. *Earth and Planetary Science Letters* **310**, 334–339 (2011).
- Hönisch, B., Hemming, N. G., Loose, B. Comment on ‘A critical evaluation of the boron isotope-pH proxy: the accuracy of ancient ocean pH estimates’ by M. Pagani, D. Lemarchand, A. Spivak, J. Gaillardet. *Geochimica et Cosmochimica Acta* **71**, 1636–1641 (2007).
- Hönisch, B., Hemming, N. G. Surface ocean pH response to variations in *p*CO₂ through two full glacial cycles. *Earth and Planetary Science Letters* **236**, 305–314 (2005).
- Hönisch, B., Hemming, N. G., Grottoli, A. G., Amat, A., Hanson, G. N., Bijma, J. Assessing scleractinian corals as recorders for paleo-pH: Empirical calibration and vital effects. *Geochimica et Cosmochimica Acta* **68**, 3675–3685 (2004).
- Hönisch, B., Hemming, N. G., Archer, D., Siddall, M., McManus, J. F. Atmospheric Carbon Dioxide Concentration Across the Mid-Pleistocene Transition. *Science* **324**, 1551–1554 (2009).

- Iguchi, A., Ozaki, S., Nakamura, T., Inoue, M., Tanaka, Y., Suzuki, A., Kawahata, H., Sakai, K. Effects of acidified seawater on coral calcification and symbiotic algae on the massive coral *Porites australiensis*. *Marine Environmental Research* **73**, 32–36 (2012).
- Iguchi, A., Kumagai, N. H., Nakamura, T., Suzuki, A., Sakai, K., Nojiri, Y. Responses of calcification of massive and encrusting corals to past, present, and near-future ocean carbon dioxide concentrations. *Marine Pollution Bulletin* (2014).
- Inoue, M., Yokoyama, Y., Harada, M., Suzuki, A., Kawahata, H., Matsuzaki, H., Iryu, Y. Trace element variations in fossil corals from Tahiti collected by IODP Expedition 310: Reconstruction of marine environments during the last deglaciation (15 to 9 ka). *Marine Geology* **271**, 303–306 (2010).
- Inoue, S., Kayanne, H., Yamamoto, S., Kurihara, H. Spatial community shift from hard to soft corals in acidified water. *Nature Climate Change* **3**, 683–687 (2013).
- Ishii, M., Kosugi, N., Sasano, D., Saito, S., Midorikawa, T., Inoue, H. Y. Ocean acidification off the south coast of Japan: A result from time series observations of CO₂ parameters from 1994 to 2008. *Journal of Geophysical Research*, doi:10.1029/2010JC006831 (2011).
- Ishii, M., Inoue, H. Y., Matsueda, H., Saito, S., Fushimi, K., Nemoto, K., Yano, T., Nagai, H., Midorikawa, T. Seasonal variation in total inorganic carbon and its controlling processes in surface waters of the western North Pacific subtropical gyre. *Marine Chemistry* **75**, 17–32 (2001).
- Ishikawa, T., Nagaishi, K. High-precision isotopic analysis of boron by positive thermal ionization mass spectrometry with sample preheating. *Journal of Analytical Atomic Spectrometry* **26**, 359–365 (2011).
- Ito, T., Mazloff, M. Anthropogenic carbon dioxide transport in the Southern Ocean driven by Ekman flow. *Nature* **463**, 80–83 (2010).
- Iudicone, D., Rodgers, K. B., Stendardo, I., Aumont, O., Madec, G., Bopp, L., Mangoni, O., Ribera d'Alcala', M. Water masses as a unifying framework for understanding the Southern Ocean Carbon Cycle. *Biogeosciences* **8**, 1031–1052 (2011).
- Kaczmarek, K., Horn, I., Nehrke, G., Bijma, J. Simultaneous determination of $\delta^{11}\text{B}$ and B/Ca ratio in marine biogenic carbonates at nanogram level. *Chemical Geology* **392**, 32–42 (2015).
- Kakihana, H., Kotaka, M., Satoh, S., Nomura, M., Okamoto, M. Fundamental Studies on the Ion-Exchange Separation of Boron Isotopes. *Bulletin of the Chemical Society of Japan* **50**, 158–163 (1977).
- Kasemann, S. A., Schmidt, D. N., Bijma, J., Foster, G. L., *In situ* analysis in marine carbonates and its application for foraminifera and paleo-pH. *Chemical Geology* **260**, 138–147 (2009).
- Kawakubo, Y., Yokoyama, Y., Suzuki, A., Okai, T., Alibert, C., Kinsley, L., Eggins, S. Precise determination of Sr/Ca by laser ablation ICP-MS compared to ICP-AES and application to multi-century temperate corals. *Geochemical Journal* **48**, 145–152 (2014).
- Keeling, C. D., Brix, H., Gruber, N. Seasonal and long-term dynamics of the upper

- ocean carbon cycle at Station ALOHA near Hawaii. *Global Biogeochemical Cycles* doi:10.1029/2004GB002227 (2004).
- Key, R. M., Kozyr, A., Sabine, C. L., Lee, K., Wanninkhof, R., Bullister, J. L., Feely, R. A., Millero, F. J., Mordy, C., Peng, T.-H. A global ocean carbon climatology: Results from Global Data Analysis Project (GLODAP). *Global Biogeochemical Cycle*, doi:10.1029/2004GB002247 (2004).
- Kiefer, T., Kienast, M. Patterns of deglacial warming in the Pacific Ocean: a review with emphasis on the time interval of Heinrich event 1. *Quaternary Science Reviews* **24**, 1063–1081 (2005).
- Kleypas, J. A., Yates, K. K. Coral Reefs and Ocean Acidification. *Oceanography* **22**, 108–117 (2009).
- Kleypas, J. A., Buddemeier, R. W., Archer, D., Gattuso, J.-P., Langdon, C., Opdyke, B. N. Geochemical Consequences of Increased Atmospheric Carbon Dioxide on Coral Reefs. *Science* **284**, 118–120 (1999).
- Kleypas, J.A., Langdon, C. in *Coastal and Estuarine Studies: Coral Reefs and Climate Change Science and Management* (eds Phinney, J. T. *et al.*) 73–110 (Geophysical Monograph Series 61, American Geophysical Union, 2006).
- Klochko, K., Kaufman, A. J., Yao, W., Byrne, R. H., Tossell, J. A. Experimental measurement of boron isotope fractionation in seawater. *Earth and Planetary Science Letters* **248**, 276–285 (2006).
- Kohfeld, K. E., Le Quere, C., Harrison, S. P., Anderson, R. F. Role of Marine Biology in Glacial-Interglacial CO₂ Cycles. *Science* **308**, 74–78 (2005).
- Krief, S., Hendy, E. J., Fine, M., Yam, R., Meibom, A., Foster, G. L., Shemesh, A. Physiological and isotopic responses of scleractinian corals to ocean acidification. *Geochimica et Cosmochimica Acta* **74**, 4988–5001 (2010).
- Kubota, K., Yokoyama, Y., Ishikawa, T., Obrochta, S., Suzuki, A. Larger CO₂ source at the equatorial Pacific during the last deglaciation. *Scientific Reports*, doi:10.1038/srep05261 (2014).
- Kuchinke, M., Tilbrook, B., Lenton, A. Seasonal variability of aragonite saturation state in the Western Pacific. *Marine Chemistry* **161**, 1–13 (2014).
- Kwon, E. Y., Hain, M. P., Sigman, D. M., Galbraith, E. D., Sarmiento, J. L., Toggweiler, J. R. North Atlantic ventilation of “southern-sourced” deep water in the glacial ocean. *Paleoceanography*, doi:10.1029/2011PA002211 (2012).
- Le Quéré, C., Raupach, M. R., Canadell, J. G., Marland, G., Bopp, L., Ciais, P., Conway, T. J., Doney, S. C., Feely, R. A., Foster, P., Friedlingstein, P., Gurney, K., Houghton, R. A., House, J. I., Huntingford, C., Levy, P. E., Lomas, M. R., Majkut, J., Metz, N., Ometto, J. P., Peters, G. P., Prentice, I. C., Randerson, J. T., Running, S. W., Sarmiento, J. L., Schuster, U., Sitch, S., Takahashi, T., Viovy, N., van der Werf, G. R., Woodward, F. I. Trends in the sources and sinks of carbon dioxide. *Nature Geoscience* **2**, 831–836 (2009).
- Lee, K., Tong, L. T., Millero, F. J., Sabine, C. L., Dickson, A. G., Goyet, C., Park, G.-H., Wanninkhof, R., Feely, R. A., Key, R. M. Global relationships of total alkalinity with salinity and temperature in surface waters of the world’s oceans.

- Geophysical Research Letters* **33**, doi:10.1029/2006GL027207 (2006).
- Lenton, A., Metzl, N., Takahashi, T., Kuchinke, M., Matear, R. J., Roy, T., Sutherland, S. C., Sweeney, C., Tilbrook, B. The observed evolution of oceanic $p\text{CO}_2$ and its drivers over the last two decades. *Global Biogeochemical Cycles*, doi:10.1029/2011GB004095 (2012).
- Liu, Y., Peng, Z., Zhou, R., Song, S., Liu, W., You, C.-F., Lin, Y.-P., Yu, K., Wu, C.-C., Wei, G., Xie, L., Burr, G. S., Shen, C.-C. A 1400-year terrigenous dust record on a coral island in South China Sea. *Scientific Reports*, doi:10.1038/srep04994 (2014).
- Liu, Y., Liu, W., Peng, Z., Xiao, Y., Wei, G., Sun, W., He, J., Liu, G., Chou, C.-L. Instability of seawater pH in the South China Sea during the mid-late Holocene: Evidence from boron isotopic composition of corals. *Geochimica et Cosmochimica Acta* **73**, 1264–1272 (2009).
- Loubere, P., Bennet, S. Southern Ocean biogeochemical impact on the tropical ocean: Stable isotope records from the Pacific for the past 25,000 years. *Global and Planetary Change* **63**, 333–340 (2008).
- Lourantou, A., Lavrie, J. V., Köhler, P., Barnola, J.-M., Paillard, D., Michel, E., Raynaud, D., Chappellaz, J. Constraint of the CO_2 rise by new atmospheric carbon isotopic measurements during the last deglaciation. *Global Biogeochemical Cycles*, doi: 10.1029/2009GB003545 (2010).
- Lueker, T. J., Dickson, A. G., Keeling, C. D. Ocean $p\text{CO}_2$ calculated from dissolved inorganic carbon, alkalinity, and equations for K_1 and K_2 : validation based on laboratory measurements of CO_2 in gas and seawater at equilibrium. *Marine Chemistry* **70**, 105–119 (2000).
- Lüthi, D., Le Floch, M., Bereiter, B., Blunier, T., Barnola, J.-M., Siegenthaler, U., Raynaud, D., Jouzel, J., Fischer, H., Kawamura, K., Stocker, T. F. High-resolution carbon dioxide concentration record 650,000–800,000 years before present. *Nature* **453**, 379–382 (2008).
- MARGO Project Members. Constraints on the magnitude and patterns of ocean cooling at the Last Glacial Maximum. *Nature Geoscience* **2**, 127–132 (2009).
- Marchitto, T. M., Lehman, S. J., Ortiz, J. D., Flückiger, J., van Geen, A. Marine Radiocarbon Evidence for the Mechanism of Deglacial Atmospheric CO_2 Rise. *Science* **316**, 1456–1459 (2007).
- Marcott, S. A., Bauska, T. K., Buizert, C., Steig, E. J., Rosen, J. L., Cuffey, K. M., Fudge, T. J., Severinghaus, J. P., Ahn, J., Kalk, M. L., McConnell, J. R., Sowers, T., Taylor, K. C., White, J. W. C., Brook, E. J. Centennial-scale changes in the global carbon cycle during the last deglaciation. *Nature* **514**, 616–619 (2014).
- Marshall, J. F., McCulloch, M. T. An assessment of the Sr/Ca ratio in shallow water hermatypic corals as a proxy for sea surface temperature. *Geochimica et Cosmochimica Acta* **66**, 3263–3280 (2002).
- Martínez-García, A., Sigman, D. M., Ren, H., Anderson, R. F., Straub, M., Hodell, D. A., Jaccard, S. L., Eglinton, T. I., Haug, G. H. Iron Fertilization of the Subantarctic Ocean During the Last Ice Age. *Science* **343**, 1347–1350 (2014).
- Matsumoto, K., Yokoyama, Y. Atmospheric $\Delta^{14}\text{C}$ reduction in simulations of Atlantic

- overturning circulation shutdown. *Global Biogeochemical Cycles* **27**, 296–304 (2013).
- McConnaughey, T. A. ^{13}C and ^{18}O isotopic disequilibrium in biological carbonates: I. Patterns. *Geochimica et Cosmochimica Acta* **53**, 151–162 (1989).
- McCulloch, M., Falter, J., Trotter, J., Montagna, P. Coral resilience to ocean acidification and global warming through pH up-regulation. *Nature Climate Change* **2**, 623–627 (2012a).
- McCulloch, M., Trotter, J., Montagna, P., Falter, J., Dunbar, R., Freiwald, A., Fořterra, G., Correa, M. L., Maier, C., Ruggeberg, A., Taviani, M. Resilience of cold-water scleractinian corals to ocean acidification: Boron isotopic systematics of pH and saturation state up-regulation. *Geochimica et Cosmochimica Acta* **87**, 21–34 (2012b).
- McCulloch, M. T., Holcomb, M., Rankenburg, K., Trotter, J. A. Rapid, high-precision measurements of boron isotopic compositions in marine carbonates. *Rapid Communications in Mass Spectrometry* **28**, 2704–2712 (2014).
- McMullen, C. C., Cragg, C. B., Thode, H. G. Absolute ratio of $^{11}\text{B}/^{10}\text{B}$ in Searles Lake borax. *Geochimica et Cosmochimica Acta* **23**, 147–150 (1961).
- Midorikawa, T., Ishii, M., Saito, S., Sasano, D., Kosugi, N., Motoi, T., Kamiya, H., Nakadate, A., Nemoto, K., Inoue, H. Y. Decreasing pH trend estimated from 25-yr time series of carbonate parameters in the western North Pacific. *Tellus* **62B**, 649–659 (2010).
- Midorikawa, T., Ishii, M., Kosugi, N., Sasano, D., Nakano, T., Saito, S., Sakamoto, N., Nakano, H., Inoue, H. Y. Recent deceleration of oceanic $p\text{CO}_2$ increase in the western North Pacific in winter. *Geophysical Research Letters* **39**, L12601 (2012).
- Millero, F. J. The thermodynamics of the carbonate system in seawater. *Geochimica et Cosmochimica Acta* **43**, 1651–1661 (1979).
- Misra, S., Owen, R., Kerr, J., Greaves, M., Elderfield, H. Determination of $\delta^{11}\text{B}$ by HR-ICP-MS from mass limited samples: Application to natural carbonates and water samples. *Geochimica et Cosmochimica Acta* **140**, 531–552 (2014).
- Mishima, M., Suzuki, A., Nagao, M., Ishimura, T., Inoue, M., Kawahata, H. Abrupt shift toward cooler condition in the earliest 20th century detected in a 165 year coral record from Ishigaki Island, southwestern Japan. *Geophysical Research Letters*, doi:10.1029/2010GL043451 (2010).
- Monnin, E., Indermuhle, A., Dallenbach, A., Fluckiger, J., Stauffer, B., Stocker, T. F., Raynaud, D., Barnola, J.-M. Atmospheric CO_2 Concentrations over the Last Glacial Termination. *Science* **291**, 112–114 (2001).
- Nozaki, Y., Rye, D. M., Turekian, K. K., Dodge, R. E. A 200 year record of carbon-13 and carbon-14 variations in a Bermuda coral. *Geophysical Research Letters* **5**, 825–828 (1978).
- Okai, T., Suzuki, A., Kawahata, H., Terashima, S., Imai, N. Preparation of a New Geological Survey of Japan Geochemical Reference Material: Coral JCp-1. *Geostandards Newsletter* **26**, 95–99 (2002).
- Orr, J. C., Fabry, V. J., Aumont, O., Bopp, L., Doney, S. C., Feely, R. A., Gnanadesikan,

- A., Gruber, N., Ishida, A., Joos, F., Key, R. M., Lindsay, K., Maier-Reimer, E., Matear, R., Monfray, P., Mouchet, A., Najjar, R. G., Plattner, G.-K., Rodgers, K. B., Sabine, C. L., Sarmiento, J. L., Schlitzer, R., Slater, R. D., Totterdell, I. J., Weirig, M.-F., Yamanaka, Y., Yool, A. Anthropogenic ocean acidification over the twenty-first century and its impact on calcifying organisms. *Nature* **437**, 681–686 (2005).
- Osborne, M. C., Dunbar, R. B., Mucciarone, D. A., Druffel, E., Sanchez-Cabeza, J. A. A 215-yr coral $\delta^{18}\text{O}$ time series from Palau records dynamics of the West Pacific Warm Pool following the end of the Little Ice Age. *Coral Reefs* **33**, 719–731 (2014).
- Palmer, M. R., Pearson, P. N. A 23,000-Year Record of Surface Water pH and $p\text{CO}_2$ in the Western Equatorial Pacific Ocean. *Science* **300**, 480–482 (2003).
- Pandolfi, J. M., Connolly, S. R., Marshall, D. J., Cohen, A. L. Projecting Coral Reef Futures Under Global Warming and Ocean Acidification. *Science* **333**, 418–422 (2011).
- Paterne, M., Ayliffe, L. K., Arnold, M., Cabioch, G., Tisnérat-Laborde, N., Hatté, C., Douville, E., Bard, E. Paired ^{14}C and $^{230}\text{Th}/\text{U}$ dating of surface corals from the Marquesas and Vanuatu (sub-equatorial Pacific) in the 3,000 to 15,000 cal yr interval. *Radiocarbon* **46**, 551–566 (2004).
- Pedro, J. B., van Ommen, T. D., Rasmussen, S. O., Morgan, V. I., Chappellaz, J., Moy, A. D., Masson-Delmotte, V., Delmotte, M. The last deglaciation: timing the bipolar seesaw. *Climate of the Past* **7**, 671–683 (2011).
- Pelejero, C., Calvo, E., McCulloch, M. T., Marshall, J. F., Gagan, M. K., Lough, J. M., Opdyke, B. N. Preindustrial to Modern Interdecadal Variability in Coral Reef pH. *Science* **309**, 2204–2207 (2005).
- Pena, L. D., Cacho, I., Ferretti, P., Hall, M. A. El Niño–Southern Oscillation–like variability during glacial terminations and interlatitudinal teleconnections. *Paleoceanography*, doi:10.1029/2008PA001620 (2008).
- Pena, L. D., Goldstein, S. L., Hemming, S. R., Jones, K. M., Calvo, E., Pelejero, C., Cacho, I. Rapid changes in meridional advection of Southern Ocean intermediate waters to the tropical Pacific during the last 30 kyr. *Earth and Planetary Science Letters* **368**, 20–32 (2013).
- Quay, P. D., Stutsman, J. Surface layer carbon budget for the subtropical N. Pacific: $\delta^{13}\text{C}$ constraints at station ALOHA. *Deep-Sea Research I* **50**, 1045–1061 (2003).
- Quay, P., Sonnerup, R., Westby, T., Stutsman, J., McNichol, A. Changes in the $^{13}\text{C}/^{12}\text{C}$ of dissolved inorganic carbon in the ocean as a tracer of anthropogenic CO_2 uptake. *Global Biogeochemical Cycles*, doi:10.1029/2001GB001817 (2003).
- Quay, P. D., Tilbrook, B., Wong, C. S. Oceanic Uptake of Fossil Fuel CO_2 : Carbon-13 Evidence. *Science* **256**, 74–79 (1992).
- Rae, J. W. B., Foster, G. L., Schmidt, D. N., Elliott, T. Boron isotopes and B/Ca in benthic foraminifera: Proxies for the deep ocean carbonate system. *Earth and Planetary Science Letters* **302**, 403–413 (2011).
- Reimer, P. J., Baillie, M. G. L., Bard, E., Bayliss, A., Beck, J. W., Blackwell, P. G., Bronk-Ramsey, C., Buck, C. E., Burr, G. S., Edwards, R. L., Friedrich, M., Grootes,

- P. M., Guilderson, T. P., Hajdas, I., Heaton, T. J., Hogg, A. G., Hughen, K. A., Kaiser, K. F., Kromer, B., McCormac, F. G., Manning, S. W., Reimer, R. W., Richards, D. A., Southon, J. R., Talamo, S., Turney, C. S. M., van der Plicht, J., Weyhenmeyer, C. E. IntCal09 and Marine09 radiocarbon age calibration curves, 0–50,000 years cal BP. *Radiocarbon* **51**, 1111–1150 (2009).
- Reimer, P. J., Bard, E., Bayliss, A., Beck, J. W., Blackwell, P. G., Bronk-Ramsey, C., Buck, C. E., Cheng, H., Edwards, R. L., Friedrich, M., Grootes, P. M., Guilderson, T. P., Haflidason, H., Hajdas, I., Hatté, C., Heaton, T. J., Hoffman, D. L., Hogg, A. G., Hughen, K. A., Kaiser, K. F., Kromer, B., Manning, S. W., Niu, M., Reimer, R. W., Richards, D. A., Scott, E. M., Southon, J. R., Staff, R. A., Turney, C. S. M., van der Plicht, J. IntCal13 and Marine13 radiocarbon age calibration curves 0–50,000 years cal BP. *Radiocarbon* **55**, 1869–1887 (2013a).
- Reimer, P. J., Bard, E., Bayliss, A., Beck, J. W., Blackwell, P. G., Bronk-Ramsey, C., Buck, C. E., Edwards, R. L., Friedrich, M., Grootes, P. M., Guilderson, T. P., Haflidason, H., Hajdas, I., Hatté, C., Heaton, T. J., Hogg, A. G., Hughen, K. A., Kaiser, K. F., Kromer, B., Manning, S. W., Reimer, R. W., Richards, D. A., Scott, E. M., Southon, J. R., Turney, C. S. M., van der Plicht, J. Selection and treatment of data for radiocarbon calibration: An update to the International Calibration (IntCal) criteria. *Radiocarbon* **55**, 1923–1945 (2013b).
- Revelle, R., Suess, H. E. Carbon Dioxide Exchange Between Atmosphere and Ocean and the Question of an Increase of Atmospheric CO₂ during the Past Decades. *Tellus* **9**, 18–27 (1957).
- Reynaud, S., Hemming, N. G., Juillet-Leclerc, A., Gattuso, J.-P. Effect of *p*CO₂ and temperature on the boron isotopic composition of the zooxanthellate coral *Acropora* sp. *Coral Reefs* **23**, 539–546 (2004).
- Riebesell, U., Fabry, V. J., Hansson, L., Gattuso, J.-P. in *Guide to best practices for ocean acidification research and data reporting* (Publications Office of European Union, Luxembourg, 2010).
- Robbins, L. L., Hansen, M. E., Kleypas, J. A., Meylan, S. C. CO₂calc—A user-friendly seawater carbon calculator for Windows, Max OS X, and iOS (iPhone). *U.S. Geological Survey Open-File Report* 2010–1280 (2010).
- Rollion-Bard, C., Chaussidon, M., France-Lanord, C. Biological control of internal pH in scleractinian corals: Implications on paleo-pH and paleo-temperature reconstructions. *C. R. Geoscience* **343**, 397–405 (2011a).
- Rollion-Bard, C., Blamart, D., Trebosc, J., Tricot, G., Mussi, A., Cuif, J.-P. Boron isotopes as pH proxy: A new look at boron speciation in deep-sea corals using 11B MAS NMR and EELS. *Geochimica et Cosmochimica Acta* **75**, 1003–1012 (2011b).
- Rollion-Bard, C., Chaussidon, M., France-Lanord, C. pH control on oxygen isotopic composition of symbiotic corals. *Earth and Planetary Science Letters* **215**, 275–288 (2003).
- Rose, K. A., Sikes, E. L., Guilderson, T. P., Shane, P., Hill, T. M., Zahn, R., Spero, H. J. Upper-ocean-to-atmosphere radiocarbon offsets imply fast deglacial carbon dioxide release. *Nature* **466**, 1093–1097 (2010).

- Rubino, M., Etheridge, D. M., Trudinger, C. M., Allison, C. E., Battle, M. O., Langenfelds, R. L., Steele, L. P., Curran, M., Bender, M., White, J. W. C., Jenk, T. M., Blunier, T., Francey, R. J. A revised 1000 year atmospheric $\delta^{13}\text{C}$ -CO₂ record from Law Dome and South Pole, Antarctica. *Journal of Geophysical Research (Atmosphere)* **118**, 8482–8499 (2013).
- Sabine, C. L., Feely, R. A., Key, R. M., Bullister, J. L., Millero, F. J., Lee, K., Peng, T.-H., Tilbrook, B., Ono, T., Wong, C. S. Distribution of anthropogenic CO₂ in the Pacific Ocean. *Global Biogeochemical Cycles*, doi:10.1029/2001GB001639 (2002).
- Sabine, C. L., Feely, R. A., Gruber, N., Key, R. M., Lee, K., Bullister, J. L., Wannikhof, R., Wong, C. S., Wallace, D. W. R., Tilbrook, B., Millero, F. J., Peng, T. H., Kozyr, A., Ono, T., Rios, A. F. The Oceanic Sink for Anthropogenic CO₂. *Science* **305**, 367–371 (2004).
- Sallée, J.-B., Matear, R. J., Rintoul, S. R., Lenton, A. Localized subduction of anthropogenic carbon dioxide in the Southern Hemisphere oceans. *Nature Geoscience* **5**, 579–584 (2012).
- Sarmiento, J. L., Gruber, N. in *Ocean Biogeochemical Dynamics*. (Princeton Univ. Press, 2011)
- Schlitzer, R. Ocean Data View. <<http://odv.awi.de>>, (2014).
- Schmitt, J., Schneider, R., Elsig, J., Leuenberger, D., Laurantou, A., Chappellaz, J., Kohler, P., Joos, F., Stocker, T. F., Leuenberger, M., Fischer, H. Carbon Isotope Constraints on the Deglacial CO₂ Rise from Ice Cores. *Science* **336**, 711–714 (2012).
- Schmittner, A., Gruber, N., Mix, A. C., Key, R. M., Tagliabue, A., Westberry, T. K. Biology and air–sea gas exchange controls on the distribution of carbon isotope ratios ($\delta^{13}\text{C}$) in the ocean. *Biogeosciences* **10**, 5793–5816 (2013).
- Schneider, T., Bischoff, T., Haug, G. H. Migrations and dynamics of the intertropical convergence zone. *Nature* **513**, 45–53 (2014).
- Seard, C., Camoin, G., Yokoyama, Y., Matsuzaki, H., Durand, N., Bard, E., Sepulcre, S., Deschamps, P. Microbialite development patterns in the last deglacial reefs from Tahiti (French Polynesia; IODP Expedition #310): Implications on reef framework architecture, *Marine Geology* **279**, 63–86 (2011).
- Seki, O., Foster, G. L., Schmidt, D. N., Mackensen, A., Kawamura, K., Pancost, R. D. Alkenone and boron-based Pliocene $p\text{CO}_2$ records. *Earth and Planetary Science Letters* **292**, 201–211 (2010).
- Shinjo, R., Asami, R., Huang, K.-F., You, C.-F., Iryu, Y. Ocean acidification trend in the tropical North Pacific since the mid-20th century reconstructed from a coral archive. *Marine Geology*. **342**, 58–64 (2013).
- Siani, G., Michel, E., De Pol-Holz, R., DeVries, T., Lamy, F., Carel, M., Isguder, G., Dewilde, F., Laurantou, A. Carbon isotope records reveal precise timing of enhanced Southern Ocean upwelling during the last deglaciation. *Nature Communications*, doi: 10.1038/ncomms3758 (2013).
- Sigman, D. M., Boyle, E. A. Glacial/interglacial variations in atmospheric carbon dioxide. *Nature* **407**, 859-869 (2000).

- Sigman, D. M., Hain, M. P., Haug, G. H. The polar ocean and glacial cycles in atmospheric CO₂ concentration. *Nature* **466**, 47–55 (2010).
- Sikes, E. L., Samson, C. R., Guilderson, T. P., Howard, W. R. Old radiocarbon ages in the southwest Pacific Ocean during the last glacial period and deglaciation. *Nature* **405**, 555–559 (2000).
- Skinner, L., McCave, I. N., Carter, L., Fallon, S., Scrivner, A. E., Primeau, F. Reduced ventilation and enhanced magnitude of the deep Pacific carbon pool during the last glacial period. *Earth and Planetary Science Letters* **411**, 45–52 (2015).
- Skinner, L. C., Fallon, S., Waelbroeck, C., Michel, E., Barker, S. Ventilation of the Deep Southern Ocean and Deglacial CO₂ Rise. *Science* **328**, 1147–1151 (2010).
- Southon, J., Noronha, A. L., Cheng, H., Edwards, R. L., Wang, Y. A high-resolution record of atmospheric ¹⁴C based on Hulu Cave speleothem H82. *Quaternary Science Reviews* **33**, 32–41 (2012).
- Spero, H. J., Lea, D. W. The Cause of Carbon Isotope Minimum Events on Glacial Terminations. *Science* **296**, 522–525 (2002).
- Spivack, A. J., Edmond, J. M. Boron isotope exchange between seawater and the oceanic crust. *Geochimica et Cosmochimica Acta* **51**, 1033–1043 (1987).
- Stott, L., Southon, J., Timmermann, A., Koutavas, A. Radiocarbon age anomaly at intermediate water depth in the Pacific Ocean during the last deglaciation. *Paleoceanography*, doi: 10.1029/2008PA001690 (2009).
- Stute, M., Forster, M., Frischkorn, H., Serejo, A., Clark, J. F., Schlosser, P., Broecker, W. S., Bonani, G. Cooling of Tropical Brazil (5°C) During the Last Glacial Maximum. *Science* **269**, 379–383 (1995).
- Sutton, A. J., Feely, R. A., Sabine, C. L., McPhaden, M. J., Takahashi, T., Chavez, F. P., Friederich, G. E., Mathis, J. T. Natural variability and anthropogenic change in equatorial Pacific surface ocean pCO₂ and pH. *Global Biogeochemical Cycles*, doi:10.1002/2013GB004679 (2014).
- Suzuki, A., Hibino, K., Iwase, A., Kawahata, H. Intercolony variability of skeletal oxygen and carbon isotope signatures of cultured *Porites* corals: Temperature-controlled experiments. *Geochimica et Cosmochimica Acta* **69**, 4453–4462 (2005).
- Swart, P. K., Greer, L., Rosenheim, B. E., Moses, C. S., Waite, A. J., Winter, A., Dodge, R. E., Helmle, K. The ¹³C Suess effect in scleractinian corals mirror changes in the anthropogenic CO₂ inventory of the surface oceans. *Geophysical Research Letters*, doi:10.1029/2009GL041397 (2010).
- Takahashi, T., Sutherland, S. C., Chipman, D. W., Goddard, J. G., Ho, C., Newberger, T., Sweeney, C., Munro, D. R. Climatological distributions of pH, pCO₂, total CO₂, alkalinity, and CaCO₃ saturation in the global surface ocean, and temporal changes at selected locations. *Marine Chemistry* **164**, 95–125 (2014).
- Takahashi, T., Sutherland, S. C., Wanninkhof, R., Sweeney, C., Feely, R. A., Chipman, D. W., Hales, B., Friederich, G., Chavez, F., Sabine, C., Watson, A., Bakker, D. C. E., Schuster, U., Metzl, N., Yoshikawa-Inoue, H., Ishii, M., Midorikawa, T., Nojiri, Y., Kortzinger, A., Steinhoff, T., Hoppema, M., Olafsson, J., Arnarson, T. S., Tilbrook,

- B., Johannessen, T., Olsen, A., Bellerby, R., Wong, C. S., Delille, B., Bates, N. R., and de Baar, H. J. W. Climatological mean and decadal change in surface ocean $p\text{CO}_2$, and net sea–air CO_2 flux over the global oceans. *Deep-Sea Research II* **56**, 554–577 (2009).
- Talley, L. D., Pickard, G. L., Emery, W. J., Swift, J. H. in *Descriptive Physical Oceanography: An Introduction*. (Elsevier Academic Press, Amsterdam, 2011).
- Tans, P., Keeling, D. Trends in Atmospheric Carbon Dioxide. <<http://www.esrl.noaa.gov/gmd/ccgg/trends/>>, (2014).
- Tans, P. An Accounting of the Observed Increase in Oceanic and Atmospheric CO_2 and an Outlook for the Future. *Oceanography* **22**, 26–35 (2009).
- Thomas, A. L., Henderson, G. M., Deschamps, P., Yokoyama, Y., Mason, A. J., Bard, E., Hamelin, B., Durand, N., Camoin, G. Penultimate Deglacial Sea-Level Timing from Uranium/Thorium Dating of Tahitian Corals. *Science* **324**, 1186–1189 (2009).
- Toggweiler, J. R., Russel, J. L., Carson, S. R. Midlatitude westerlies, atmospheric CO_2 , and climate change during the ice ages. *Paleoceanography*, doi:10.1029/2005PA001154 (2006).
- Trotter, J., Montagna, P., McCulloch, M., Silenzi, S., Reynaud, S., Mortimer, G., Martin, S., Ferrier-Pagès, C., Gattuso, J., Rodolfo-Metalpa, R. Quantifying the pH ‘vital effect’ in the temperate zooxanthellate coral *Cladocora caespitosa*: Validation of the boron seawater pH proxy. *Earth and Planetary Science Letters* **303**, 163–173 (2011).
- Tseng, C.-M., Wong, G. T. F., Chou, W.-C., Lee, B.-S., Sheu, D.-D., Liu, K.-K. Temporal variations in the carbonate system in the upper layer at the SEATS station. *Deep-Sea Research II* **54**, 1448–1468 (2007).
- Usui, N., Ishizaki, S., Fujii, Y., Tsujino, H., Yasuda, T., Kamachi, M. Meteorological Research Institute multivariate ocean variational estimation (MOVE) system: Some early results. *Advances in Space Research* **37**, 806–822 (2006).
- Vengosh, A., Kolodny, Y., Starinsky, A., Chivas, A. R., McCulloch, M. T. Coprecipitation and isotopic fractionation of boron in modern biogenic carbonates. *Geochimica et Cosmochimica Acta* **55**, 2901–2910 (1991).
- Venn, A. A., Tambutte, E., Holcomb, M., Laurent, J., Allemand, D., Tambutte, S. Impact of seawater acidification on pH at the tissue–skeleton interface and calcification in reef corals. *Proceedings of the National Academy of Sciences* **110**, 1634–1639 (2013).
- Venn, A., Tambutte, E., Holcomb, M., Allemand, D., Tambutte, S. Live Tissue Imaging Shows Reef Corals Elevate pH under Their Calcifying Tissue Relative to Seawater. *PLoS ONE* **6**, doi:10.1371/journal.pone.0020013 (2011).
- Vincent, D. G. The South Pacific Convergence Zone (SPCZ): A Review. *Monthly Weather Review* **122**, 1949–1970 (1994).
- Waters, J. F., Millero, F. J., Sabine, C. L. Changes in South Pacific anthropogenic carbon. *Global Biogeochemical Cycles*, doi:10.1029/2010GB003988 (2011).
- Wei, G., McCulloch, M. T., Mortimer, G., Deng, W., Xie, L. Evidence for ocean

- acidification in the Great Barrier Reef of Australia. *Geochimica et Cosmochimica Acta* **73**, 2332–2346 (2009).
- Wu, H.-P., Jiang, S.-Y., Wei, H.-Z., Yan, X. An experimental study of organic matters that cause isobaric ions interference for boron isotopic measurement by thermal ionization mass spectrometry. *International Journal of Mass Spectrometry* **328–329**, 67–77 (2012).
- Yamano, H., Sugihara, K., Nomura, K. Rapid poleward range expansion of tropical reef corals in response to rising sea surface temperatures. *Geophysical Research Letters*, doi:10.1029/2010GL046474 (2011).
- Yara, Y., Vogt, M., Fujii, M., Yamano, H., Hauri, C., Steinacher, M., Gruber, N., Yamanaka, Y. Ocean acidification limits temperature-induced poleward expansion of coral habitats around Japan. *Biogeosciences* **9**, 4955–4968 (2012).
- Yokoyama, Y., Esat, T. M. Global climate and sea level- enduring variability and rapid fluctuations over the past 150,000 years. *Oceanography* **24**, 54–69 (2011).
- Yokoyama, Y., Webster, J. M., Cotterill, C., Braga, J. C., Jovane, L., Mills, H., Morgan, S., Suzuki, A. IODP Expedition 325: Great Barrier Reefs Reveals Past Sea-Level, Climate and Environmental Changes Since the Last Ice Age. *Scientific Drilling*, doi:10.2204/iodp.sd.12.04.2011 (2011).
- Yu, J., Thornalley, D. J. R., Rae, J. W. B., McCave, N. I. Calibration and application of B/Ca, Cd/Ca, and $\delta^{11}\text{B}$ in *Neogloboquadrina pachyderma* (sinistral) to constrain CO_2 uptake in the subpolar North Atlantic during the last deglaciation. *Paleoceanography* **28**, 237–252 (2013).
- Yu, J. M., Broecker, W. S., Elderfield, H., Jin, Z. D., McManus, J., Zhang, F. Loss of Carbon from the Deep Sea Since the Last Glacial Maximum. *Science* **330**, 1084–1087 (2010).
- Zeebe, R. E., Wolf-Gladrow, D. in *CO₂ in Seawater: Equilibrium, kinetics, isotopes*. (Elsevier Oceanography Series, 2001).
- Zeebe, R. E. History of Seawater Carbonate Chemistry, Atmospheric CO_2 , and Ocean Acidification. *Annual Review of Earth and Planetary Sciences* **40**, 141–165 (2012).
- Zhang, R., Delworth, T. L. Simulated Tropical Response to a Substantial Weakening of the Atlantic Thermohaline Circulation. *Journal of Climate* **18**, 1853–1860 (2005).
- Ziegler, M., Diz, P., Hall, I. R., Zahn, R. Millennial-scale changes in atmospheric CO_2 levels linked to the Southern Ocean carbon isotope gradient and dust flux. *Nature Geoscience* **6**, 457–461 (2013).

Appendix A. Abbreviation

Abbreviation	Definition
AAIW	Antarctic Intermediate Water
ACR	Antarctic Cold Reversal
ALOHA	A Long-Term Oligotrophic Habitat Assessment
B/A	Bølling/Allerød
CLIVAR	Climate Variability and Predictability
DCF	Dead Carbon Fraction
DIC	Dissolved Inorganic Carbon
ECC	Equatorial Countercurrent
EDC	EPICA Dome C
EEP	Eastern Equatorial Pacific
EUC	Equatorial Undercurrent
GICC05	Greenland Ice Core Chronology 2005
GLODAP	Global Data Analysis Project
HS1	Heinrich Stadial 1
IODP	Integrated Ocean Drilling Program (International Ocean Discovery Program)
IPCC	Intergovernmental Panel on Climate Change
ITCZ	Intertropical Convergence Zone
JGOFS	Joint Global Ocean Flux Study
JMA	Japanese Meteorological Agency
LER	Linear Extension Rate
LGM	Last Glacial Maximum
MC-ICPMS	Multicollector-Inductively Coupled Plasma Massspectrometry
MLO	Mauna Loa Observatory
MOVE-G	Multivariate Ocean Variational Estimation—the global
NEC	North Equatorial Current
SAMW	Subantarctic Mode Water
SCS	South China Sea
SEC	South Equatorial Current

Continued

SOCAT	Surface Ocean CO ₂ Atlas
SODA	Simple Ocean Data Assimilation
SPCZ	South Pacific Convergence Zone
SSS	Sea Surface Salinity
SST	Sea Surface Temperature
TA	Total Alkalinity
TIMS	Thermal Ionization Mass Spectrometry
TTO	Transient Tracers in the Oceans
WDC	West Antarctica Divide ice core
WEP	Western Equatorial Pacific
WOCE	World Ocean Circulation Experiment
WPWP	Western Pacific Warm Pool
YD	Younger Dryas

Appendix B. A script used to extract SOCAT v2 data set.

```

$intxt="/SOCATv2_TropicalPacific.tsv";
$outtxt="/SOCATv2_TropicalPacific_ogw.csv";
$="" ;
#-=-#-=-#-=-#-=-#-=-#-=-#-=-#-=-#
# set range : if not use, set extra large (or small) value (ex. -999 or 999)
$latmin=26.6;
$latmax=27.6;
$lonmin=139.7;
$lonmax=144.7;
$yrmin=1960;
$ymax=2014;
#-=-#-=-#-=-#-=-#-=-#-=-#-=-#-=-#
# "¥" must be translated into "back slash".

if(-f $outtxt){
    print "¥n$outtxt exist! Overwrite it¥n";
    print " yes -> y // no -> any other key¥n";
    $yesno=<STDIN>;
    chomp($yesno);
    if($yesno ne "y"){exit;}
}
open(IN,"<$intxt");
print "Read $intxt¥n";
#
#
for($i=1;$i<=627;$i++){
    $header=<IN>;
    # print $header
}
$label=<IN>;
chomp($label);

```

```

@olabel=("Expocode", "Yr", "Mon", "Day", "Hour", "Min", "Longitude", "Latitude", "Temp",
"Sal(measured)", "Sal(WOA05)", "fCO2_rec", "WOCE_flag");
open(OUT, ">$outtxt");
    print OUT "@olabel¥n";
while(<IN>){
    chomp;
    @indat=split("¥t");
    if($indat[22]<0){next;}                # fco2<0
    if($indat[10]<$latmin || $indat[10]>$latmax){next;}
    if($indat[9]<$lonmin || $indat[9]>$lonmax){next;}
    if($indat[3]<$yrmin || $indat[3]>$yrmax){next;}

    printf OUT "%14s", $indat[0];        #Expocode
    printf OUT ",%5d", $indat[3];        #year
    printf OUT ",%2d", $indat[4];        #month
    printf OUT ",%2d", $indat[5];        #day
    printf OUT ",%2d", $indat[7];        #hour
    printf OUT ",%2d", $indat[8];        #min
    printf OUT ",%9.4f", $indat[9];      #longitude
    printf OUT ",%9.4f", $indat[10];     #latitude
    printf OUT ",%7.3f", $indat[13];     #temperature
    printf OUT ",%7.3f", $indat[12];     #salinity (measured)
    printf OUT ",%7.3f", $indat[17];     #salinity (WOA05)
    printf OUT ",%7.2f", $indat[22];     #fco2_rec
    printf OUT ",%2d", $indat[24];       #WOCE_flag
    printf OUT "¥n"
}
close(IN);
close(OUT);
print "Output $outtxt¥n";

```

Appendix C. A script used to draw bathymetrical map of Fig. 2-1.

```

range=142.05/142.35/27/27.25
#size is in cm scale
size=6
reso=f
file=Ogasawara_bathymetry
xy=Ogasawara_coral_location

grdcut ETOPO1_Bed_c_gmt4.grd -R${range} -G${file}.grd
makecpt -Cocean -T-2000/0/50 -Z > ${file}.cpt
#
grdimage ${file}.grd -R${range} -JM${size} -C${file}.cpt -E100 -P -K > ${file}.eps
#
grdcontour ${file}.grd -JM${size} -C50 -W0.5 -L-500/-50 -A50tf6 -O -K >>
${file}.eps
pscoast -R${range} -JM${size} -D${reso} -W1 -A -G220 -O -K -Lf142.2/27.3/27.3/5k
>> ${file}.eps
psscale -Ba500g500f500 -C${file}.cpt -D3c/-1c/6c/0.3ch -O -K >> ${file}.eps
psxy ${xy}.txt -JM -R -W -Sd6p -Gblack -O -K >> ${file}.eps
#pstext ${xy}.txt -JM -R -O -Gblue -D0.2/0 >> ${file}.eps
psbasemap -R${range} -JM -Ba0.1f0.1/a0.1f0.1WSne -O >> ${file}.eps

```